

**MECHANISTIC STUDIES ON THE RADICAL S-ADENOSYLMETHIONINE
ENZYMES INVOLVED IN MOLYBDOPTERIN, THIAMIN AND VITAMIN B₁₂
BIOSYNTHESIS**

A Dissertation

by

ANGAD PANKAJ MEHTA

Submitted to the Office of Graduate and Professional Studies of
Texas A&M University
in partial fulfillment of the requirements for the degree of

DOCTOR OF PHILOSOPHY

Chair of Committee,	Tadhg P. Begley
Committee Members,	Frank M. Raushel
	David P. Barondeau
	Paul D. Straight
Head of Department,	François P. Gabbaï

May 2015

Major Subject: Chemistry

Copyright 2015 Angad Pankaj Mehta

ABSTRACT

This dissertation focuses on radical S-adenosylmethionine enzymes involved in cofactor biosynthesis. Mechanistic studies discussed here include: (i) molybdenum cofactor biosynthetic enzyme - MoaA, (ii) thiamin pyrimidine synthase – ThiC (iii) hydroxybenzimidazole synthase, HBI synthase, involved in anaerobic vitamin B₁₂ biosynthesis.

MoaA catalyzes the first step in molybdopterin biosynthesis where GTP is converted to pterin. This catalysis involves a remarkable rearrangement reaction where the C8 of guanosine-5'-triphosphate (GTP) is inserted between the C2' and C3' carbon atoms of GTP to give the final pterin. Mechanistic studies involved characterization of the products of the reaction, identification of the position of hydrogen atom abstraction by 5'-deoxyadenosyl radical and trapping of intermediates by using 2',3'-dideoxyGTP, 2'-deoxyGTP and 2'-chloroGTP as substrate analogs.

Thiamin pyrimidine synthase, ThiC, catalyzes a complex rearrangement reaction involving the conversion of aminoimidazole ribotide (AIR) to thiamin pyrimidine (HMP-P). A hydrogen atom transfer from S-adenosylmethionine (AdoMet) to HMP-P was demonstrated. Also, the stereochemistry of this transfer was elucidated.

Bioinformatics studies on ThiC revealed that a paralog of ThiC was clustered with vitamin B₁₂ biosynthetic genes in several anaerobic microorganisms. The gene responsible for the anaerobic vitamin B₁₂ – benzimidazole biosynthesis was previously unknown. We demonstrate that the gene product of this ThiC paralog is a radical S-

adenosylmethionine enzyme. Remarkably it catalyzes the conversion of aminoimidazole ribotide (AIR) to 5-hydroxybenzimidazole (5-HBI) and formate, and S-adenosylmethionine to 5'-deoxyadenosine. We determine the hydrogen atom abstracted by 5'-deoxyadenosyl radical. We also performed carbon, nitrogen and hydrogen labeling studies and characterized the labeling pattern on 5-HBI. Based on these studies we propose a reaction mechanism of this remarkable conversion of AIR to 5-HBI.

To all my teachers...

ACKNOWLEDGEMENTS

First and foremost, I would like to thank Tadhg. If it were not for Tadhg, I would never have entered this amazing field of enzyme chemistry and chemical biology. Tadhg is a spectacular mentor and I have learnt more than just science from him. Tadhg has been a great source of inspiration for me over all these years. Thank you, Tadhg, for all the opportunities and all your trust. Also, I would like to thank my committee members for their support and valuable insights.

I am grateful to all the past and the present Begley Lab members. Thanks to Amrita Hazra for helping me get started in the lab and for bearing with all my stupid questions. My research would not have been possible without all my collaborators. Sameh, apart from being a spectacular chemist, you are a “magician artist” and a great friend! Cynthia and Hui, I bothered you with non-stop requests for all kinds of constructs. Thanks for all your help and thanks for bearing with me. Mike (Ealick Lab) and Derek (Britt Lab), I absolutely enjoyed working with both of you. Bill Russell, thanks for all the scientific discussions and hour long lunches! Sean Kong, thanks for all the NMR time. Kalyan, thanks for all the useful scientific advice. Seán, BJ, Bekir thanks for all your help with “fancy” instruments!

Mom and Dad, thanks for your love and support. Dad, thank you for inculcating scientific curiosity. Mom, thank you for teaching me the values of self-motivation, hard work, discipline and sacrifice. My brother, Rugved, thanks for understanding me and being my best friend!

NOMENCLATURE

AdoMet	S-adenosyl-L-methionine
5'dA	5'-deoxyadenosine
5'dA radical	5'-deoxyadenosyl radical
GTP	guanosine-5'-triphosphate
cPMP	cyclicpyranopterintriphosphate
HPLC	high performance liquid chromatography
LCMS	liquid chromatography mass spectrometry
NMR	nuclear magnetic resonance
COSY	correlation spectroscopy
HSQC	heteronuclear single quantum coherence
PFBHA	<i>o</i> -(pentafluorobenzyl)-hydroxylamine
2',3'-dideoxyGTP	2'-3'-anhydro-2',3'-dideoxyguanosine-5'-triphosphate
2'-chloroGTP	2'-chloro-2'-deoxyguanosine-5'-triphosphate
AIR	aminoimidazole ribotide
HMP-P	4-amino-5-hydroxymethyl-2-methylpyrimidine phosphate
HMP	4-amino-5-hydroxymethyl-2-methylpyrimidine
5-HB	5-hydroxybenzimidazole
CO	carbon monoxide
FMN	Flavin mononucleotide
DMB	dimethylbenzimidazole

EPR	electron paramagnetic resonance
MS	Mass spectrometry
CIP	Calf intestine phosphatase

TABLE OF CONTENTS

	Page
ABSTRACT.....	ii
DEDICATION.....	iv
ACKNOWLEDGEMENTS.....	v
NOMENCLATURE.....	vi
TABLE OF CONTENTS.....	viii
LIST OF FIGURES.....	xiv
LIST OF TABLES.....	xvii
1. INTRODUCTION TO RADICAL ADO MET ENZYMES.....	1
1.1 Introduction to radical S-adenosylmethionine (AdoMet, 1) enzymes.....	1
1.2 Diverse rearrangement reactions catalyzed by radical AdoMet enzymes.....	3
1.3 Research opportunity.....	5
2. MOLYBDOPTERIN BIOSYNTHESIS.....	7
2.1 Introduction to molybdenum cofactor.....	7
2.2 Background.....	8
2.3 Results and discussion.....	10
2.3.1 LCMS analysis of MoaA reaction products – 5'-dA (6) formation..	10
2.3.2 Characterization of MoaA reaction product derived from GTP.....	11
2.3.3 o-(pentafluorobenzyl) hydroxylamine (PFBHA) derivatization of the reaction product.....	12
2.3.4 Reconstitution of MoaA purified from <i>E. coli</i> (MoaC ⁻) strain.....	14
2.3.5 5'-dA (6) formation in the MoaA/ deuterated GTP isotopomers reactions.....	16
2.3.6 Mechanistic proposal for MoaA catalyzed reaction.....	19
2.3.7 MoaA reactions with 2',3'-dideoxyGTP – LCMS analysis.....	20
2.3.8 MoaA reactions 2',3'-dideoxyGTP – product characterization.....	22
2.3.9 MoaA reactions 2'-chloroGTP – HPLC and LCMS analysis.....	25
2.3.10 MoaA reactions with 2'-deoxyGTP – LCMS analysis.....	28
2.3.11 Revised mechanistic proposal for MoaA-catalyzed reaction.....	30
2.4 Conclusion.....	31

2.5 Experimental.....	33
2.5.1 Overexpression and purification of MoaA.....	33
2.5.2 Overexpression and purification of guanylate kinase.....	34
2.5.3 Enzymatic assays for MoaA reactions for LCMS characterization of 5'dA (6)	34
2.5.4 Enzymatic assays for MoaA reactions for LCMS/NMR characterization of pterin (8).....	35
2.5.5 MoaA over-expressed and purified from <i>E. coli</i> (MoaC ⁻).....	36
2.5.6 PFBHA derivatization of the reaction product.....	36
2.5.7 Assay conditions for MoaA reactions with 2',3'-dideoxyGTP (21)..	36
2.5.8 Phosphatase treatment of MoaA/2',3'-dideoxyGTP reaction mixtures.....	37
2.5.9 Acid hydrolysis of phosphatase treated MoaA/2',3'-dideoxyGTP reaction mixtures.....	37
2.5.10 Assay conditions for MoaA reactions with 2'-chloroGTP (21) for guanine characterization.....	38
2.5.11 Assay conditions for MoaA reactions with 2'-chloroGTP (21) for trapping of ribose derived product.....	38
2.5.12 MoaA reactions with 2'-deoxyGTP.....	39
2.5.13 LCMS conditions for MoaA reactions for LCMS characterization of 5'dA (6)	39
2.5.14 HPLC conditions for the purification of 5'-dA formed in the MoaA reactions.....	40
2.5.15 LCMS characterization of the dephosphorylated product of MoaA reactions with GTP and hydroxylamine derivatized product (10).....	40
2.5.16 HPLC purification of the MoaA/GTP reaction product.....	41
2.5.17 LCMS parameters for the product detection of MoaA reactions with 2',3'-dideoxyGTP.....	41
2.5.18 LCMS parameters for comparing the dephosphorylated, acid hydrolyzed product of MoaA with 2',3'-dideoxyGTP with reference standards.....	42
2.5.19 LCMS conditions for MoaA assays with 2'-chloroGTP – detection of guanine.....	42
2.5.20 LCMS conditions for MoaA assays with 2'-chloroGTP – detection of 3-mercaptopbenzoic acid derivatized product.....	43
2.5.21 LC conditions for MoaA assays with 2'-deoxyGTP – product isolation and co-elution experiment.....	43
2.5.22 Synthetic scheme for guanosine-5'-monophosphate (65).....	44
2.5.23 Synthesis of [2- ² H] and [2- ² H] 1,2,3,5-tetra-O-acetylribofuranoside (62)	44
2.5.24 Synthesis of 2-acetyl-amino-2',3',5'-tri-O-acetyl-6-O-(N,N- diphenylcarbamoyl)-guanosine (63)	46
2.5.25 Synthesis of guanosine (64).....	46

2.5.26	Synthesis of guanosine-5'-monophosphate (65, GMP).....	47
2.5.27	HPLC conditions for purification of GMP isotopomers.....	47
2.5.28	Synthesis of [8- ² H] guanosine-5'-monophosphate.....	48
2.5.29	Synthetic scheme for 2',3'-anhydro-2',3'-dideoxyguanosine (24)...	48
2.5.30	Synthesis of 2',3'-anhydro-2',3'-dideoxyguanosine (24).....	48
2.5.31	Synthetic scheme for 2-amino-8-((3S)-5-hydroxy-2- (hydroxymethyl)tetrahydrofuran-3-yl)-9H-purin-6-ol (29).....	50
2.5.32	Synthesis of methyl-6-O-(tert-butyldimethylsilyl)- α -D- glucopyranoside (70)	50
2.5.33	Synthesis of methyl-2,3-anhydro-6-O-(tert-butyldimethylsilyl)- α -D-allopyranoside (71)	51
2.5.34	Synthesis of (2S,5S)-2-(tert-butyldimethyl silanyloxymethyl)-5- methoxy-2,5-dihydrofuran-3- carbaldehyde (72).....	52
2.5.35	Synthesis of (2S,3R/S, 5S)-2-(tert-butyldimethyl silanyloxy methyl)- 5-methoxytetrahydrofuran-3- carbaldehyde (73).....	52
2.5.36	Synthesis of 2-amino-8-((2S, 3R/S, 5S)-2-(tert-butyldimethyl silanyloxymethyl)-5-methoxytetrahydrofuran-3-yl)-9H- purin-6-ol (74)	53
2.5.37	Synthesis of 2-amino-8-((2S, 3S,5S)-2-(hydroxymethyl)-5- methoxytetrahydrofuran-3-yl)-9H-purin-6-ol (75).....	54
2.5.38	Synthesis of 2-amino-8-((3S)-5-hydroxy-2- (hydroxymethyl)tetrahydrofuran-3-yl)-9H-purin-6-ol (29).....	54
2.5.39	Synthetic scheme for 2'-chloroGMP (81).....	55
2.5.40	Synthesis of 9-(3',5'-O-(1,1',3,3'-tetrakisopropylidisiloxane- 1,3-diyl)- β -D-arabinofuranosyl) guanine (77).....	56
2.5.41	Synthesis of 9-(3',5'-O-(1,1',3,3'-tetrakisopropylidisiloxane- 1,3-diyl))-2'-O-[(trifluoromethyl)sulfonyl] arabinofuranosyl guanine (78)	56
2.5.42	Synthesis of 3',5'-O-(1,1',3,3'-tetrakisopropylidisiloxane- 1,3-diyl) -2'-chloro-2'-deoxy- β -D-guanosine (79).....	57
2.5.43	Synthesis of 2'-chloro-2'-anhydroguanosine (80).....	58
2.5.44	Synthesis of 2'-chloro-2'-anhydroguanosine-5'-monophosphate (81)	58
2.5.45	Synthetic scheme for 5-(3-mercaptopbenzoic acid)-3-furanone (35)..	59
2.5.46	Synthesis of 5'-O-tosylthymidine (83).....	59
2.5.47	Synthesis of 3'-keto-5'-tosylthymidine (84).....	60
2.5.48	Synthesis of 2-methylene-3(2H)-furanone (33).....	60
2.5.49	Synthesis of 5-(3-mercaptopbenzoic acid)-3-furanone (35).....	60
2.5.50	Synthetic scheme for 2-amino-6-((2S/2R,3S)-2,3,4- trihydroxybutyl)pteridin-4(3H)-one (40, 41).....	61
2.5.51	Synthesis of (2R,3S,4R,5R)-2-((p-toluidino)methyl)-tetrahydro- 2H-pyran-2,3,4,5-tetraol (87).....	62
2.5.52	Synthesis of 2-amino-6-((2S,3S)-2,3,4-trihydroxybutyl) pteridin-4(3H)-one (40)	62

2.5.53	Synthesis of (2R,3S,4R,5R)-2-((<i>p</i> -toluidino)methyl)-tetrahydro-2H-pyran-2,3,4,5-tetraol (90)	63
2.5.54	Synthesis of 2-amino-6-((2R,3S)-2,3,4-trihydroxybutyl)pteridin-4(3H)-one (41)	63
3.	THIAMIN PYRIMIDINE SYNTHASE – ThiC	65
3.1	Introduction to thiamin pyrimidine synthase – ThiC	65
3.2	Results and discussion	68
3.2.1	Identification of the origin of the C5' hydrogen of HMP-P	68
3.2.2	Stereochemistry of the transfer of hydrogen atom from 5' dA on to HMP-P	69
3.2.3	Summary of active-site mutant studies for ThiC	71
3.3	Conclusion	74
3.4	Experimental	75
3.4.1	Over-expression of C.c. ThiC	75
3.4.2	Over-expression of A.t. ThiC	76
3.4.3	Purification of A.t. ThiC and C.c. ThiC	77
3.4.4	Over-expression and purification of S-adenosylmethionine synthetase	77
3.4.5	ThiC-SAM synthetase coupled assays	78
3.4.6	ThiC assay conditions	78
3.4.7	Alkaline phosphate treatment of HMP-P purified after ThiC reconstitution	79
3.4.8	Sample preparation for mass spectrometry experiments	79
3.4.9	Enzymatic sample - derivatization for stereochemistry experiment	79
3.4.10	Reference standard sample - derivatization for stereochemistry experiment	80
3.4.11	HPLC purification of HMP-P from ThiC reconstitution mixture	80
3.4.12	HPLC buffer exchange of alkaline phosphatase mixture	81
3.4.13	Synthetic scheme for camphanic esters of HMP (31, 32, 33)	81
3.4.14	Synthesis of 4-amino-5-(hydroxymethyl)-2-methylpyrimidine (HMP, 35)	82
3.4.15	Synthesis of 4-amino-5-cyano-2-methylpyrimidine (38)	82
3.4.16	Synthesis of 4-amino-5-carbaldehyde-2-methylpyrimidine (39)	82
3.4.17	Synthesis of 4-amino-5-R-D-(hydroxymethyl)-2-methylpyrimidine (41)	83
3.4.18	Synthesis of 4-amino-5-S-D-(hydroxymethyl)-2-methylpyrimidine (40)	83
3.4.19	Preparation of camphanic ester of HMP (31, 32, 33)	83
4.	ANAEROBIC VITAMIN B ₁₂ BIOSYNTHESIS – HYDROXYBENZIMIDAZOLE SYNTHASE	85

4.1	Background and introduction.....	85
4.2	Results and discussion.....	87
4.2.1	Reconstitution of ThiC-1 as hydroxybenzimidazole synthase (HBI synthase)	87
4.2.2	HBI synthase reactions with ¹³ C-labeled AIR isotopomers.....	89
4.2.3	HBI synthase – fate of 1'-C of AIR.....	92
4.2.4	HBI synthase reactions with ² H-labeled AIR isotopomers.....	93
4.2.5	HBI synthase reactions with ¹⁵ N-AIR.....	97
4.2.6	Characterization of labeling pattern on 5-HB.....	98
4.2.7	Discussion.....	99
4.2.8	ThiC-HBI synthase homology model (Steve Ealick Lab, Cornell University)	100
4.2.9	Mechanistic proposal for HBI synthase catalyzed reaction.....	103
4.3	Conclusion.....	104
4.4	Experimental.....	105
4.4.1	Over-expression and purification of HBI synthase.....	105
4.4.2	HBI synthase assays for LCMS and HPLC purification of 5-HB... ..	106
4.4.3	Enzymatic assays for NMR analysis to determine the fate of 1'-C of AIR.....	107
4.4.4	HPLC conditions for co-elution experiment and purification of 5-HB.....	107
4.4.5	LCMS conditions for HBI synthase assays.....	107
4.4.6	Synthetic scheme for AIRs (36).....	108
4.4.7	Synthesis of methyl a/b-D-ribofuranoside (29).....	109
4.4.8	Synthesis of 1-O-methyl-2,3,5-tri-O-acetyl-a/b-D-ribofuranoside (30)	109
4.4.9	Synthesis of 1,2,3,5-tetra-O-acetyl-a/b-D-ribofuranoside (31).....	110
4.4.10	Synthesis of 5-nitro-1-(2,3,5-tri-O-acetyl-b-D-ribofuranoside (34)	110
4.4.11	Synthesis of 5-nitro-1-(b-D-ribofuranoside)imidazole (35).....	111
4.4.12	Synthesis of 5-amino-1-(b-D-ribofuranoside)imidazole (36).....	111
5.	SUMMARY AND OUTLOOK.....	112
5.1	Summary.....	112
5.1.1	Molybdopterin biosynthesis.....	112
5.1.2	Thiamin pyrimidine synthase – ThiC.....	114
5.1.3	Anaerobic vitamin B ₁₂ biosynthesis – hydroxybenzimidazole biosynthesis.....	115
5.2	Outlook.....	117
5.2.1	Molybdopterin biosynthesis – crystallography.....	118
5.2.2	Thiamin pyrimidine synthase – ThiC – trapping of organic radicals.....	118

5.2.3	Testing HBI synthase homologs– anaerobic vitamin B ₁₂ biosynthesis.....	118
5.2.4	HBI synthase – EPR studies.....	119
5.2.5	AIR analogs to study HBI synthase and ThiC reactions.....	119
	REFERENCES.....	120
	APPENDIX.....	127

LIST OF FIGURES

	Page
Figure 1.1 5'dA radical mediated chemistry.....	2
Figure 1.2 Examples of major reactions found in organic radical chemistry.....	3
Figure 1.3 Complex radical rearrangement reactions catalyzed by radical AdoMet enzymes.....	4
Figure 2.1 Molybdopterin biosynthetic pathway.....	8
Figure 2.2 Labeling studies indicating the carbon-insertion reaction characterized by MoaA-MoaC.....	9
Figure 2.3 MoaA active site.....	9
Figure 2.4 MoaA reactions – characterization of 5'dA formed.....	10
Figure 2.5 MoaA reactions – characterization of stable oxidized pterin.....	11
Figure 2.6 Trapping of the ketone-containing MoaA reaction product by oxime formation.....	13
Figure 2.7 Trapping of the ketone-containing MoaA (MoaC ⁺) reaction product.....	15
Figure 2.8 Mass spectrometry data for 5'-dA formation with GTP isotopomers.....	16
Figure 2.9 Mechanistic proposal for MoaA catalyzed reaction.....	19
Figure 2.10 Analysis of the product formed when 2',3'-dideoxyGTP 21 is treated with MoaA.....	21
Figure 2.11 Mechanistic analysis to suggest possible products formed from 2',3'-dideoxyGTP (21)	22
Figure 2.12 MoaA reactions with 2',3'-dideoxyGTP – product comparison with reference standard (24).....	23
Figure 2.13 MoaA reactions with 2',3'-dideoxyGTP – hydrolyzed product comparison with reference standard (29)	24
Figure 2.14 Mechanistic proposal for the product formed in the MoaA catalyzed	

reaction with 2',3'-dideoxyGTP and subsequent derivatization.....	25
Figure 2.15 MoaA reactions with 2'-chloroGTP – product characterization.....	26
Figure 2.16 Mechanism of the MoaA-catalyzed reaction of 2'-chloroGTP (31).....	27
Figure 2.17 Two possible mechanistic proposals for the carbon insertion step.....	28
Figure 2.18 MoaA reactions with 2'-deoxyGTP (42b) – product characterization.....	29
Figure 2.19 Revised mechanistic proposal for the MoaA-catalyzed reaction.....	31
Figure 2.20 Synthetic scheme for GMP (65)	44
Figure 2.21 Synthetic scheme for 2',3'-anhydro-2',3'-dideoxyguanosine (24).....	48
Figure 2.22 Synthetic scheme for 2-amino-8-((3S)-5-hydroxy-2-(hydroxymethyl)tetrahydrofuran-3-yl)-9H-purin-6-ol (29).....	50
Figure 2.23 Synthetic scheme for 2'-chloroGMP (81).....	55
Figure 2.24 Synthetic scheme for 5-(3-mercaptopbenzoic acid)-3-furanone (35).....	59
Figure 2.25 Synthetic scheme for 2-amino-6-((2S/2R,3S)-2,3,4-trihydroxybutyl)pteridin-4(3H)-one (40, 41).....	61
Figure 3.1 ThiC catalyzed conversion of AIR (1) to HMP-P (2) and AdoMet (3) to 5'dA (5) and methionine (6)	65
Figure 3.2 C, N and H labeling pattern on HMP-P and 5'dA in the ThiC-catalyzed reaction and active site of ThiC.....	66
Figure 3.3 Mechanistic proposal for ThiC-catalyzed reaction.....	67
Figure 3.4 Incorporation of a deuterium atom from AdoMet.....	69
Figure 3.5 Stereochemical analysis of the deuterium atom incorporated from AdoMet.....	70
Figure 3.6 Synthetic scheme for camphanic esters of HMP (31, 32, 33).....	81
Figure 4.1 ThiC-catalyzed reaction - C, N and H labeling pattern on HMP-P and 5'dA.....	85

Figure 4.2 BluB catalyzed DMB biosynthesis.....	86
Figure 4.3 Reconstitution of ThiC-1 as HBI synthase.....	88
Figure 4.4 Reconstitution of ThiC-1 as a radical SAM enzyme as hydroxybenzimidazole synthase (HBI synthase).....	89
Figure 4.5 HBI synthase reaction with ^{13}C -AIR.....	90
Figure 4.6 HBI synthase – fate of 1'-C of AIR.....	92
Figure 4.7 HBI synthase reaction with ^2H -AIR.....	94
Figure 4.8 HBI synthase reaction with ^{15}N -AIR - LCMS data for 5-HB.....	98
Figure 4.9 Characterization of the labeling pattern on 5-HB.....	99
Figure 4.10 HBI synthase homology model based on ThiC structure.....	102
Figure 4.11 A mechanistic proposal for the HBI synthase catalyzed reaction.....	103
Figure 4.12 Synthetic scheme for AIRs (36)	108
Figure 5.1 Mechanistic proposal for MoaA-catalyzed transformation.....	114
Figure 5.2 Mechanistic proposal for HBI synthase-catalyzed transformation.....	117
Figure A1 Substrate analogs that were tested for ThiC-catalyzed reactions.....	127

LIST OF TABLES

	Page
Table 2.1 5'-dA (6) formed in the MoaA reactions with several site-specifically deuterated GTP isotopomers.....	18
Table 3.1 ThiC - active site mutant studies.....	71
Table 4.1 Summary of HBI synthase reactions with ¹³ C-AIR.....	91
Table 4.2 HBI synthase reaction with ² H-AIR isotopomers.....	97

1. INTRODUCTION TO RADICAL ADO MET ENZYMES

1.1 Introduction to radical S-adenosylmethionine (AdoMet, 1) enzymes

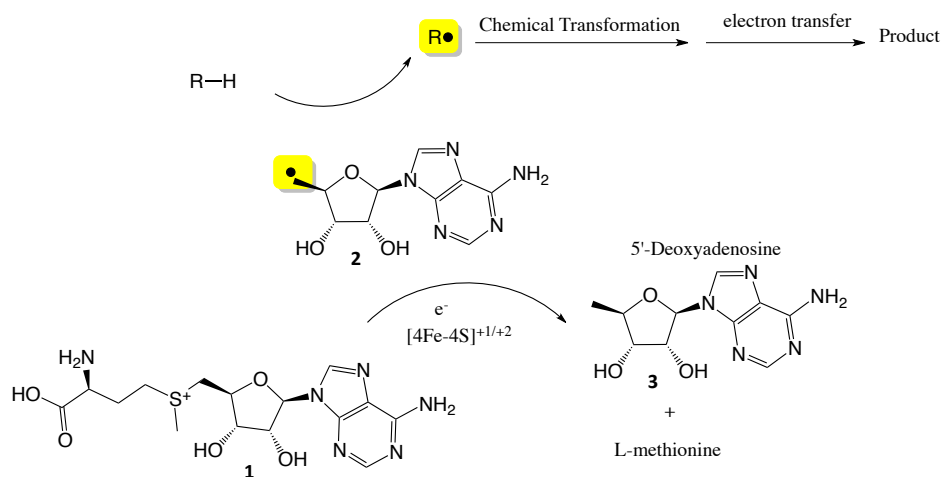
Complex chemical transformations in biological systems are often radical mediated transformations. Some of these transformations commonly include rearrangement reactions¹, carbon insertion reactions², radical addition reactions³, chemically high energy C-C, C-N, C-P bond fragmentation reactions⁴⁻⁶ and epimerization reactions⁷. These transformations are commonly initiated by hydrogen atom abstractions from unactivated C-H bonds to generate radical intermediates, which undergo remarkable transformations.

These radical transformations are mainly catalyzed by cytochrome P450 dependent enzymes⁸, non-heme iron containing enzymes⁹, vitamin B₁₂ containing-adenosyl cobalamin dependent enzymes¹⁰ and [4Fe-4S] cluster containing radical S-adenosylmethionine (**AdoMet**) enzymes¹¹.

Radical AdoMet enzymes usually generate a 5'-deoxyadenosyl radical (**5'dA radical, 2**) and L-methionine using a reduced [4Fe-4S]⁺ cluster and AdoMet. This 5'dA radical abstracts a hydrogen atom to form 5'-deoxyadenosine (5'dA) and generates a substrate derived radical intermediate (Figure 1.1).

In contrast to iron(IV)oxo-derived radicals, where the dominant chemistry involves radical addition to the iron-bound oxygen, radicals formed by hydrogen atom transfer to the adenosyl radical are more persistent because the reverse reaction is relatively slow. This allows time for complex rearrangements to occur (Figure 1.1).

(A)



(B)

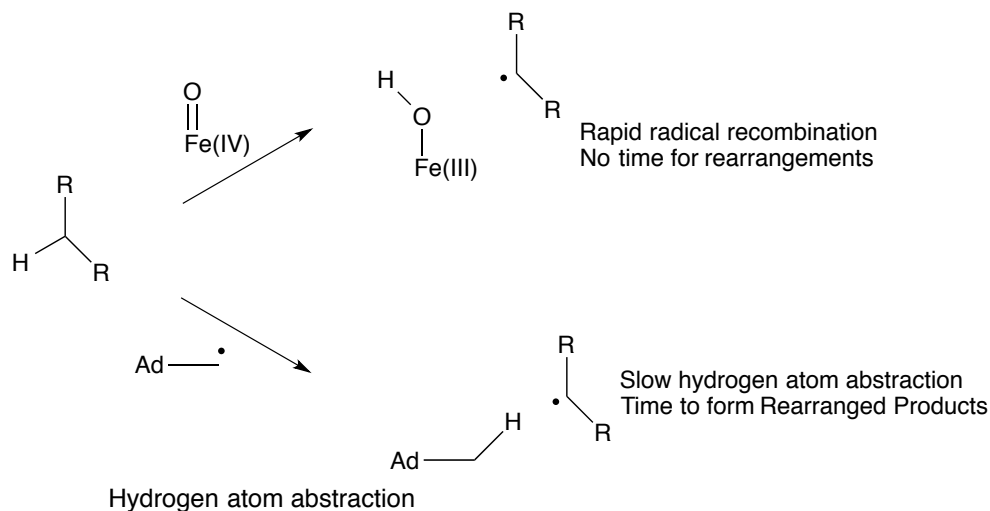


Figure 1.1: 5'dA radical mediated chemistry. (A, B) In contrast to radicals generated using iron(IV)oxo, radical SAM enzymes generate persistent radicals that can undergo complex rearrangements.

Radical AdoMet enzymes catalyze a remarkable range of reactions. This is due to the high intrinsic reactivity of organic radicals, which can undergo rapid hydrogen atom abstraction, double bond addition and fragmentation reaction (Figure 1.2). Examples of

all of these reactions can be found in the radical SAM enzymes used for cofactor biosynthesis.

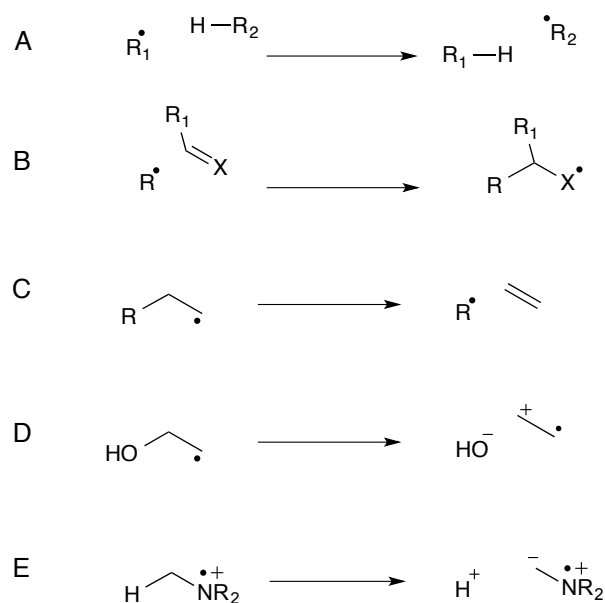


Figure 1.2: Examples of major reactions found in organic radical chemistry. A) Hydrogen atom abstraction reactions. B) Addition to double bonds. C-E) β bond scission reactions.

1.2 Diverse rearrangement reactions catalyzed by radical AdoMet enzymes

Radical AdoMet enzymes catalyze several complex radical rearrangement reactions as shown in Figure 1.3.

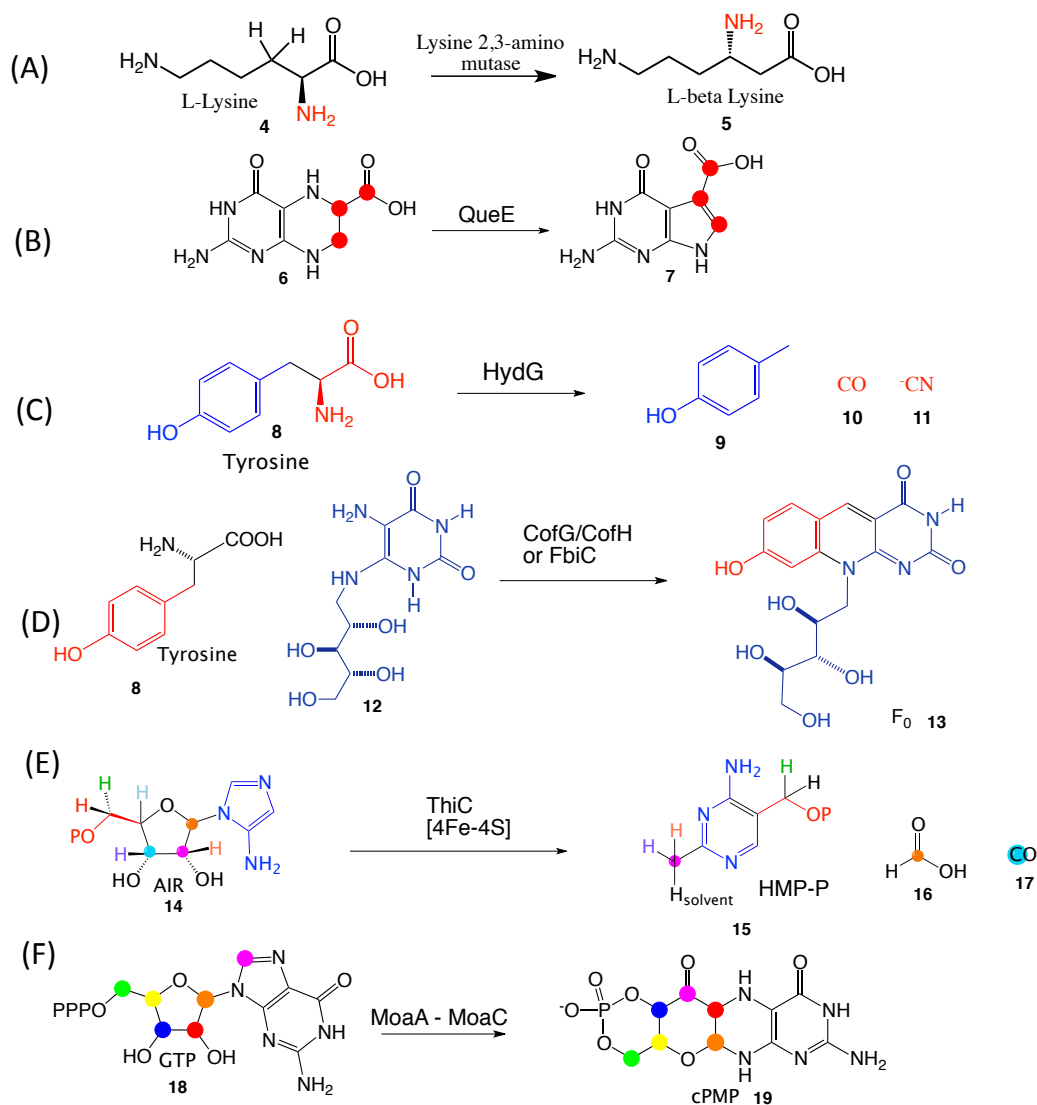


Figure 1.3: Complex radical rearrangement reactions catalyzed by radical AdoMet enzymes. (A) Lysine 2,3-aminomutase catalyzed rearrangement of L-lysine to L-beta Lysine. (B) QueE catalyzes the radical mediated ring contraction step (6 to 7) in the deazapurine biosynthesis. (C) HydG catalyzes the conversion of tyrosine (8) to p-cresol (9), CO (10) and cyanide (11) in the H cluster containing FeFe hydrogenase maturation. (D) CofG/CofH catalyzed tyrosine (8) and ribityl-daminouracil (12) to F₀ in the F420 biosynthesis (13). (E) ThiC catalyzed conversion of AIR (14) to HMP-P (15) in the prokaryotic thiamin biosynthesis. (F) MoaA-MoaC catalyzed conversion of GTP (18) to cPMP (19) in the molybdopterin biosynthesis.

Lysine 2,3-aminomutase catalyzes the conversion of L-lysine to L-beta Lysine (Figure 1.3A) in the lysine fermenting bacteria.¹²⁻¹⁵ It was one of the first radical AdoMet enzyme to be reconstituted in vitro. QueE catalyzes the radical mediated ring contraction step (6) to (7) in the deazapurine biosynthesis.¹⁶⁻¹⁹ This step is common to the biosynthetic pathways of all deazapurine-containing compounds. HydG catalyzes the the conversion of tyrosine (8) to p-cresol (9), CO (10) and cyanide (11) in the H cluster containing FeFe hydrogenase maturation.²⁰⁻²⁴ CofG/CofH catalyzes the conversion of tyrosine (8) and ribityl-daminouracil (12) to Fo in the F420 biosynthesis (13).²⁵ ThiC catalyzes the conversion of AIR (14) to HMP-P (15) in the prokaryotic thiamin biosynthesis.^{1,26-28} MoaA-MoaC catalyzes the conversion of GTP (18) to cPMP (19) in the molybdopterin biosynthesis.^{2,29-32} MoaA is a radical AdoMet enzyme involved in molybdopterin biosynthesis. It uses GTP as a substrate. The product of MoaA was unknown before our studies.

1.3 Research opportunity

It can be seen from the reactions shown in Figure 1.3A-F that Radical AdoMet enzymes catalyze several complex radical rearrangement reactions. Mechanistic studies have been extensively performed on Lysine 2,3-aminomutase. However, till recently, the mechanistic details of reactions B-F (Figure 1.3) were poorly understood.

This dissertation describes the mechanistic studies on (i) MoaA catalyzed GTP transformation in molybdopterin biosynthesis (ii) ThiC catalyzed HMP-P biosynthesis

and (iii) ThiC homolog (HBI synthase) catalyzed benzimidazole biosynthesis in the anaerobic vitamin B₁₂ biosynthetic pathway.

2. MOLYBDOPTERIN BIOSYNTHESIS*

2.1 Introduction to molybdenum cofactor

Molybdenum is a required nutrient for plants, animals and microorganisms and is involved in many redox reactions implicated in the global carbon, sulfur, and nitrogen cycles.^{33,34} With the exception of nitrogenase, all molybdenum requiring enzymes use molybdopterin as the metal binding ligand. Nitrate reductase, sulfite oxidase, xanthine dehydrogenase and aldehyde oxidase are well known molybdenum cofactor dependent enzymes. Molybdopterin forms the core pterin structure of different forms of molybdenum cofactor. In humans the deficiency of molybdopterin biosynthetic genes leads to death within months of birth.³⁵ Molybdopterin cofactor biosynthetic studies have played a critical role in finding the right supplement that overcomes this genetic deficiency.³⁶ The genes responsible for molybdopterin biosynthesis have been known since 1980s. However, the chemical details of the early steps of this biosynthetic pathway were yet to be elucidated.³²

*Reprinted in part with permission from Mehta, A. P.; Hanes, J. W.; Abdelwahed, S. H.; Hilmey, D. G.; Hanzelmann, P.; Begley, T. P. *Biochemistry* **2013**, *52*, 1134. Copyright 2013 American Chemical Society and from Mehta, A. P.; Abdelwahed, S. H.; Xu, H.; Begley, T. P. *J. Am. Chem. Soc.* **2014**, *136*, 10609. Copyright 2014 American Chemical Society and from Mehta, A. P.; Abdelwahed, S. H.; Begley, T. P. *J Am Chem Soc* **2013**, *135*, 10883. Copyright 2013 American Chemical Society.

2.2 Background

The biosynthesis of molybdopterin is similar in plants, animals and microorganisms. The biosynthetic pathway is shown in Figure 2.1. The first steps catalyzed by MoeA and MoeC use guanosine-5'-triphosphate (**1**; GTP) as the precursor to synthesize cyclicpyranopterin monophosphate (cPMP). The next steps involve the thiolation of molybdopterin to form **3** followed by the metal incorporation to give **5**.³²

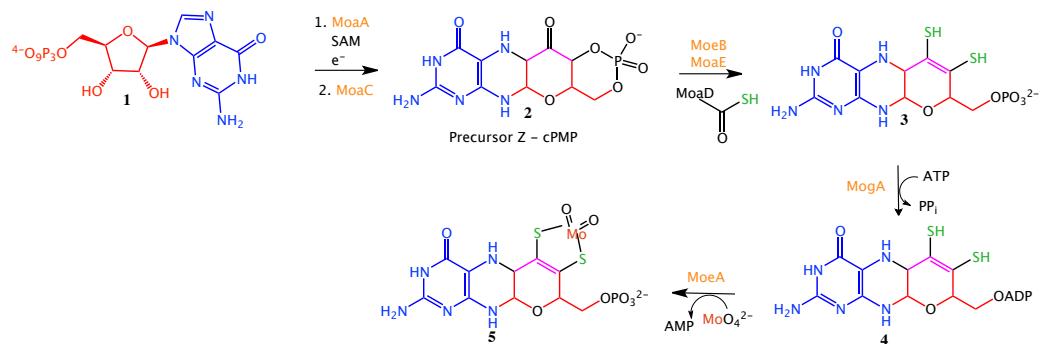


Figure 2.1: Molybdopterin biosynthetic pathway.

Previous labeling studies had established that in the conversion of GTP to cPMP by MoeA-MoeC, the C8 of GTP is inserted between the C2' and C3' carbons as shown in the Figure 2.2. This is an unprecedented reaction catalyzed in ribose chemistry.³⁷



Figure 2.2: Labeling studies indicating the carbon-insertion reaction characterized by MoaA-MoaC.

Also, it was shown that MoaA is a member of the radical-AdoMet superfamily of proteins and harbors two $[4\text{Fe-4S}]^{2+,1+}$ clusters. The N-terminal $[4\text{Fe-4S}]$ cluster is likely to be responsible for the reductive cleavage of AdoMet to the 5'-deoxyadenosyl (5'-dA) radical and L-methionine^{3,4} and the second cluster binds to N1 of GTP.⁵ A 2.35 Å crystal structure of MoaA shows the two clusters at the active site as well as the orientation of 5'-deoxyadenosine (5'dA) as compared to GTP (Figure 2.3).²⁹⁻³¹

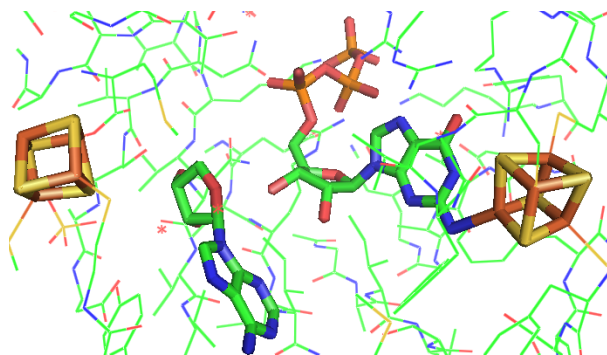


Figure 2.3: MoaA active site. A 2.35 Å crystal structure of MoaA shows the two clusters at the active site as well as the orientation of 5'-deoxyadenosine (5'dA) as compared to GTP.

The crystal structure does not indicate the regiochemistry of hydrogen atom abstraction by 5'dA radical. Based on all these previous studies, we decided to mechanistically investigate this fascinating reaction catalyzed by MoaA-MoaC.

2.3 Results and discussion

2.3.1 LCMS analysis of MoaA reaction products – 5'-dA (6) formation

MoaA assay reactions with GTP, AdoMet and dithionite as reductant were incubated in the anaerobic chamber for 3 hrs. The protein was filtered off and the small molecule pool was analyzed by LCMS. Figure 2.4 shows the formation and characterization of 5'dA formed in the MoaA reaction where all the components were present.³⁸

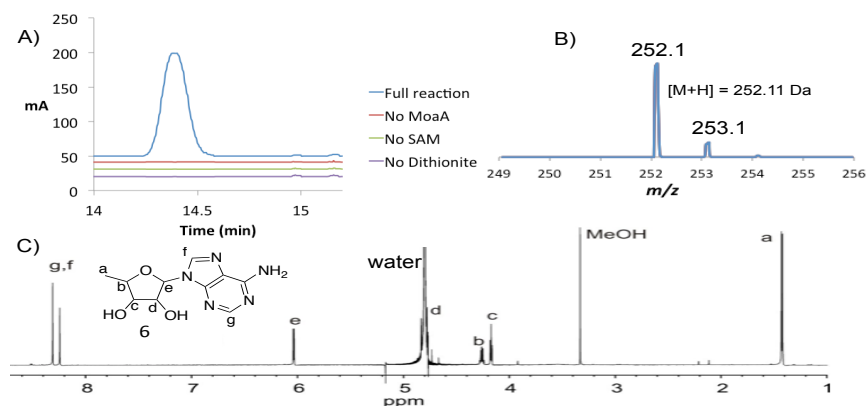


Figure 2.4: MoaA reactions – characterization of 5'dA formed. A) HPLC analysis of the MoaA reaction mixture. The red trace is from the reaction containing MoaA, SAM, GTP and dithionite. The blue, green and pink traces are controls in which MoaA, SAM or sodium dithionite were omitted respectively. The peak at 14.5 min is 5'-dA. All the reactions were performed under anaerobic conditions. B) ESI-MS analysis of the 14.5 min peak indicates an m/z of 252.1 Da corresponding to the $[M+H]$ for 5'-dA. C) ¹H NMR of the 14.5 min peak confirms its identity as 5'-dA.

2.3.2 Characterization of MoaA reaction product derived from GTP

The GTP derived product of the MoaA reaction was also analyzed. This reaction product is highly oxygen sensitive, undergoing decomposition to a mixture of products. Hence, the MoaA reaction was treated with alkaline phosphatase and it was cleanly oxidized using KI/I₂ before exposure to air.³⁸⁻⁴¹ The resulting product was purified by HPLC as a fluorescent compound eluting at 17.4 min (Figure 2.5).

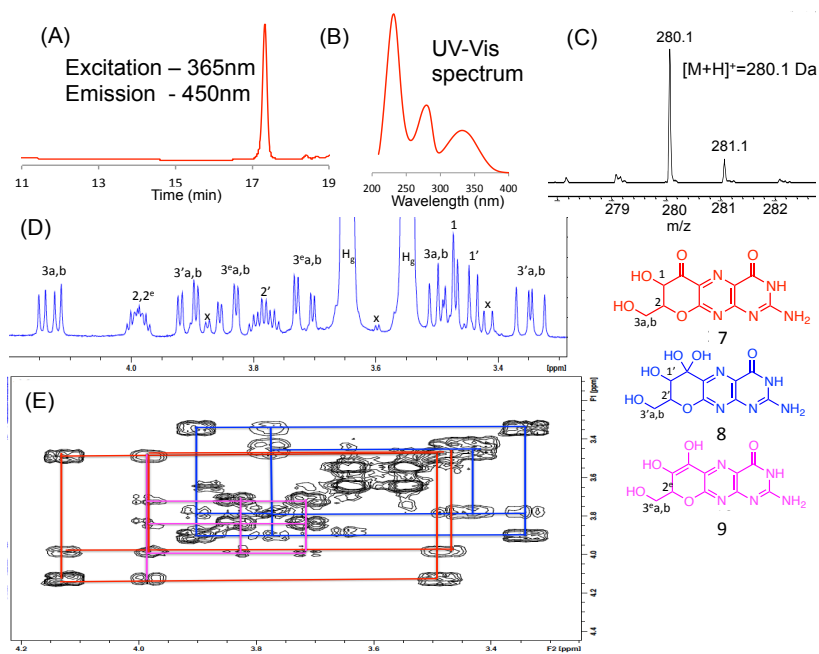


Figure 2.5: MoaA reactions – characterization of stable oxidized pterin. A) MoaA assays with GTP are treated with phosphatase followed by oxidation with KI/I₂. The HPLC traces show the formation of the fluorescent product eluting at 17.4min. (B) UV-Vis spectrum of the product. The UV-Vis spectrum of the compound was similar to that of a pterin. (C) The mass spectrum $[M+H]^+$ of the MoaA product shown in the HPLC trace in Figure 2.5A. (D) ¹H NMR of the purified product. 1,2,3a,b are the signals for compound (7), 2^e, 3^ea,b are the signals for compound (9) and 1',2',3'ab are the signals for compound (9). x is unknown impurity in the sample. (E) dqfCOSY of the purified product. The signals at 3.55ppm and 3.65ppm are glycerol impurities. (F) HSQC of the purified product.⁴¹

(F)

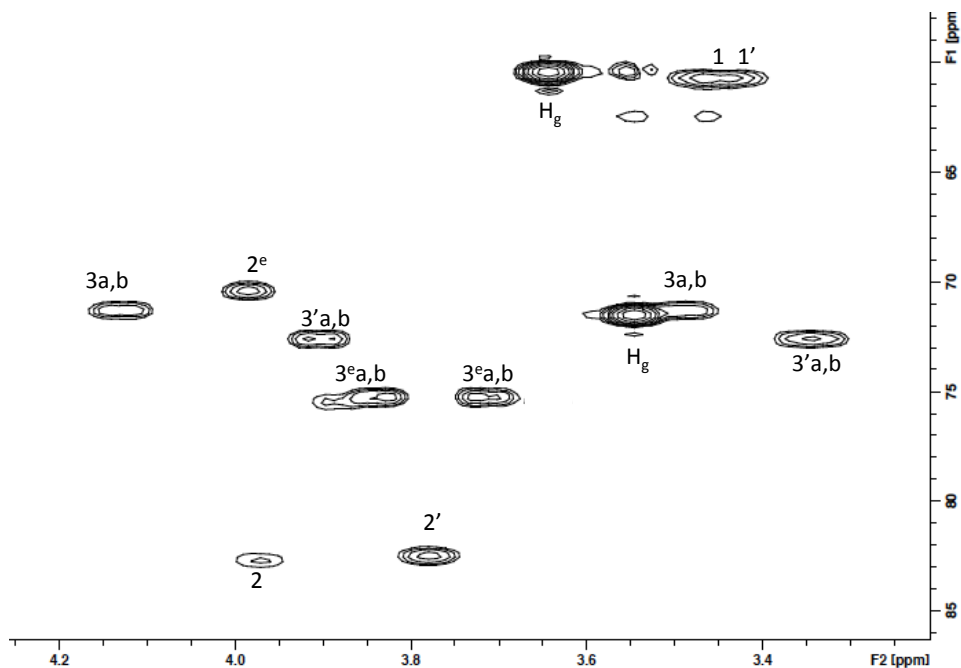


Figure 2.5 Continued.

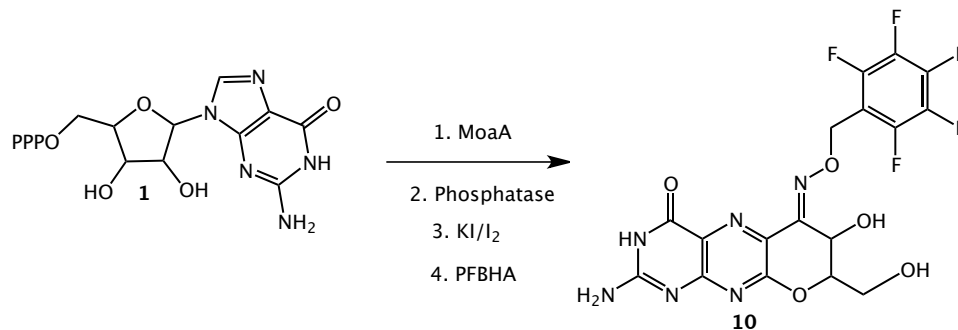
The UV-Visible spectrum of the purified product shows the characteristic features of a pterin (Figure 2.5).^{42,43} Multiple small- scale MoaA reactions were run to give sufficient product for characterization by LCMS and NMR spectroscopy (Figure 2.5).⁴¹

2.3.3 *o*-(pentafluorobenzyl) hydroxylamine (PFBHA) derivatization of the reaction product

The oxidized reaction mixture prepared as described above was treated with *o*-(pentafluorobenzyl) hydroxylamine (PFBHA) and analyzed for oxime formation by LCMS. Figure 2.6 shows the extracted ion chromatograms for 475.1Da which

corresponds to the $[M+H]^+$ for the E and Z isomers of compound **(10)**. These were absent in controls where MoaA, GTP, AdoMet or dithionite is absent.

(A)



(B)

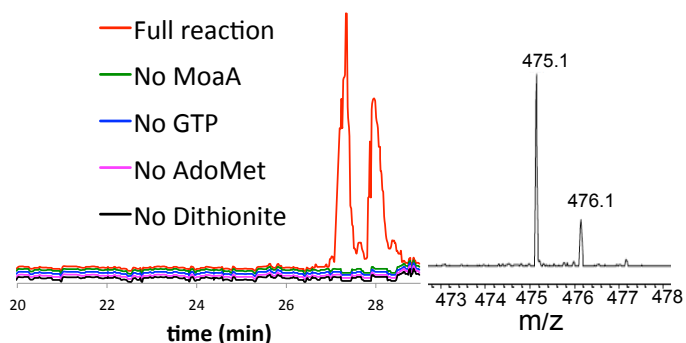


Figure 2.6: Trapping of the ketone-containing MoaA reaction product by oxime formation. A) The MoaA reaction mixture was treated with phosphatase, oxidized with KI/I₂ and converted to the oxime with PFBHA. B) Extracted ion chromatogram of the reaction mixture at 475.1Da showing two peaks consistent with a mixture of the E and Z isomers of oxime **(19)** ($[M+H]^+$ of 22(E+Z) = 475.1Da).

Figure 2.6 (B) is the extracted ion chromatogram of the reaction mixture at 475.1 Da showing two peaks consistent with a mixture of the E and Z isomers of oxime **(10)**,

Figure 2.6A) ($[M+H]^+$ of 22(E+Z) = 475.1Da). This is consistent with pterin (**20**) as the product of MoaA reactions with GTP.⁴¹

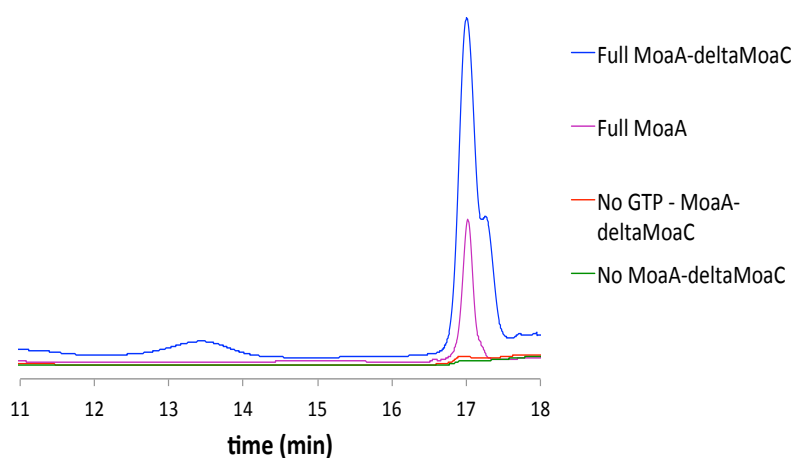
2.3.4 Reconstitution of MoaA purified from *E. coli* (MoaC⁻) strain

Meanwhile, a study from Kenichi Yokoyama's lab suggested that (**14**) was the product of MoaA⁴⁴. In order to exclude the possibility of MoaC contamination in our MoaA samples that result in the formation of the pterin, we over-expressed MoaA in a MoaC deletion mutant of *E. coli*. The MoaA reaction product isolated from this strain had an identical retention time (Figure 2.7) to the product described in Figure 2.5A. This product structure was also confirmed by derivatization with hydroxylamine and LCMS analysis (Figure 2.7).

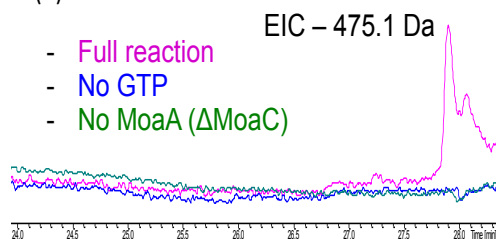
This provided the first conclusive evidence that pterin (**20**) was the product of MoaA. Thus, we demonstrated that the MoaA catalysis involves a remarkable rearrangement reaction where the C8 of GTP is inserted between the C2' and C3' carbon atoms of GTP to give the final pterin (**20**).

This confirms (Figure 2.7) the assignment of pterin as the product of MoaA reaction. These studies established that MoaA catalyzes the remarkable carbon insertion reaction where GTP is converted to pterin. The next aspect of this study was to mechanistically investigate this reaction.⁴¹

(A)



(B)



(C)

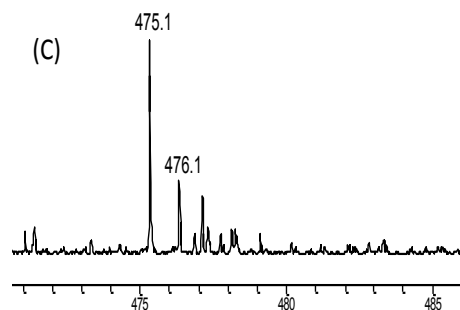


Figure 2.7: Trapping of the ketone-containing MoaA (MoaC⁻) reaction product. (A) HPLC chromatogram of the MoaA reactions carried out using MoaA isolated from a MoaC⁻ overexpression strain (Fluorescence: Excitation – 365nm, Emission – 450nm). Pink trace: Chromatogram of the reaction mixture generated using MoaA over-expressed and purified from *E. coli* BL21(DE3). Blue trace: HPLC analysis of the reaction mixture generated using MoaA over-expressed and purified from *E. coli* - MoaC⁻ subjected to λ DE3 lysogenation. The shoulder is a column artifact. Red and green are controls where either GTP or MoaA are absent. (B) Trapping of pterin **7**, formed using MoaA isolated from the MoaC⁻ overexpression strain, with PFBHA. Extracted ion chromatogram for 475.1 Da indicating a unique signal in the full reaction for the trapped pterin (**10**) (B) [M+H]⁺ for the trapped product consistent with structure **10**.

2.3.5 5'-dA (6) formation in the MoaA/ deuterated GTP isotopomers

reactions

In order to obtain mechanistic insights regarding the MoaA catalyzed rearrangement reaction catalyzed by MoaA we wanted to identify the initial site of hydrogen abstraction on GTP (**1**) by the 5'-dA radical (**6**).

Several (Table 2.1) site specifically deuterium labeled GMP isotopomers were synthesized and converted to GTP *in situ* using guanylate kinase, nucleoside diphosphate kinase and ATP/Mg²⁺. Deuterium transfer from labeled GTP to the 5'-dA was monitored by LCMS (Figure 2.8).

A.

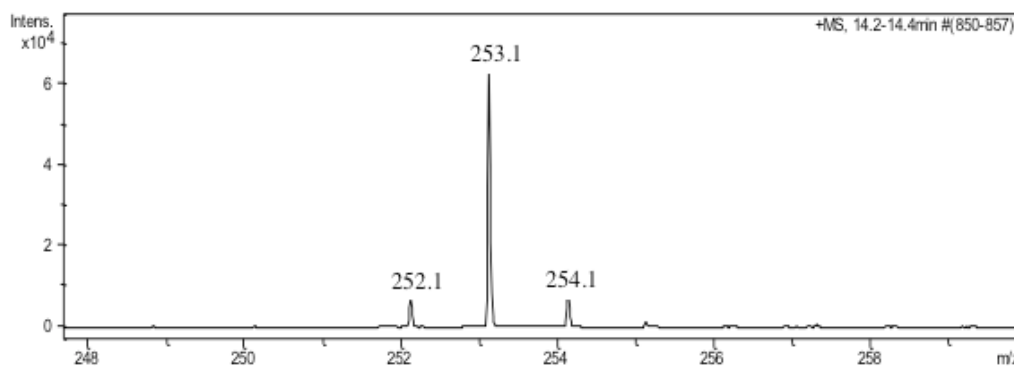
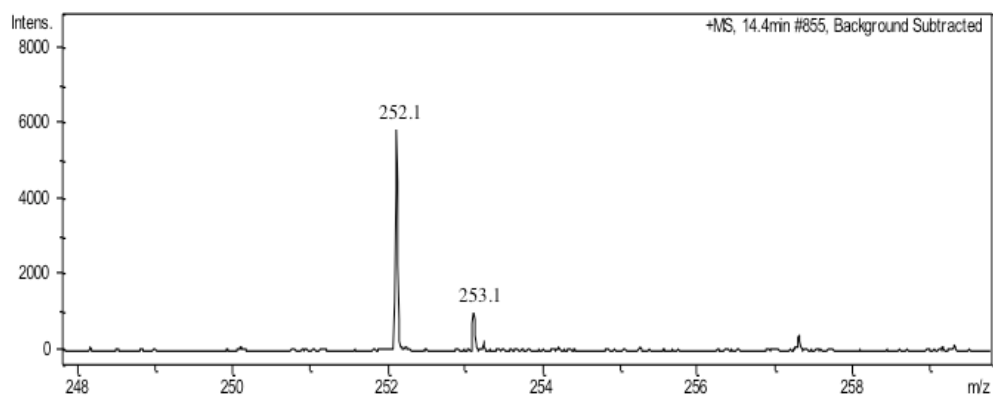
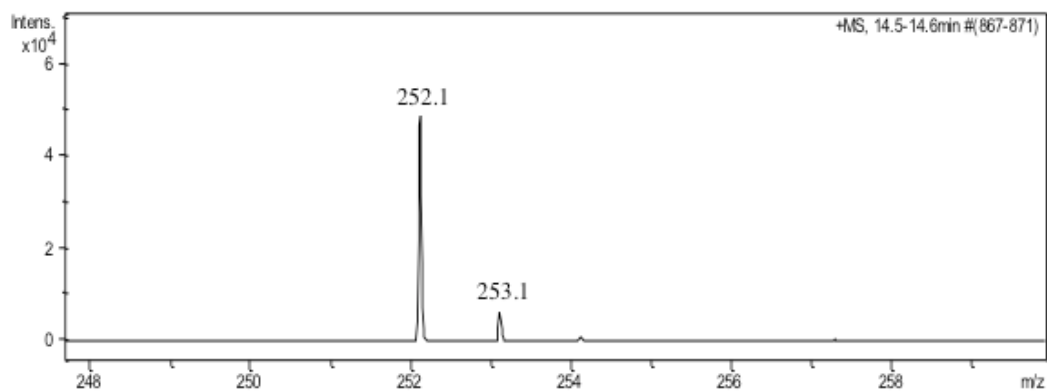


Figure 2.8: Mass spectrometry data for 5'-dA formation with GTP isotopomers. (A) MoaA assays with 3',4',5',5'-²H₄-GTP (B) MoaA assays with 8'-²H₄-GTP (C) MoaA assays with 2'-²H₄-GTP (D) MoaA assays with U-²H₁₀-GTP (universally deuteriated) (E) MoaA assays with 3'-²H₄-GTP

B.



C.



D.

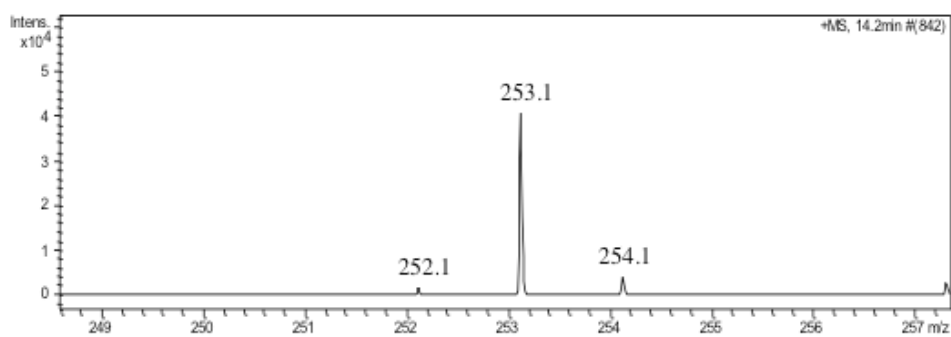


Figure 2.8 Continued.

E.

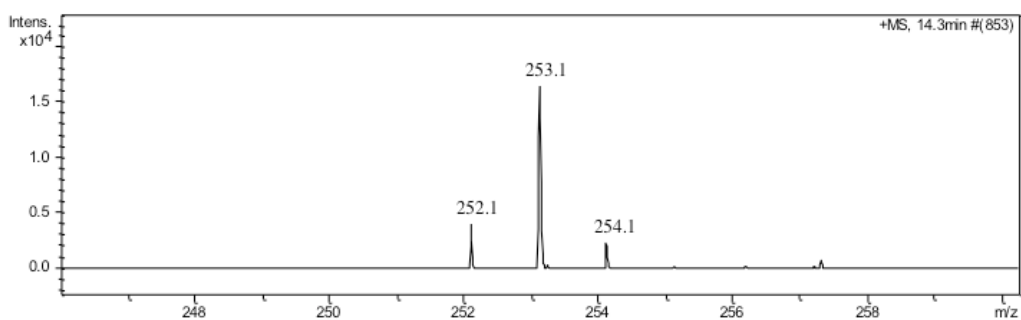


Figure 2.8 Continued.

Table 2.1: 5'-dA (**6**) formed in the MoaA reactions with several site-specifically deuterated GTP isotopomers.

Deuterated analogs of GTP	LCMS – [M+H] ⁺ for 5'-deoxyadenosine
U- ² H ₁₀ -GTP	253.1
3',4',5',5'- ² H ₄ -GTP	253.1
2'- ² H -GTP	252.1
8'- ² H -GTP	252.1
3'- ² H -GTP	253.1

Analysis of the 5'-dA generated using universally labeled GTP (i.e. deuterium on all non-exchangeable sites) revealed an increase of a single mass unit ([M+H] - 253.1Da) demonstrating that only one of the deuterium atoms was incorporated into 5'-dA (Table2.1). No deuterium incorporation was observed with 8'-²H-GTP demonstrating

that the deuterium was derived from the ribose. No deuterium incorporation was observed with 2'-²H-GTP and a single deuterium incorporation was observed with 3',4',5',5'-²H₄-GTP, further localizing the site of deuterium incorporation to C3', C4' or C5' of the ribose. Final localization of the hydrogen atom transferred was achieved by demonstrating a single deuterium transfer from 3'-²H-GTP to 5'-dA.³⁸

2.3.6 Mechanistic proposal for MoaA catalyzed reaction

The deuterium labeling studies described above, revealed the site of initial hydrogen atom abstraction by 5'dA radical. Based on these studies and the previous carbon labeling studies we advanced the first mechanistic proposal for the MoaA catalyzed reaction (Figure 2.9).³⁸

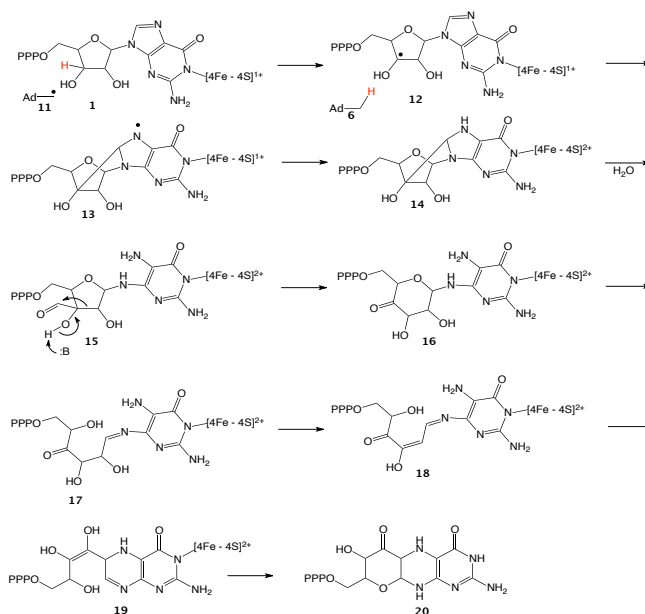


Figure 2.9: Mechanistic proposal for MoaA catalyzed reaction.³⁸

In this proposal, the 5'-dA radical **11**, generated by reductive cleavage of S-Adenosyl methionine (AdoMet), abstracts the 3' hydrogen atom from GTP to give **12**, which then undergoes cyclization to give **13**. Reduction of this radical by the purine liganded iron sulfur cluster to **14** followed by hydrolysis to **15** and a benzilic like rearrangement to **16** completes the insertion of the purine carbon into the ribose. Ring opening of **17** followed by dehydration of **18** and a conjugate addition gives **19**. Cyclization to **19** followed by a final tautomerization completes the formation of the reaction product **20**³. While ribose and deoxyribose radicals have been extensively studied in the context of enzymes such as ribonucleotide reductase and DNA damage by radiation or radical-generating antibiotics, addition of a C3' centered radical to C8 of a purine has never been reported^{5,6,7}. The successful trapping of an analog of **15** would provide a critical test of the proposed mechanism.

2.3.7 MoaA reactions with 2',3'-dideoxyGTP – LCMS analysis⁴⁵

The successful trapping of an analog of **14** would provide a critical test of the proposed mechanism. It can be seen from the above mechanistic proposal that the hydroxyl groups at the 2' and 3' positions of GTP may play an important role in the conversion of GTP to pterin. With the goal to trap an early step intermediate, we decided to test 2',3'-dideoxyGTP **21** as a substrate for MoaA reactions. MoaA reactions with 2',3'-dideoxyGTP were analyzed by LCMS as shown in Figure 2.10

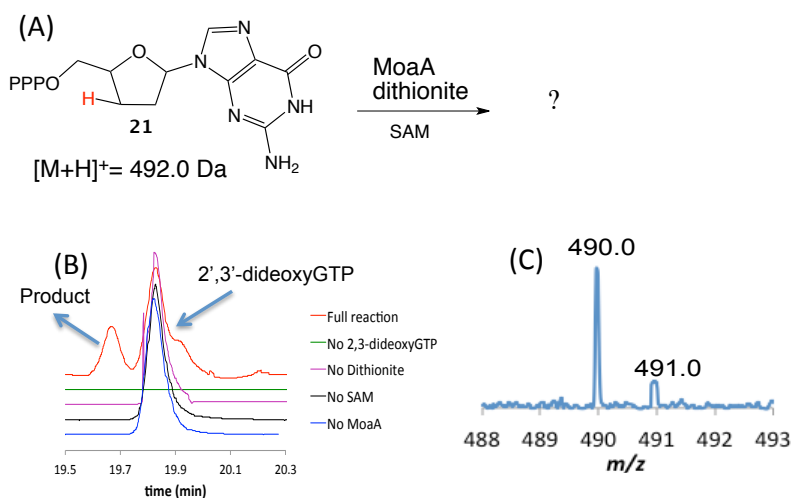


Figure 2.10: Analysis of the product formed when 2',3'-dideoxyGTP **21** is treated with MoaA. A) LC analysis of the MoaA reaction mixture and controls. Red trace is the full reaction where all the components are present. Green, pink, black and blue traces are for reaction mixtures where either 2',3'-dideoxyGTP, dithionite, SAM or MoaA is absent respectively. The unidentified signal at 19.9 min has the same $[M+H]^+$ as 2',3'-dideoxyGTP. B) MS of the compound eluting at 19.6 min. The $[M+H]^+$ is 490.0 Da - two Da less than the $[M+H]^+$ of the substrate **21**.

LCMS analysis of the MoaA/2',3'-dideoxyGTP **21** reaction mixture

demonstrated the formation of a new product eluting at 19.6 min (Figure 2.10). ESI-MS (positive mode) analysis of this product demonstrated that its mass $[M+H]^+$ was 490.0 Da - two Da less than the $[M+H]^+$ of the substrate. We considered two possible structures for this product (**23** and **27**, Figure 2.11). To test for the formation of **23**, the enzymatic product was dephosphorylated by phosphatase treatment and compared by LCMS to an authentic synthesized sample of **24**.

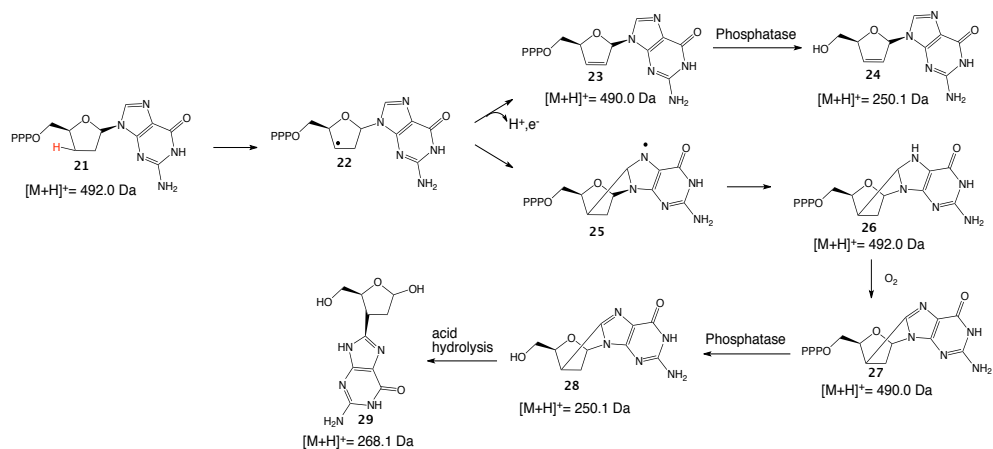


Figure 2.11: Mechanistic analysis to suggest possible products formed from 2',3'-dideoxyGTP (**21**).

2.3.8 MoaA reactions with 2',3'-dideoxyGTP – product characterization⁴⁵

Figures 2.12A-C demonstrate that the retention time of **24** and its MS/MS spectrum are different from the enzymatic product. The MS/MS spectrum of **17** showed fragmentation of the N-glycosyl bond to form guanine (152.0 Da, Figure 2.12). This fragmentation was not detected for the dephosphorylated enzymatic product (Figure 2.12) suggesting an additional bond between the sugar and the base consistent with **28**. This excludes the possibility that MoaA catalyzes the formation of **23** from **21**.

Unfortunately, NMR characterization of the enzymatic product (Figure 2.12) was not possible. Only small quantities were formed because 2',3'-dideoxyGTP **21** is a poor substrate (there is no evidence for enzyme modification by MS analysis). An identification strategy, involving comparison with a reference compound, was therefore adopted. If **26** is the product structure, oxidation and dephosphorylation, followed by N-glycosyl bond cleavage would give **29** which can be synthesized as a reference.

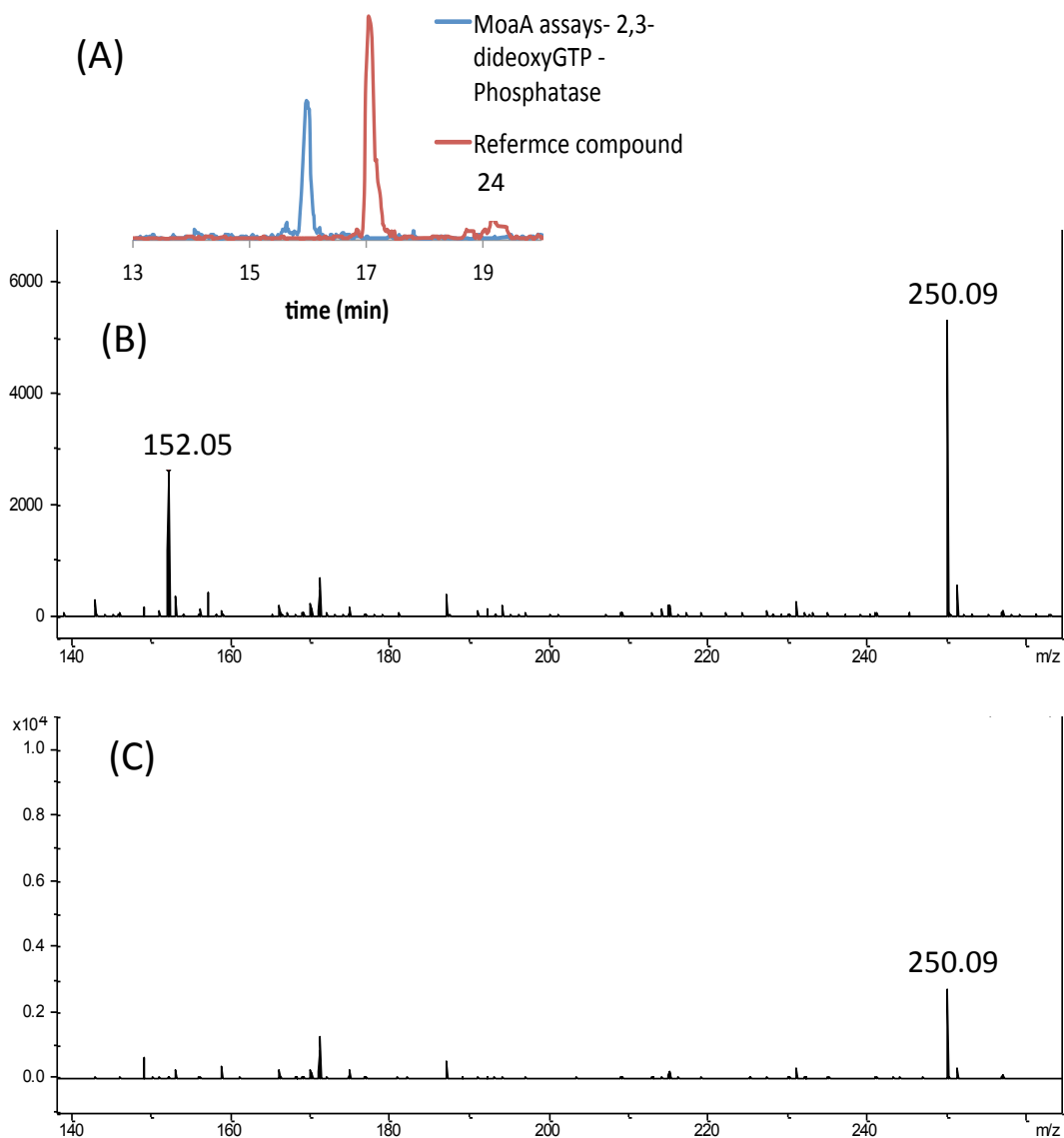


Figure 2.12: MoaA reactions with 2',3'-dideoxyGTP - product comparison with reference standard (**24**). (A) Product comparison with reference standard **24**. Extracted Ion Chromatograms for $[M+H]^+ = 250.0\text{Da}$ demonstrate that compound **24** is different from the dephosphorylated enzymatic product. (B) MS/MS of the synthetic reference standard for compound **24**. (C) MS/MS of the dephosphorylated enzymatic product.

To test this, the enzymatic product was derivatized by treating the MoaA reaction mixture with phosphatase followed by acid at 65°C for 2 hrs. The extracted ion chromatograms for 268.1Da ($\mathbf{29} + \text{H}^+ + \text{H}_2\text{O}$) are shown in Figure 2.13 and demonstrate that the acid treatment generates isomers of the product as expected from ring opening of the hemiacetal. The derivatized enzymatic product coelutes with the synthetic reference, (also generates isomers on acid treatment) and is identical by LCMS analysis. Thus, the enzymatic reaction of 2',3'-dideoxy-GTP, $\mathbf{21}$ supports the formation of the remarkable reaction intermediate $\mathbf{14}$ in the MoaA-catalyzed reaction.

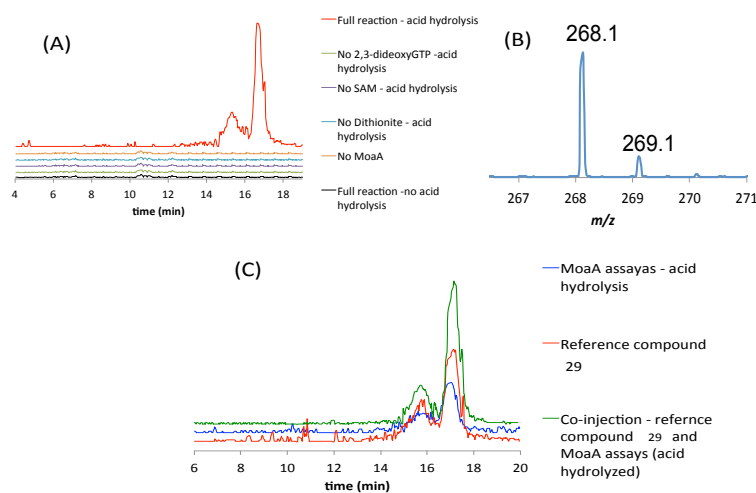


Figure 2.13: MoaA reactions with 2',3'-dideoxyGTP – hydrolyzed product comparison with reference standard ($\mathbf{29}$). A) Extracted Ion Chromatograms for $[\text{M}+\text{H}]^+ = 268.1$ Da demonstrate that the $[\text{M}+\text{H}]^+ = 268.1$ Da signal is seen only in reaction mixtures with all the components present after phosphatase treatment and acid hydrolysis. The two compounds with $[\text{M}+\text{H}]^+ = 268.1$ Da are most likely a consequence of hemiacetal isomerization during the acid hydrolysis. B) MS of the compound formed by acid hydrolysis of the dephosphorylated enzymatic product ($[\text{M}+\text{H}]^+ = 268.1$ Da). C) Extracted Ion Chromatograms for $[\text{M}+\text{H}]^+ = 268.1$ Da demonstrate that the derivatized enzymatic product has the same mass and co-elutes with compound $\mathbf{29}$.

A mechanistic proposal for the formation of **29/30**, is described in Figure 2.14. The 5'-dA radical **11** abstracts the 3' hydrogen atom from 2',3'-dideoxyGTP **21**, to give **22**, which then undergoes cyclization to give **25**. Reduction of this radical by the purine liganded iron sulfur cluster gives **26** which on aerobic oxidation results in the formation of **27**. Phosphatase treatment of **27** followed by acid hydrolysis gives **29/30** as a mixture of isomers.

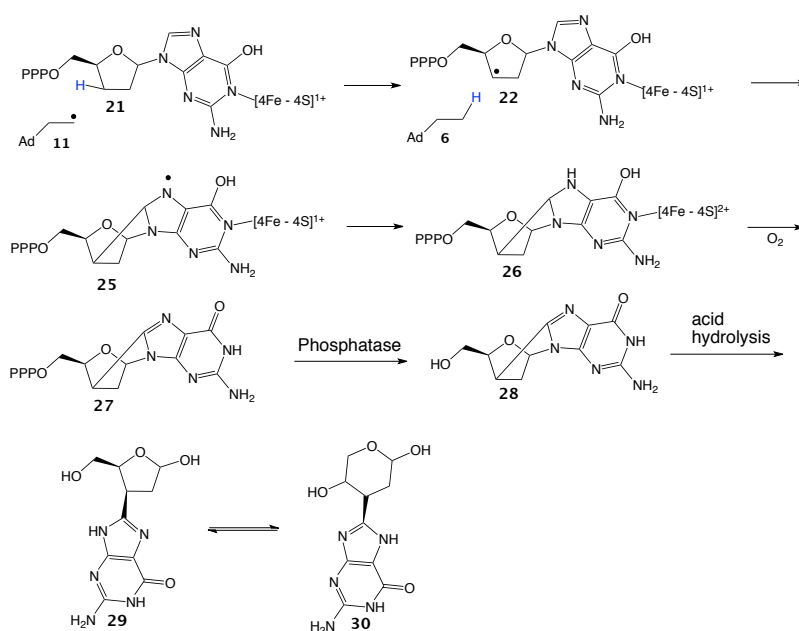


Figure 2.14: Mechanistic proposal for the product formed in the MoaA catalyzed reaction with 2',3'-dideoxyGTP and subsequent derivatization.

2.3.9 MoaA reactions 2'-chloroGTP – HPLC and LCMS analysis⁴¹

We next explored the use of 2'-chloroGTP (**31**) to trap radical (**12**, Figure 2.9). This strategy was previously developed to study the radical intermediates formed by ribonucleotide reductase, DNA irradiation, and by radical-generating antibiotics.⁴⁶⁻⁴⁸

LCMS and HPLC analysis of the MoaA/2'-chloroGTP reaction mixture

demonstrated the formation of a new compound eluting at 3 minutes and identified as guanine (**32**) by comparison with an authentic standard (Figure 2.15). Pterin was not detected in the reaction mixture.

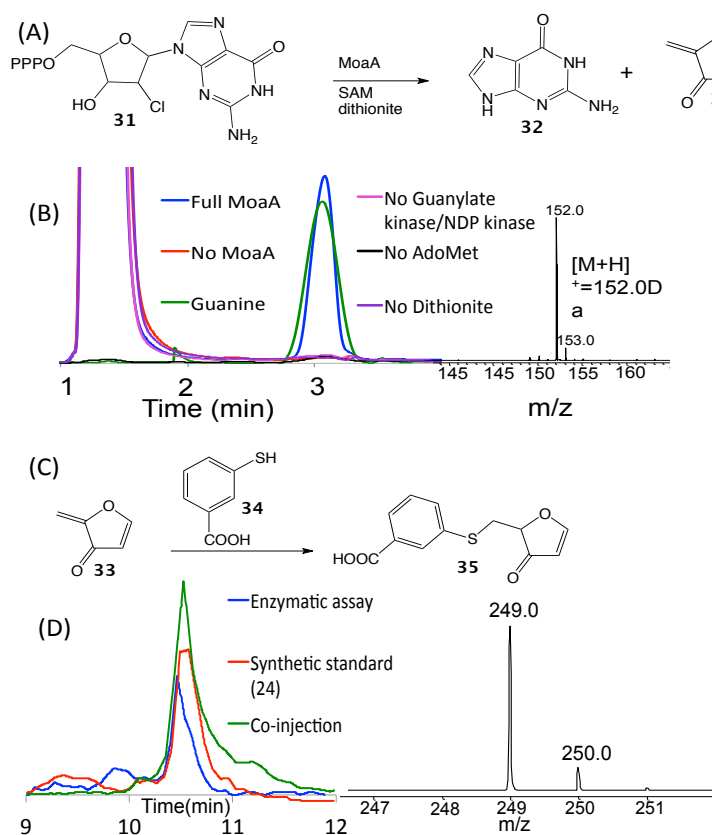


Figure 2.15: MoaA reactions with 2'-chloroGTP – product characterization. (A) The MoaA-catalyzed reaction of 2'-chloroGTP (**31**) results in the formation of guanine (**32**) and furanone (**33**). (B) LCMS traces to confirm the formation of guanine as one of the product. (C) Analysis of the MoaA-catalyzed reaction of 2'-chloroGTP (**31**) for the ribose derived product. The reaction mixture was treated with phosphatase followed by 3-mercaptobenzoic acid to yield (**35**). (D) The chromatograms are extracted ion chromatogram – 249.0 Da corresponding to the [M-H]⁻ of (**35**). Co-injection shows that that the 3-mercaptobenzoic acid derivative of the enzymatic product is identical to (**35**) by LCMS analysis.

The ribose-derived product (**33**) was trapped by treating the reaction mixture with 3'-mercaptobenzoic acid. The extracted ion chromatogram for $[M-H]^- = 249.0$ Da corresponded to the $[M-H]^-$ of compound (**35**), the expected trapped product. An authentic standard of compound (**35**) was synthesized (Figure 2.15) and found to be identical by LCMS analysis to the trapped product.

A mechanistic proposal for this reaction is shown in Figure 2.16. We also tested the 2'-chloroGTP isomer where the 2'-chloro was in the S orientation as a substrate analog. No reaction was observed.

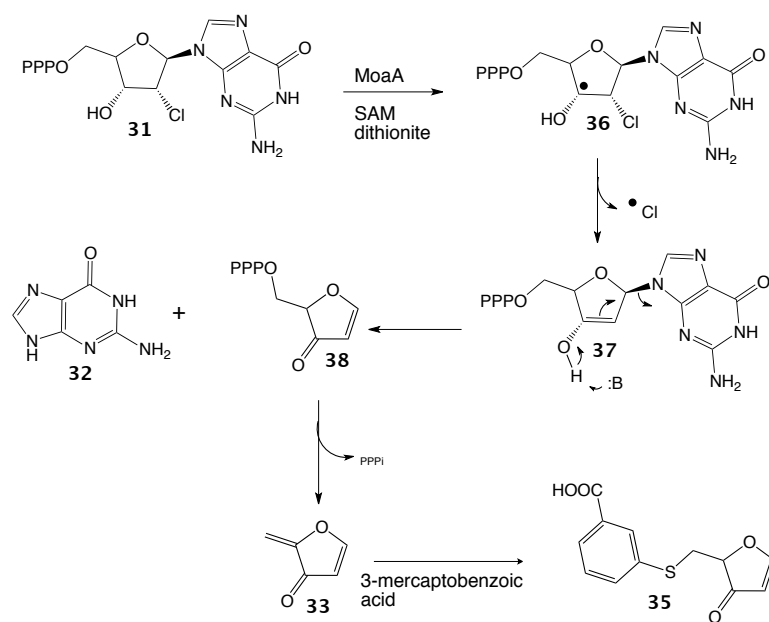


Figure 2.16: Mechanism of the MoeA-catalyzed reaction of 2'-chloroGTP (**31**).

2.3.10 MoaA reactions with 2'-deoxyGTP – LCMS analysis⁴¹

Next, we wanted to investigate the conversion of **15** to **16**, which involves the carbon insertion step. There are two possible mechanistic proposals for this step as shown in the Figure 2.17.

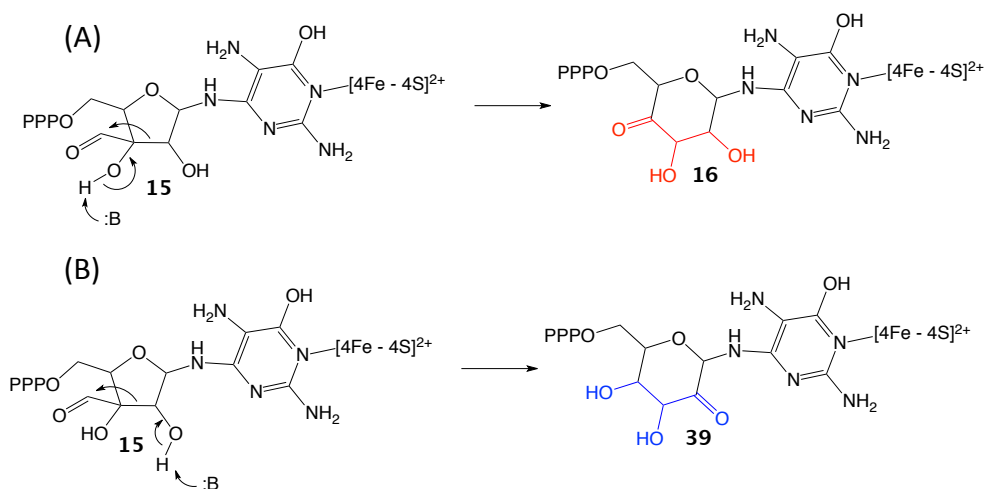


Figure 2.17: The two possible mechanistic proposals for the carbon insertion step. (A) involves the hydroxyl group at 3' position and (B) involves the hydroxyl group at 2' position.

We decided to explore the use of 2'-deoxyGTP (**42b**) to probe the later steps of the reaction. The proposal in Figure 2.9 suggests that this compound might block the conversion of (**14**) to (**20**) and that any trapped species would elucidate the later steps in the MoaA-catalyzed reaction.

MoaA reactions with 2'-deoxyGTP were set up. The enzymatic reaction mixture was treated with alkaline phosphatase and analyzed by HPLC. In order to collect sufficient product, multiple reactions were run. A fluorescent product was observed at

excitation wavelength of 365nm and an emission wavelength of 450nm. The UV-Vis spectrum of the compound was similar to that of a pterin.^{42,43} Oxidation with KI/I₂ was not necessary to stabilize this reaction product. LCMS analysis revealed an [M+H]⁺ = 268.1 Da. The UV-Vis spectrum and LCMS experiments suggested that structures **(40)** or **(41)** with undetermined stereochemistry at the site of initial hydrogen atom abstraction. To resolve this, we synthesized both isomers and compared them with the enzymatic product by HPLC. This analysis demonstrated that the reaction product has the stereochemistry shown in **(40)** (Figure 2.18).

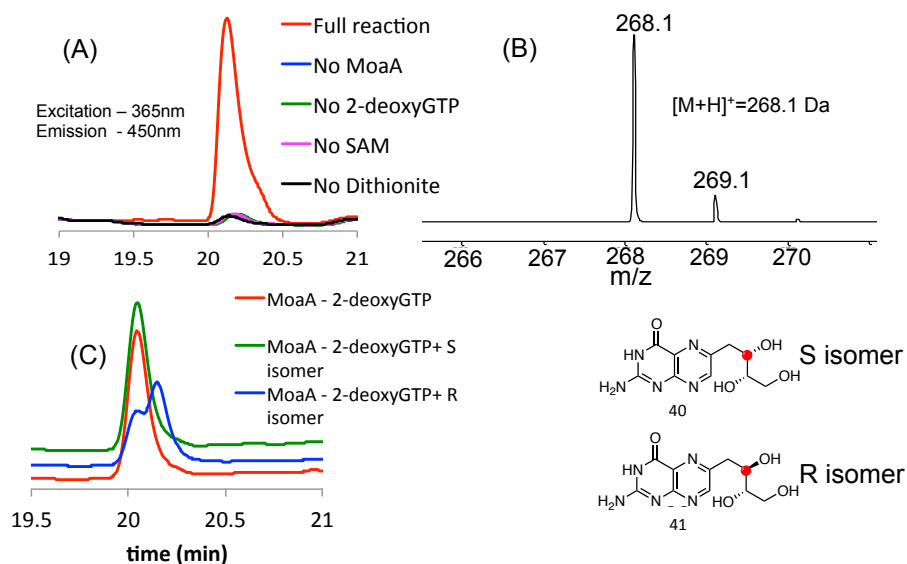


Figure 2.18: MoaA reactions with 2'-deoxyGTP (**42b**) – product characterization. (A) The HPLC chromatograms (Fluorescence – Excitation -365nm and emission – 450nm) show that a unique signal is seen only in the full reaction and not in the controls where either of MoaA, GTP, AdoMet or dithionite are absent. (B) [M+H]⁺ of the unique signal in the full reaction. (C) HPLC co-injection experiment to determine the stereochemistry at the purine derived carbon of the product.

The stereochemistry at C2 of the 2,3,4-trihydroxybutyl substituent is assumed to be the same as that in the starting 2'-deoxy-GTP because this center does not participate in the reaction (Figure 2.9). The S-stereochemistry at C3 (the site of initial hydrogen atom abstraction) was determined by HPLC comparison of the enzymatic product with synthetic standard (Figure 2.18C). This suggests that the formation of **(40)** is primarily or exclusively occurring at the MoaA active site because non-enzymatic chemistry would result in the scrambling of stereochemistry at C3 of the pterin substituent. The formation of **(40)** is not consistent with the proposed conversion of **(14)** to **(20)** shown in Figure 2.9. A revised mechanistic proposal for the MoaA-catalyzed reaction is outlined in Figure 2.19.

2.3.11 Revised mechanistic proposal for MoaA-catalyzed reaction⁴¹

When 2'-deoxyGTP (**42b**) is used as a substrate, we propose that **(47b)**, formed as shown in Figures 2.9 and Figure 2.19, undergoes ring opening, tautomerization (**50b**). Conjugate addition followed by a double tautomerization would give **(57)**. Loss of water and a final tautomerization would give the observed enzymatic product **(40)**. For the native MoaA-catalyzed reaction, using GTP as the substrate (**42a**, X=OH), hydrogen atom abstraction from C3' of GTP gives radical **(43a)** which then adds to C8 of the purine to give **(44a)**. Electron transfer from the purine liganded [4Fe-4S] cluster gives **(45a)**. Amino hydrolysis to **(46a)** followed by a benzylic-like rearrangement gives **(47a)**. Ring opening followed by tautomerization gives **(50a)**, which is converted to **(20)** by a conjugate addition, water elimination, tautomerization and a final ring closure.

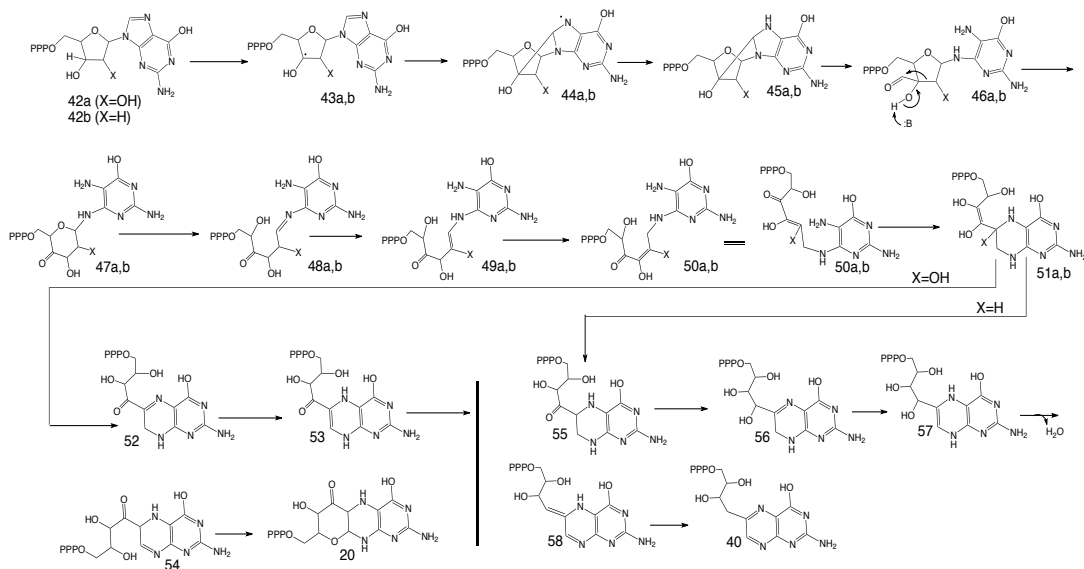


Figure 2.19: Revised mechanistic proposal for the MoaA-catalyzed reaction. MoaA –catalyzed conversion of GTP (**42a**) (also **1**) to (**20**) and 2'-deoxyGTP (**42b**) to (**40**).

This mechanism (Figure 2.19) is consistent with the regiochemistry of hydrogen atom abstraction by the 5'-deoxyadenosyl radical, with the trapping of (**14**) directly or using 2',3'-dideoxyGTP, the trapping of radical (**43a**) using 2'-Cl-GTP and the conversion of 2'-deoxyGTP to (**40**).

2.4 Conclusion

We reconstituted MoaA-catalyzed transformation. MoaA catalyzes the first step in molybdopterin biosynthesis where GTP is converted to pterin (**20**). This catalysis involves a remarkable rearrangement reaction where the C8 of guanosine-5'-triphosphate (GTP) is inserted between the C2' and C3' carbon atoms of GTP to give the final pterin. We characterized the reaction products and identification of the position of

hydrogen atom abstraction by 5'-deoxyadenosyl radical. Based on this we put forth the first mechanistic proposal for MoaA catalyzed reaction (Figure 2.9).

An independent study from Kenichi Yokoyama's lab suggested that **45a** was the product of MoaA. We expressed MoaA in *E. coli* (MoaC⁻) and showed that in our hands, pterin was the product of MoaA. We did not see any accumulation of **45a** in our assays.⁴¹ This provided the first conclusive evidence that pterin (**20**) was the product of MoaA. Thus, we demonstrated that MoaA catalysis involves a remarkable rearrangement reaction where the C8 of GTP is inserted between the C2' and C3' carbon atoms of GTP to give the final pterin (**20**).

We used 2',3'-dideoxyGTP as a substrate analog and trapped a novel intermediate (**27**). This intermediate provided critical evidence in support of our first mechanistic proposal. We further trapped the radical (**43a**, **also 12**) by using 2'-chloroGTP (**31**). We characterized the products of MoaA reaction with 2'-chloroGTP.

We decided to explore the use of 2'-deoxyGTP (**42b**) to probe the later steps of the reaction. MoaA reaction with 2'-deoxyGTP resulted in the formation of a stereospecific product (**40**). This suggested that the formation of (**40**) was primarily or exclusively occurring at the MoaA active site because non-enzymatic chemistry would result in the scrambling of stereochemistry at C3 of the pterin substituent. The formation of (**40**) was not consistent with the proposed conversion of (**14**) to (**20**) shown in Figure 2.9. This study clarified the later step of MoaA-catalyzed transformation. Based on this we revised our mechanistic proposal for the MoaA-catalyzed reaction (as outlined in Figure 2.19).

2.5 Experimental

2.5.1 Overexpression and purification of MoaA³⁸

The MoaA overexpression plasmid was previously described¹. MoaA was co-expressed in the presence of a plasmid encoding the *suf* operon for in vivo [4Fe-4S] reconstitution *E. coli* BL21 (DE3). An overnight 15 ml culture was grown in LB media in the presence of ampicillin and chloramphenicol. This was then added to 1.5 L of LB media containing ampicillin and chloramphenicol. The cultures were incubated at 37⁰C with shaking (180 rpm) until the OD₆₀₀ reached 0.45. The culture was then incubated at 4⁰C without shaking for 1.5 hrs. Then 200 mg of ferrous ammonium sulfate and 200 mg of cysteine were added. This was followed by induction of the culture with 100 μM IPTG. The culture was then incubated at 15⁰C with shaking (110 rpm) for 14 - 16hrs. The culture was then incubated at 4⁰C for 3 hrs without shaking. The cells were then harvested and stored in liquid nitrogen overnight before enzyme purification. For enzyme purification, the cell pellets were thawed at room temperature in an anaerobic chamber and suspended in lysis buffer (100 mM Tris-HCl, pH 7.5) in the presence of 2mM DTT, lysozyme (0.2 mg/ml) and benzonase (100 units). This mixture was then cooled in an ice-bath for 2 hrs. The suspension of cells was then sonicated and centrifuged to give the cell-free extract. The enzyme was then purified using standard Ni-NTA chromatography. The column was first incubated with the lysis buffer. The cell-free extract was then passed over the column, which was then washed with 5-6 column volumes of wash buffer (100 mM Tris-HCl, 300 mM NaCl, 20 mM imidazole, 2mM DTT, pH 7.5). The protein was then eluted using 100 mM Tris-HCl, 300 mM NaCl, 250

mM imidazole, 2 mM DTT, pH 7.5. The purified enzyme was buffer exchanged into 100 mM potassium phosphate, 30% glycerol, 2 mM DTT, pH 7.5 using a 10DG column and the purified enzyme was stored in liquid nitrogen.

2.5.2 Overexpression and purification of guanylate kinase⁴⁹

The guanylate kinase overexpression plasmid was transformed into *E. coli* BL21 (DE3). An overnight 15ml culture was grown in LB media in the presence of ampicillin. This was then added to 1.5L of LB media containing ampicillin. The cultures were incubated at 37⁰C with shaking (180 rpm) until the OD₆₀₀ reached 0.55. This was followed by induction of the culture with 100 μM IPTG at 15⁰C for 14hrs at 180rpm. The enzyme was purified on a blue sepharose column prepared in wash buffer (15 mM Tris-HCl, 1 mM EDTA, 1 mM DTT). The column was loaded with cell free extract, washed with wash buffer until the OD₂₈₀ was less than 0.02. The enzyme was then eluted with 15 mM Tris-HCl, 1 mM EDTA, 1 mM DTT, 5 mM GMP.

2.5.3 Enzymatic assays for MoaA reactions for LCMS characterization of 5'dA (6)³⁸

The enzymatic reaction mixtures contained MoaA (125 μM), GTP (1 mM), SAM (1.5 mM), and sodium dithionite (in excess) and were incubated at room temperature in an anaerobic chamber for 3 hrs. For HPLC and LCMS analysis the enzyme was removed by ultrafiltration using a 10kDa cut-off filter. The samples were then prepared in the anaerobic chamber and sealed before HPLC or LCMS analysis.

For a reaction mixture using a GMP isotopomer as substrate, guanylate kinase (20 μ M), NDP kinase (20 μ M), ATP (5 mM), MgCl₂ (2 mM), MoaA (125 μ M) and GMP (1 mM) were incubated at room temperature for 10 mins. SAM (1.5mM) and sodium dithionite (in excess) were then added and the reactions were run as described above.

2.5.4 Enzymatic assays for MoaA reactions for LCMS/NMR characterization of pterin (8)⁴¹

The reaction mixture consisted of 250 μ M MoaA, 2mM GTP, 3mM AdoMet and 10mM dithionite and was incubated in an anaerobic chamber for 5h at room temperature. The protein was then removed by ultrafiltration using a 10kDa cut-off filter. The resulting small molecule pool was treated with 3 μ l of alkaline phosphatases in the presence of 1mM MgCl₂, incubated in the anaerobic chamber for an additional 3h and quenched with 100 μ l of oxygen-free KI/I₂ (5% I₂ (w/v) and 10% KI (w/v) in water).³⁸⁻⁴⁰ The reaction was analyzed by LCMS. For NMR characterization, the reaction mixture was purified by HPLC. The fluorescent product eluting at 17min (Figure 2.5) was collected and dried using a vacuum centrifuge. Several such reaction mixtures were purified to yield sufficient product for NMR characterization. The dried samples were dissolved in 250 μ l of a 90%:10% H₂O/D₂O mixture and analyzed by NMR (Bruker, 500MHz).

MoaA reactions were also performed with MoaA over-expressed and purified from the *E. coli*-MoaC deletion strain. An identical fluorescent compound eluting at 17min was observed (Figure 2.7).

2.5.5 MoaA over-expressed and purified from *E. coli* (MoaC⁻)⁴¹

The *E. coli* - MoaC deletion strain was obtained from CGSC, Yale and rendered compatible with a pET vector using a λ DE3 lysogenation kit. MoaA was over-expressed in this strain and purified. Reaction with GTP yielded a product that was derivatized by treatment with alkaline phosphatase and KI/I₂. This fluorescent product was identical by HPLC analysis with the product produced by MoaA isolated from the MoaC⁺ strain (Figure 2.7).

2.5.6 PFBHA derivatization of the reaction product⁴¹

The reaction mixture consisted of 250 μ M MoaA, 2mM GTP, AdoMet and 10mM dithionite and was incubated in an anaerobic chamber for 5h. The protein was then removed by ultrafiltration using a 10kDa cut-off filter. The resulting small molecule pool was treated with 3 μ l of alkaline phosphatase in the presence of 1mM MgCl₂, incubated in the anaerobic chamber for an additional 3h and quenched with 100 μ l of oxygen free KI/I₂ (5% I₂ (w/v) and 10% KI (w/v) in water).³⁸⁻⁴⁰ PFBHA (100 μ l of 40mM) was then added, the mixture was heated at 65^oC for 1.5h and analyzed by LCMS. Control reactions, lacking MoaA, GTP, SAM or dithionite were also run and similarly analyzed.

2.5.7 Assay conditions for MoaA reactions with 2',3'-dideoxyGTP (21)⁴⁵

The enzymatic reaction mixtures contained MoaA (125 μ M), 2',3'-dideoxyGTP (1.8 mM), S-Adenosyl methionine (AdoMet) (2.7 mM), and sodium dithionite (10mM)

and were incubated at room temperature in an anaerobic chamber for 3 hrs. Controls were set up where either MoaA, AdoMet, dithionite or 2',3'-dideoxyGTP was missing. For HPLC and LCMS analysis the enzyme was removed by ultrafiltration using a 10kDa cut-off filter.

2.5.8 Phosphatase treatment of MoaA/2',3'-dideoxyGTP reaction mixtures⁴⁵

Calf intestinal phosphatase (CIP) was purchased from New England Biolabs. MoaA reactions were set up as described above. From the 200µl of the reaction mixtures, the enzyme was removed by ultrafiltration using a 10kDa cut-off filter. The reaction mixtures were stored aerobically for 2 hrs before CIP treatment. Then 5µl of 1M NaOH was added to each of the assays so that the pH of the reaction mixture was 7.5-8. 2µl of 1M MgCl₂ and 400 units of CIP were added. The reaction mixtures were incubated at 37°C for 3.5 hrs. CIP was removed by ultrafiltration using a 10 kDa cut-off filter.

2.5.9 Acid hydrolysis of phosphatase treated MoaA/2',3'-dideoxyGTP reaction mixtures⁴⁵

MoaA assays with 2',3'-dideoxyGTP were set up and dephosphorylated as described above. CIP was separated from the small molecule pool by using 10kDa cut off filters. 1M HCl was added to the above reaction mixture to make the final concentration of HCl to 0.5M. The reactions were incubated at 65°C for 2 hrs. The

reactions were then cooled to room temperature and then neutralized by NaOH. The neutralized assays were then analyzed by LCMS.

2.5.10 Assay conditions for MoaA reactions with 2'-chloroGTP (21) for guanine characterization⁴¹

2'-chloroGMP (3mM) was synthesized and phosphorylated using NDP kinase (100 units), guanylate kinase (50 μ M) and ATP (10mM). Guanylate kinase was over-expressed and purified as described earlier.³⁸ This crude reaction mixture was used as a source of 2'-chloroGTP. For the MoaA-catalyzed reaction, 250 μ M MoaA, 2mM 2'-chloroGTP, 3mM AdoMet and 10mM dithionite were mixed and incubated in the anaerobic chamber for 5h. Controls were set up for this reaction where either MoaA, AdoMet, dithionite or NDP kinase/Guanylate kinase were absent. The small molecule pool was analyzed by LCMS.

2.5.11 Assay conditions for MoaA reactions with 2'-chloroGTP (21) for trapping of ribose derived product⁴¹

For the trapping of the reactive 2'-Cl-ribose-derived product, all the above reactions were performed in DTT free buffer. 50 μ l of the small molecule pool were treated with 3 μ L of alkaline phosphatase followed by 3-mercaptobenzoic acid (50 μ l of 100mM solution) at 70⁰C for 1hr.

2.5.12 MoaA reactions with 2'-deoxyGTP (42b)⁴¹

MoaA (250 μ M), 2mM 2'-deoxyGTP, 3mM AdoMet and 10mM dithionite were mixed and incubated in the anaerobic chamber for 5h at room temperature. Controls were also set up in which MoaA, 2'-deoxyGTP, AdoMet or dithionite were absent. The protein was removed by ultrafiltration using a 10kDa cut-off filter. The small molecule pool was treated with 3 μ l of alkaline phosphatases in the presence of 1mM MgCl₂ and incubated in the anaerobic chamber for 3h. The reaction mixture was analyzed by LCMS and the product was purified by reverse phase HPLC. The isolated product was concentrated using a vacuum centrifuge. For the co-elution experiment 100 μ M stock solutions of compounds (40) and (41) were made. Standards (50 μ l) and 50 μ l of the concentrated product were mixed and analyzed by HPLC.

2.5.13 LCMS conditions for MoaA reactions for LCMS characterization of 5'dA (6)³⁸

LC-ESI-TOF-MS analysis was performed using an Agilent 1260 HPLC system equipped with a binary pump and autosampler and a 1200 diode array detector upstream of a MicroToF-Q II mass spectrometer (Bruker Daltonics, Billerica, MA) using the ESI source in positive ionization mode. LC conditions: A – 20mM *N,N*-dimethylhexylamine, 10mM ammonium acetate, pH 6.4 B – 75% methanol, 25% water
Column – Agilent Poroshell 120, EC-C18, 2.7 μ m, 3x10mm LC method: 0 min – 100% A, 5 mins – 100% A, 15 mins - 60% A 40% B, 27 mins – 10% A 90% B, 36min – 100% A. MS parameters: Capillary, -4500 V; Capillary offset, -500 V; Nebulizer gas, 3.0 bar;

Dry gas, 10.0 L/min; Dry gas temperature, 200°C; Funnel 1 RF, 200.0 Vpp; Funnel 2 RF, 250.0 Vpp; ISCID, 0.0 eV; Hexapole RF, 150 Vpp; Quadrupole, Ion energy, 5.0 eV; Low mass, 80 *m/z*; Collision cell, collision energy, 10.0 eV; Collision RF, 150.0 Vpp, Transfer time, 100.0 μ s; Prepulse storage, 5.0 μ s. Data was processed with DataAnalysis ver. 4.0 SP4 (Bruker Daltonics, Billerica, MA)

2.5.14 HPLC conditions for the purification of 5'-dA formed in the MoaA reactions³⁸

Agilent 1260 HPLC was used with a fraction collector for the purification of both 5'-dA and compound Z. LC-18-T column (3.0 x 150 mm, 3 μ m, Supelco) was used for the purification. Chromatography conditions were as follows: A: water B: 5mM ammonium formate pH 6.6 C: methanol. HPLC method: 0 min – 100%B, 4 mins- 10%A 90%B, 9 mins – 25%A 60%B 15%C, 14 min – 25%A 10%B 65%C, 17 mins – 100% B, 24 mins – 100%A.

2.5.15 LCMS characterization of the dephosphorylated product of MoaA reactions with GTP and hydroxylamine derivatized product (10)⁴¹

LC conditions: A – 5mM ammonium acetate, pH 6.7 B – 75% methanol, 25% water. Column – Agilent Poroshell 120, EC-C18, 2.7 μ m, 3x10mm LC method: 0 min – 100% A, 7 mins – 100% A, 15 mins - 80% A 20% B, 20 mins – 70%A 30%B, 26 mins – 0% A 100% B, 28 min – 0% A 100%B, 29 min – 100%A MS parameters: Capillary, -4500 V; Capillary offset, -500 V; Nebulizer gas, 3.0 bar; Dry gas, 10.0 L/min; Dry gas

temperature, 200°C; Funnel 1 RF, 200.0 Vpp; Funnel 2 RF, 250.0 Vpp; ISCID, 0.0 eV; Hexapole RF, 200 Vpp; Quadrupole, Ion energy, 5.0 eV; Low mass, 150 *m/z*; Collision cell, collision energy, 10.0 eV; Collision RF, 150.0 Vpp, Transfer time, 100.0 μ s; Prepulse storage, 5.0 μ s. Data was processed with DataAnalysis ver. 4.0 SP4 (Bruker Daltonics, Billerica, MA).

2.5.16 HPLC purification of the MoaA/GTP reaction product⁴¹

HPLC -1260 series Agilent. LC-18 column - ((Supelcosil SPLC-18 column (25cm x 10mm, 5 μ m)). Following gradient was used - A:water, B: 5mM ammonium formate, C: methanol. 0 min: 100%B, 7 min: 10%A 90%B, 12 min: 25%A 60%B 15%C, 17 min: 25%A 10%B 65%C, 19 min-29min: 100%B)

2.5.17 LCMS parameters for the product detection of MoaA reactions with 2',3'-dideoxyGTP⁴⁵

LC-ESI-TOF-MS analysis was performed using an Agilent 1260 HPLC system equipped with a binary pump and autosampler and a 1200 diode array detector upstream of a MicroToF-Q II mass spectrometer (Bruker Daltonics, Billerica, MA) using the ESI source in positive ionization mode. LC conditions: A – 20mM *N,N*-dimethylhexylamine, 10mM ammonium acetate, pH 6.4 B – 75% methanol, 25% water Column – Agilent Poroshell 120, EC-C18, 2.7 μ m, 3x10mm LC method: 0 min – 100% A, 5 mins – 100% A, 15 mins - 60% A 40% B, 27 mins – 10% A 90% B, 36min – 100% A. MS parameters are the same as those described in 2.4.13.

2.5.18 LCMS parameters for comparing the dephosphorylated, acid hydrolyzed product of MoaA with 2',3'-dideoxyGTP with reference standards⁴⁵

LC conditions: A – 5mM ammonium acetate, pH 6.7 B – 75% methanol, 25% water
Column – Agilent Poroshell 120, EC-C18, 2.7 μ m, 3x10mm LC method: 0 min – 100% A, 7 mins – 100% A, 15 mins - 80% A 20% B, 20 mins – 70%A 30%B, 26 mins – 0% A 100% B, 28 min – 0% A 100%B, 29 min – 100%A MS parameters: Capillary, -4500 V; Capillary offset, -500 V; Nebulizer gas, 3.0 bar; Dry gas, 10.0 L/min; Dry gas temperature, 200°C; Funnel 1 RF, 200.0 Vpp; Funnel 2 RF, 200.0 Vpp; ISCID, 0.0 eV; Hexapole RF, 200 Vpp; Quadrupole, Ion energy, 5.0 eV; Low mass, 100 *m/z*; Collision cell, collision energy, 10.0 eV; Collision RF, 150.0 Vpp, Transfer time, 100.0 μ s; Prepulse storage, 5.0 μ s. Data was processed with DataAnalysis ver. 4.0 SP4 (Bruker Daltonics, Billerica, MA).

2.5.19 LCMS conditions for MoaA assays with 2'-chloroGTP – detection of guanine⁴¹

Following gradient was used - A – 10mM N,N-dimethylhexylamine, pH 6.4 B – 75% methanol, 25% water, Column – Agilent Poroshell 120, EC-C18, 2.7 μ m, 3x10mm. 0 min – 100% A, 5 mins – 100% A, 15 mins - 60% A 40% B, 27 mins – 10% A 90% B, 36min – 100% A. MS parameters are the same as those described in 1.4.18.

2.5.20 LCMS conditions for MoaA assays with 2'-chloroGTP – detection of 3-mercaptobenzoic acid derivatized product

1200 series Agilent (binary pump) LC conditions were as follows: A – 5mM ammonium acetate, pH 6.7, B – 75% methanol, 25% water. Reverse phase column – Supelcosil LC18, 3µm, 3x10mm. The gradient was as follows: 0 min – 100% A, 7 mins – 100% A, 15 mins - 80% A 20% B, 20 mins – 70%A 30%B, 26 mins – 0% A 100% B, 28 min – 0% A 100%B, 29 min – 100%A MS parameters are the same as those described in 1.4.18.

2.5.21 LC conditions for MoaA assays with 2'-deoxyGTP – product isolation and co-elution experiment⁴¹

HPLC (Supelcosil SPLC-18 column (25cm x 10mm, 5µm)). Conditions were as follows: A: water, B: 5mM ammonium formate, C: methanol. 0 min : 100%B, 7min : 10%A 90%B, 12 min: 25%A 60%B 15%C, 17min : 25%A 10%A 65%B, 19min-29min: 100%B. The LCMS conditions are the same as those described in 1.4.18.

2.5.22 Synthesis scheme for guanosine-5'-monophosphate (65)

The synthetic scheme for GMP is shown in Figure 2.20.

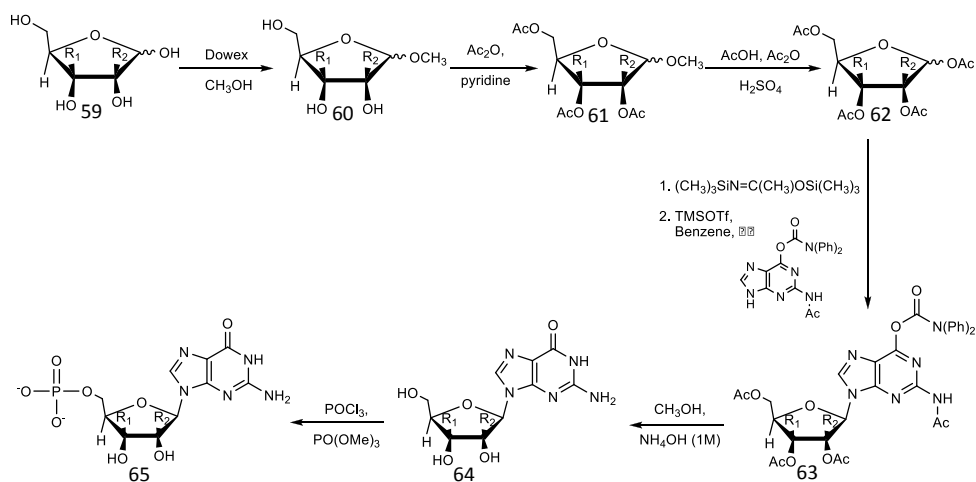


Figure 2.20: Synthetic scheme for GMP (65).

2.5.23 Synthesis of $[2\text{-}^2\text{H}]$ and $[2\text{-}^2\text{H}]$ 1,2,3,5-tetra-O-acetylribofuranoside

(62)

Dowex $8 \times 50\text{W}$, 200–400, H^+ cation-exchange resin (300 mg) was washed with anhydrous methanol and then stirred for 4.5 h at room temperature with ribose (260 mg, 1.72 mmol) in anhydrous methanol (6 mL). Reaction was monitored by TLC (CHCl_3 : MeOH , 85:15) for completion. The resin was removed by filtration and washed with anhydrous methanol. The combined filtrate and washings were evaporated to give 1-O-methyl-ribofuranoside which was dissolved in anhydrous pyridine (5 mL) and cold in ice bath then treated with acetic anhydride (0.5 mL, 564 mg, 5.48 mmol) and stirred at room temperature for 4 h. The reaction mixture was cooled (ice-bath), diluted with water

(25 mL) and the resultant aqueous solution was extracted with chloroform (4×25 mL). The combined organic extracts were washed with water (4×50 mL), dried and then co-evaporated with toluene to give 1-O-methyl-2,3,5-tri-O-acetyl-ribofuranoside which was subjected to next reaction without further purification. A cooled (ice-bath) solution of 1-O-methyl-2,3,5-tri-O-acetyl-ribofuranoside (403 mg, 1.39 mmol) and acetic anhydride (1.4 mL, 1.56 g, 15.16 mmol) in glacial acetic acid (10 mL) was treated drop-wise with conc. sulfuric acid (0.2 mL) and then stirred at room temperature for 3 h. The reaction mixture was cooled (ice-bath) and ice (10 g) was added with continued stirring. When the ice had melted, the resultant aqueous solution was extracted with chloroform (4×25 mL). The combined organic extracts were washed successively with water (2×50 mL), a saturated aqueous solution of sodium bicarbonate (2×50 mL) and water (50 mL), then dried and evaporated to give 1,2,3,5-tetra-O-acetyl-ribofuranoside (355 mg, 80%) as a virtually colorless oil which solidified after standing at room temperature. [2-²H] tetraacetyl ribofuranose: ¹H NMR (CDCl₃) δ 6.41 (d, 0.3, H1 α), 6.15 (s, 0.7, H1 β), 5.3 (d, 0.7, H3 β), 5.2 (d, 0.3, H3 α), 4.1–4.5 (m, 3, H4, H5, H5') 2.10 (s, 3, CH₃CO), 2.07 (s, 3, CH₃CO), 2.06 (s, 3, CH₃CO), 2.04 (s, 3, CH₃CO). [3-2H] tetraacetyl ribofuranose: ¹H NMR (CDCl₃) δ 6.41 (d, 0.3, H1 α), 6.15 (s, 0.7, H1 β), 5.2–5.3 (m, 1, H2), 4.1–4.5 (m, 3, H4, H5, H5'), 2.10 (s, 3, CH₃CO), 2.08 (s, 3, CH₃CO), 2.06 (s, 3, CH₃CO), 2.04 (s, 3, CH₃CO).

2.5.24 Synthesis of 2-acetylamino-2',3',5' –tri-O-acetyl-6-O-(N,N-diphenylcarbamoyle)-guanosine (63)

2-acetylamino-6-O-diphenylcarbamoyleguanine (220 mg, 0.63 mmol) was suspended in 1,2-dichloroethane (6.5 ml) under nitrogen and treated with N,O-bis-(trimethylsilyl)-acetamide (0.32 ml). The mixture was heated to 80°C and stirred for 15 min when some of the suspension dissolved. The solvents were removed in *vacuo*. The residue was suspended in dry benzene (3 ml) under nitrogen and fresh trimethylsilyltrifluoromethanesulfonate (150 μ L) was added. 1,2,3,5-tetra-O-acetyl-D-ribofuranose (200 mg, 0.62 mmol) dissolved dry benzene (3 ml) was added to the mixture which was heated to 80°C for 1 h. The solution was diluted with ethyl acetate, washed with water and brine and dried (MgSO₄). The solvent was removed in *vacuo* to yield a yellow foam, which was absorbed onto silica gel and purified by column chromatography on silica gel using hexanes : ethyl acetate (1:1) as eluent. This procedure was followed to get both the [2-²H] labeled and [3-²H] labeled compounds.

2.5.25 Synthesis of guanosine (64)

2-acetylamino-2',3',5'-tri-O-acetyl-6-O-(N,N-diphenylcarbamoyle)-guanine (180 mg, 0.28 mmol) was dissolved in methanol (3 ml). 1N aqueous ammonium hydroxide was added until turbidity. After stirring overnight at 4°C, the solvents were removed in *vacuo* and the residue was recrystallised from water as an off-white solid. This procedure was followed to get both the [2-²H] labeled and [3-²H] labeled.

2.5.26 Synthesis of guanosine-5'-monophosphate (65, GMP)

A suspension of guanosine (50 mg, 0.177 mmol) in TEP, trimethylphosphate, (0.6 mL) was heated at 50°C for 15 min and then cooled to 0°C. Water (1.59 uL, 0.0885 mmol) was added followed by POCl₃ (33uL, 0.354 mmol) at 0°C, and the entire mixture was further stirred at 0°C for 1.5 h. The mixture was poured into ice-water (1 mL) and stirred for another hour before it neutralized by ammonium bicarbonate solution. The reaction mixture was lyophilized to give white product which then purified by Prep HPLC using a SPLC-18DB column (10 x 250 mm, 5 μ, Supelco) at a flow rate of 2 mL/min using an Agilent 100 HPLC system with quaternary pump and manual injector. This procedure was followed to get both the [2-²H] labeled and [3-²H] labeled guanosine

2.5.27 HPLC conditions for purification of GMP isotopomers

Agilent 1260 HPLC was used with a fraction collector for the purification of both 5'-dA and compound Z. LC-18-T column (3.0 x 150 mm, 3 μm, Supelco) was used for the purification. Chromatography conditions were as follows: A: water B: 5mM ammonium formate pH 6.6 C: methanol 0 min – 100%B, 7 mins- 10%A 90%B, 12 mins – 25%A 60%B 15%C, 17 min – 25%A 10%B 65%C, 19 mins – 100% B, 30 mins – 100%A.

2.5.28 Synthesis of [8-²H] guanosine-5'-monophosphate ³⁸

8-²H- GMP was synthesized by H/D exchange with D₂O. GMP was heated at 80⁰C in D₂O and the completion of the reaction was monitored by NMR. Dr. Sameh H. Abdelwahed synthesized 2'-²H-GMP and 3'-²H-GMP.

2.5.29 Synthetic scheme for 2',3'-anhydro-2',3'-dideoxyguanosine (24)

The synthetic scheme for 24 is shown in Figure 2.21.

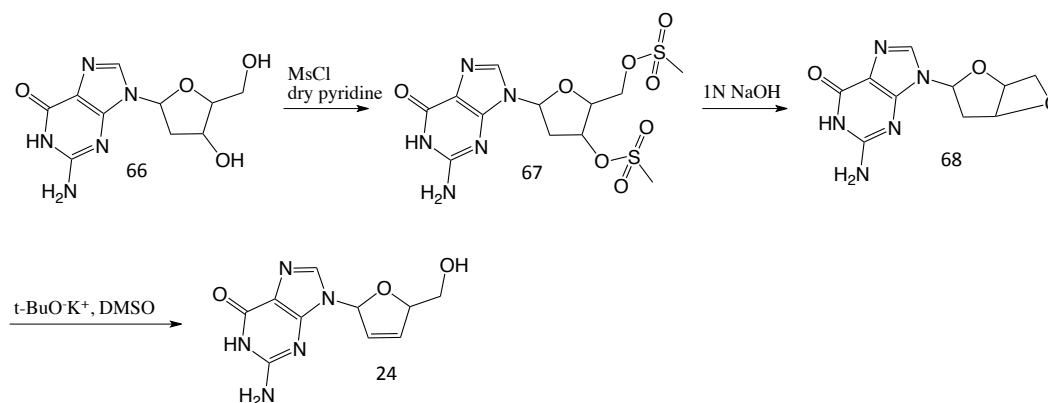


Figure 2.21: Synthetic scheme for 2',3'-anhydro-2',3'-dideoxyguanosine (24).

2.5.30 Synthesis of 2',3'-anhydro-2',3'-dideoxyguanosine (24)

Methanesulfonyl chloride (550 μ L, 7.1 mmol) was added dropwise to a solution of 600mg. (2.2 mmol) of 2'-deoxyguanosine (66) in 10 ml. of dry pyridine which, had been chilled previously to - 10⁰C. After 3 hrs at 0⁰C, the reaction mixture was treated with 5ml. of water and the solution poured slowly with vigorous stirring into ice-water. The mesylated compound precipitates out. This solid was dried and used for the next

step. A solution of 320mg. (0.75 mmoles) of **31** in 15 ml. of water containing 2.2 ml. of 1.055 M sodium hydroxide was refluxed for 2 hrs. The cooled solution was neutralized with acetic acid and evaporated to dryness. The dry residue was further purified by silica gel flash chromatography. The compound **68** was analyzed by NMR and ESI-MS. ¹H NMR (300 MHz, CD₃OD): 2.8 (m, H-2', H-2'), 2.7, 3.2 (s, CH₃-OMs), 4.3 (m, H-5'), 4.86 (m, H-4'), 5.6 (m, H-3'), 6.4 (t, H-1'), 7.9 (s, H-8).

Conversion of compound **68** to 2',3'-anhydro-2',3'-dideoxyguanosine **24**:

Purified compound **31** (40mg, 0.16mmoles) was added to 1ml of DMSO containing 22mg (0.196 mmoles) of *t*-BuOK in 2 ml. of DMSO was added to the above mixture. The mixture was stirred at 25°C for 2 hrs and then neutralized with a dilute solution of acetic acid and evaporated to dryness.

The product **24** was then extracted with chloroform, purified by silica gel flash chromatography (CH₃Cl:MeOH – 10:1) and analyzed by NMR and ESI-MS. ¹H NMR (300 MHz, CD₃OD): 4.2, 4.3 (d, H-5'), 6.1 (d, H-1'), 6.3 (m, H-2'), 6.4 (m, H-3'), 7.8 (s, H-8). The 4'-H predicted under water signal⁵.

2.5.31 Synthetic scheme for 2-amino-8-((3S)-5-hydroxy-2-(hydroxymethyl)tetrahydrofuran-3-yl)-9H-purin-6-ol (**29**)⁴⁵

The synthetic scheme for **29** is shown in Figure 2.22. This reference standard (**29**) was synthesized by Dr. Sameh H. Abdelwahed.

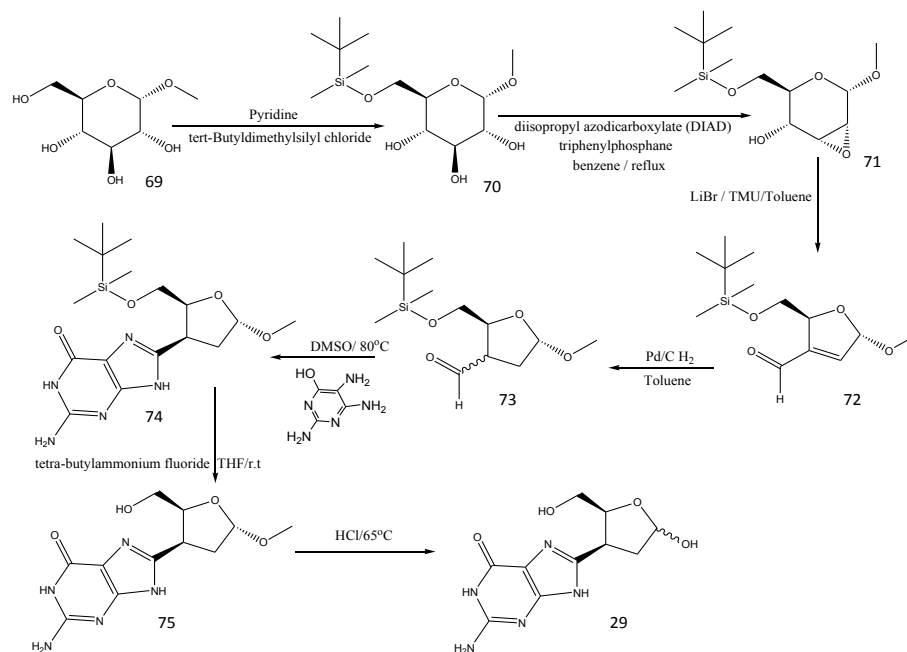


Figure 2.22: Synthetic scheme for 2-amino-8-((3S)-5-hydroxy-2-(hydroxymethyl)tetrahydrofuran-3-yl)-9H-purin-6-ol (**29**).

2.5.32 Synthesis of methyl-6-O-(*tert*-butyldimethylsilyl)- α -D-glucopyranoside (**70**)

To a stirred solution of commercially available methyl- α -D-glucopyranoside (**69**) (5 g, 25.74 mmol) in 40 ml of dry pyridine was slowly added *tert*-butyldimethylsilyl chloride (3.88, 25.74 mmol) and the mixture was kept for overnight at room temperature.

After removal of the solvent under reduced pressure, the residue was taken up in ethyl acetate and extracted with 0.5 M HCl, saturated aqueous NaHCO₃ and brine. The aqueous layers were re-extracted twice with ethyl acetate and the combined organic layers were dried over MgSO₄. After evaporation of the solvent and drying of the product in vacuo, the residue was purified by flash column chromatography (hexane/ethyl acetate, 3:1) yielding the silylether 24 (5.1 g, 65%) as a white solid, ¹H NMR (300 MHz, CD₃OD): 0.05 (s, 6H), 0.91 (s, 9H), 3.29 (m, 2H), 3.38 (s, 3H), 3.49 (m, 1H), 3.60 (m, 1H), 3.75 (m, 1H), 3.87 (m, 1H), 4.63 (d, J = 3.7 Hz, 1H)

2.5.33 Synthesis of methyl-2,3-anhydro-6-O-(tert-butyldimethylsilyl)- α -D-allopyranoside (71)

Compound **70** (4.0 g, 12.98 mmol) and triphenylphosphine (4.25 g, 16.21 mmol) were dissolved in 80 ml of benzene (dried using sodium metal). Diisopropyl azodicarboxylate (2.8 ml, 14.27 mmol) was added dropwise over a period of 30 min at room temperature. The mixture was stirred for 1 hr at room temperature and then refluxed for 4 hrs. After washing with 0.5 N HCl and with brine, the aqueous layers were twice re-extracted with ethyl acetate and the combined organic layers were dried over MgSO₄. After filtration and removal of the solvents under reduced pressure, the residue was purified by flash column chromatography (hexane/ethyl acetate, 3:1) yielding 3.1 g **71** (83%) ¹H NMR (300 MHz, CDCl₃): 0.01 (s, 6H), 0.85 (s, 9H), 3.44 (s, 3H), 3.47 (m, 1H), 3.50 (m, 1H), 3.60 (m, 1H), 3.72 (m, 1H), 3.86 (m, 2H), 3.93 (d, J = 8.7, 1H).

2.5.34 Synthesis of (2S,5S)-2-(*tert*-butyldimethyl silanyloxymethyl)-5-methoxy-2,5-dihydrofuran-3- carbaldehyde (72)

A mixture of lithium bromide (3.8 g, 44.5 mmol) and tetramethylurea (4.5 ml) in 160 ml of toluene was refluxed in a Dean-Stark apparatus while a solution of the epoxide **71** (3.0 g, 10.34 mmol) in 90 ml of toluene was added dropwise over 3 hrs. The reaction mixture was then refluxed for another 1 hr. After removal of the solvents under reduced pressure, hexane (50 ml) was added and the crude reaction mixture was filtered through a plug of celite. The filtrate was concentrated under reduced pressure and purified by flash column chromatography (hexane/ethyl acetate, 3:1) yielding 2.1 g (75%) of aldehyde **72**. ¹H NMR (300 MHz, CDCl₃): -0.03 (s, 3H), 0.01 (s, 3H), 0.80 (s, 9H), 3.41 (s, 3H), 3.86 (m, 2H), 5.12 (m, 1H), 5.89 (d, J = 4.3 Hz, 1H), 6.66 (d, J = 1.8 Hz, 1H), 9.85 (s, 1H).

2.5.35 Synthesis of (2S,3R/S, 5S)-2-(*tert*-butyldimethyl silanyloxymethyl)- 5-methoxytetrahydrofuran-3- carbaldehyde (73)

(2S,5S)-2-(*tert*-butyldimethylsilanyloxymethyl)-5-methoxy-2,5-dihydrofuran-3-carbaldehyde (**72**, 2.1 gm) was dissolved in toluene (100 ml) and hydrogenated (H₂, Pd/C, 100 mg, 10%) after 30 min the solvent was filtered through a plug of celite and evaporated, the residue was chromatographed on silica-gel (hexane/ ethyl acetate, 3:1) to yield a quantitative amount 0.7:1.0 mixture of S/R epimers of the corresponding aldehyde **73**. ¹H NMR (300 MHz, CD₃OD): 0.03 (4s, 6H), 0.83 (2s, 9H), 2.22 (m, 1H), 2.3 (m, 1H), 2.82 (m, 1H), 3.29, 3.33 (2s, 3H), 3.59-3.83 (m, 3H), 5.04, 4.92 (m, 1H),

9.62, 9.71 (2d, 1H). The R and the S isomers were distinguished from each other by NOESY. The NMR signals for the R and the S isomers were as follows: R-isomer ¹H NMR (400 MHz, CDCl₃): -0.01 (s, 3H), -0.007 (s, 3H), 0.81 (s, 9H), 1.92 (dd, J_{AB} = 13.3 Hz, J = 8.5 Hz, 1H), 2.33 (ddd, J_{AB} = 13.3 Hz, J = 8.1 Hz, 5.0 Hz, 1H), 3.2 (m, 1H), 3.27 (s, 3H), 3.72 (m, 2H), 4.38 (ddd, J = 8.6 Hz, 4.7 Hz, 3.4 Hz, 1H), 5.07 (d, J = 5.0 Hz, 2.15 Hz, 1H). S-isomer ¹H NMR (400 MHz, CDCl₃): 0.006 (s, 3H), 0.01 (s, 3H), 0.83 (s, 9H), 2.16 (m, 2H), 2.8 (m, 1H), 3.22 (s, 3H), 3.67 (m, 2H), 4.32 (q, J = 4.3 Hz, 1H), 4.98 (dd, J = 3.8 Hz, 1.9 Hz, 1H). The characteristic feature of the two isomers is the proton signal at C4 of compound **73**. In case of the R isomer, the NMR signals for the protons on C4 are separated from each other by 0.5 ppm. In case of S isomer these signals overlap. This feature will be useful while assigning the stereochemistry of compound **75**.

2.5.36 Synthesis of 2-amino-8-((2S, 3R/S, 5S)-2-(*tert*-butyldimethylsilyloxy)methyl)-5-methoxytetrahydrofuran-3-yl)-9H-purin-6-ol (74**)**

2,5,6-triaminopyrimidin-4-ol (110 mg, 0.78 mmol) was dissolved in DMSO (1.5 ml). A solution of **73** (180 mg, 0.66 mmol) in 0.5 ml of DMSO was added dropwise over 3 min. and the reaction mixture was heated to 80°C for 4 hrs. After evaporation of the solvent and drying of the product in vacuo, the residue was chromatographed on silica-gel (hexane/ ethyl acetate, 1:1) to yield 155 mg (60%) of **74** as a white solid, which was used in the next reaction without further purification.

2.5.37 Synthesis of 2-amino-8-((2S, 3S,5S)-2-(hydroxymethyl)-5-methoxytetrahydrofuran-3-yl)-9H-purin-6-ol (75)

Compound **74** (100 mg, 0.25 mmol) was dissolved in dry tetrahydrofuran (5 ml). Tetrabutylammonium fluoride (1.0 M in THF, 0.5 ml) was added to this solution at room temperature. After 10 min, TLC analysis indicated that the reaction was complete. The solvent was removed under reduced pressure and the product was dried in vacuo, the residue was chromatographed on silica-gel (hexane/ ethyl acetate, 1:1) to give the corresponding purine 54 mg (76%). ¹H NMR (300 MHz, D₂O): 2.31 (m, 1H), 2.72 (m, 1H), 2.75 (m, 1H), 3.49 (2s, 3H), 3.86 (m, 2H), 4.52 (m, 1H), 5.41(m, 1H). The NMR signals for protons at C4 are separated by around 0.5 ppm. This is similar to the R isomer of compound **73**. By this analogy we confirm the stereochemistry at C3 of compound **75**.

2.5.38 Synthesis of 2-amino-8-((3S)-5-hydroxy-2-(hydroxymethyl)tetrahydrofuran-3-yl)-9H-purin-6-ol (29)

10 mg of compound **29** was dissolved in 0.5N HCl and heated to 65°C for 2 hrs. The solvent was removed under reduced pressure and the product was dried in vacuum to give a mixture of isomers of compound **22** (compounds 22a, 22b, 22c, 22d). ¹H NMR (400 MHz, D₂O): 1.9-2.5 (m, H-4), 3.5- 4.2 (m, H-1, H-2, H-3), 4.86, 5.4, 5.57 (m, H-5). The acid deprotection reaction generates isomers of the product **29**. One set of isomers could be the α and β isomers at C5. The other isomer could be the pyranose from of compound **29** (compound 30 shown in Figure 2.14). The enzymatic N-glycosyl bond

hydrolysis reaction for conversion of compound **28** to compound **29** (shown in Figure 2.14) is carried out under identical conditions mentioned above. These synthesized set of isomers co-elute with the enzymatically-generated products during LCMS analysis.

2.5.39 Synthetic scheme for 2'-chloroGMP (**81**)⁴¹

The synthetic scheme for (**81**) is shown in Figure 2.23. Dr. Sameh H. Abdelwahed synthesized (**81**).

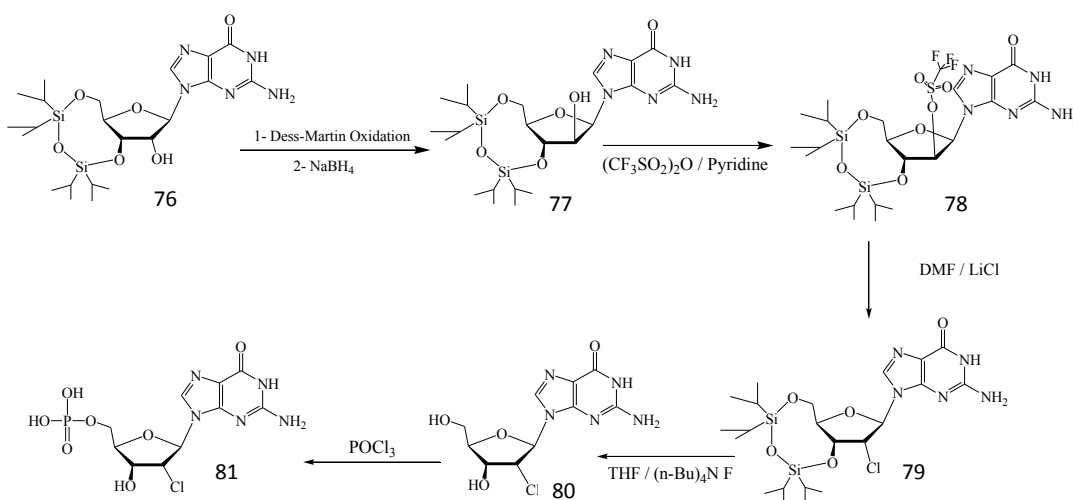


Figure 2.23: Synthetic scheme for 2'-chloroGMP (**81**)

2.5.40 Synthesis of 9-(3',5'-O-(1,1',3,3'-tetraisopropylidisiloxane-1,3-diyl)-β-D-arabinofuranosyl) guanine (77)

Treatment of 0.44 g (0.80 mmol) of 3',5'-O-(1,1',3,3'-tetraisopropylidisiloxane-1,3-diyl)-α-D-guanosine (76) with 2.3 equiv of Dess-Martin periodinane reagent, gave 0.4 g of a yellow glass whose ¹H NMR spectrum (DMSO-*d*₆) indicated formation of the 2'-ketoguanosine derivative plus its hydrate. Reduction of this material with sodium borohydride afforded 9-(3',5'-O-(1,1',3,3'-tetraisopropylidisiloxane-1,3-diyl) arabinofuranosyl)guanine which was purified by flash column chromatography (chloroform/methanol 5%). Yield 0.3 g (68%). ¹H NMR (DMSO-*d*₆) ppm 10.6 (s, NH amide), 7.7 (s, H8), 6.5 (s, NH₂), 5.95 (d, H1'), 5.82 (d, OH), 4.35 (t, H2'), 4.25 (m, H3'), 4.1 (d, H4'), 3.95 (dd, H5' and H5''), 1.00 [m, Si-CH(CH₃)₂ and CH₃]. ESI MS of 77: calculated for C₂₂H₃₉N₅O₆Si₂ 525.2, observed 526.2 m/z ([M+H]⁺).

2.5.41 Synthesis of 9-(3',5'-O-(1,1',3,3'-tetraisopropylidisiloxane-1,3-diyl)-2'-O-[(trifluoromethyl)sulfonyl] arabinofuranosyl)guanine (78)

A solution of 77 (0.27 g, 0.52 mmol) and 4-(dimethylamino)pyridine (0.13 g, 1.5 mmol) in pyridine (0.4 mL, 4.6 mmol)-dichloromethane (10 mL) was cooled to 0 °C (1 h) and treated with trifluoromethanesulfonic anhydride (0.13 mL, 0.77 mmol). The mixture was stirred at 0 °C for 5 min and then at room temperature for 3 h and finally partitioned between dichloromethane (10 mL) and water (10 mL). The organic layer was washed with water (2 x 20 mL), brine (2 x 20 mL) and finally dried over magnesium sulfate. Flash column chromatography (Hexane /ethylacetate 15%) yielded 78: 0.2 g

(60%). ¹H NMR (CDCl₃) ppm 11.9 (s, NH amide), 7.8 (s, H8), 6.15 (bs, NH₂), 6.15 (d, H1'), 5.3 (t, H2'), 4.82 (m, H3'), 3.9-4.1(m, H4', H5' and H5''), 1.00 [m, Si-CH(CH₃)₂ and CH₃]. ESI MS of **78**: calculated for C₂₃H₃₈F₃N₅O₈SSi₂ 657.2, observed 658.2 m/z ([M+H]⁺).

2.5.42 Synthesis of 3',5'-O-(1,1',3,3'-tetraisopropylidisiloxane-1,3-diyl)-2'-chloro-2'-deoxy-β-D-guanosine (79)

The trifluoromethanesulfonate **54** (0.2 g, 0.3 mmol) and lithium chloride (0.13 g, 0.3 mmol) were dissolved in 10 mL of dimethylformamide (DMF) and the solution was stirred at 50°C for 30 min, then cooled to room temperature and stirred overnight at room temperature. The reaction was monitored by TLC in chloroform/methanol (10:1). After removal of the solvent under reduced pressure, the residue was taken up in ethylacetate and washed with water. The aqueous phase were re-extracted twice with ethylacetate and the combined organic phase was dried over magnesium sulfate. After evaporation of the solvent and drying of the product under vacuum, the residue was purified by flash column chromatography (Hexane/ethylacetate 15%) yielding **79**: 0.1 g (60%). ¹H NMR (CDCl₃) ppm 11.9 (bs, NH amide), 7.8 (s, H8), 6.3 (bs, NH₂), 6.12 (s, H1'), 4.65 (m, H3' and H4'), 4.1-4.25 (m, H2', H5' and H5''), 1.10 [m, Si-CH(CH₃)₂ and CH₃]. ESI MS of **79**: calculated for C₂₂H₃₈ClN₅O₅Si₂ 543.2, observed 544.2m/z ([M+H]⁺)

2.5.43 Synthesis of 2'-chloro-2'-anhydroguanosine (80)

Deprotection of the bifunctional silyl group: a 1 molar solution of tetra-n-butylammonium fluoride (2eq) was added to a solution of **79** in tetrahydrofuran (THF) at room temperature and the deprotection reaction was followed by TLC (CHCl₃: MeOH, 5:1). The reaction was almost completed within 10 min. The reaction mixture was then concentrated under reduced pressure and the residue was purified by flash column chromatography (chloroform/methanol 5%). ¹H NMR (MeOD, *d*₄) ppm 8.02 (s, H8), 6.13 (d, H1'), 4.91 (m, H3'), 4.43 (m, H4'), 4.2 (m, H2'), 3.8 (m, H5' and H5'').

2.5.44 Synthesis of 2'-chloro-2'-anhydroguanosine-5'-monophosphate (81)

A suspension of 2'-chloro-2'-deoxyguanosine, **56** (50 mg, 0.177 mmol) in trimethylphosphate, (0.6 mL) was heated at 50°C for 15 min and then cooled to 0°C. Water (1.6 μL, 0.09 mmol) was added followed by POCl₃ (33 μL, 0.35 mmol) at 0°C, and the entire mixture was further stirred at 0°C for 1.5 h. The mixture was poured into ice-water (1 mL) and stirred for another hour before it was neutralized with ammonium bicarbonate solution. The reaction mixture was lyophilized to give white product which was then purified by Prep HPLC using a SPLC-18DB column (10 x 250 mm, 5 μ, Supelco) at a flow rate of 2 mL/min using an Agilent 100 HPLC system with a quaternary pump and manual injector. ¹H NMR (D₂O) ppm 8.1 (s, H8), 6.25 (s, H1'), 4.55 (m, H3' and H4'), 4.3 (m, H2'), 4.0 (m, H5' and H5'').

2.5.45 Synthetic scheme for 5-(3-mercaptopbenzoic acid)-3-furanone (**35**)⁴¹

The synthetic scheme for (**35**) is shown in Figure 2.24. This reference standard (**35**) was synthesized by Dr. Sameh H. Abdelwahed.

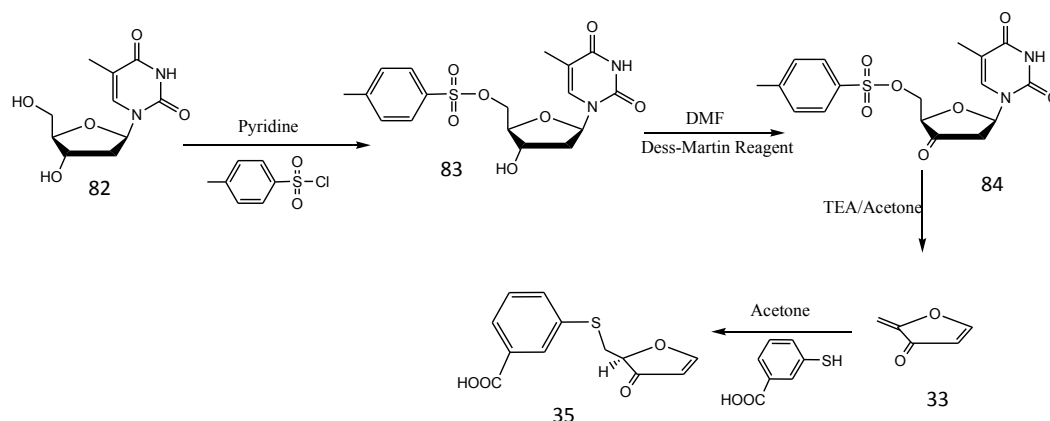


Figure 2.24: Synthetic scheme for 5-(3-mercaptopbenzoic acid)-3-furanone (**35**).

2.5.46 Synthesis of 5'-*O*-tosylthymidine (**83**)

Tosylthymidine was prepared according to the literature procedure⁷ and is summarized as follows. Briefly, thymidine (2.0 mmol) was treated with a 1.2 equivalents of *p*-TsCl in 15 mL dry pyridine at $-5\text{ }^{\circ}\text{C}$. After 16 h at $0\text{ }^{\circ}\text{C}$, the reaction was quenched with ice-water and extracted with chloroform. The combined chloroform extracts were washed consecutively with saturated NaHCO_3 and water and dried over anhydrous MgSO_4 . Flash chromatography on silica (methanol/chloroform 5%) yielded pure 5'-*O*-tosyl thymidine in 56% yields. ^1H NMR (MeOD) ppm 7.83 (d, H_A), 7.51 (s, H_T), 7.74 (d, H_B), 6.25 (t, $\text{H}_{1'}$), 4.33 (m, $\text{H}_{4'}$), 4.41 (m, $\text{H}_{5'}$ and $\text{H}_{5''}$), 2.47 (s, CH_3), 2.26 (m, CH_2), 1.90 (s, CH_3).

2.5.47 Synthesis of 3'-keto-5'-tosylthymidine (**84**)

Compound **83** was oxidized by the Dess-Martin method A cold (0 °C) solution of tosylthymidine (0.5 g, 1.26 mmol) in DMF (5 ml) was added to a solution of the Dess-Martin periodinane reagent (0.55 g, 1.3 mmol) in DMF (5 ml) at 0°C. Stirring was continued for 15 min at 0 °C and 3 h at ambient temperature. The solvent was removed by vacuo at ambient temperature, the solid crude material was dissolved in ethanol (50 ml) and filtered. The solvent was evaporated in vacuo at ambient temperature to give **84** (0.42 g, 85 %; ~ 95% purity). ¹HNMR (acetone-*d*₆) ppm 7.80 (d, H_A), 7.52 (s, H_T), 7.45 (d, H_B), 6.25 (dd, H_{1'}), 4.33-4.43 (m, H_{4'}, H_{5'} and H_{5''}), 2.46 (s, CH₃), 1.85 (s, CH₃).

2.4.48 Synthesis of 2-methylene-3(2H)-furanone (**33**)

Generation of **60** was catalyzed by the addition of 5 uL of triethylamine to 15 mg (0.038 mmol) of 3'-keto-5'-tosylthymidine in 0.5 mL of acetone-*d*₆, ¹HNMR (acetone-*d*₆) ppm 8.47 (d, H_{1'}, J = 2.42 Hz), 5.93 (d, H_{2'}, J = 2.4 Hz), 5.49 (d, H_{5'}, J = 2.0 Hz), 5.30 (d, H_{5''}, J = 2.0 Hz)

2.5.49 Synthesis of 5-(3-mercaptopbenzoic acid)-3-furanone (**35**)

3'-keto-5'-tosylthymidine (100 mg, 0.25 mmol) was dissolved in 2.0 mL of chloroform, and 10 uL of purified triethylamine was added. After 10 min at room temperature, (48 mg, 0.3 mmol) of 3-mercaptopbenzoic acid and 20 uL of triethylamine were added. The solvent was evaporated in vacuo at ambient temperature to give a crude material that was purified by silica gel column chromatography in (methanol :

chloroform 5-10%). It was noticed that there is only one compound formed and isolated even if 3-mercaptobenzoic acid was added in excess. $^1\text{H NMR}$ (CDCl_3) ppm 8.51 (d, H1'), 8.26 (s, H_A), 8.00 (d, H_D), 7.76 (d, H_B), 7.44 (t, H_C), 5.77 (d, H_{2'}), 4.58 (dd, H_{4'}), 3.57 (dd, H_{5'}), 3.23 (dd, H_{5''}).

2.5.50 Synthetic scheme for 2-amino-6-((2S/2R,3S)-2,3,4-trihydroxybutyl)pteridin-4(3H)-one (40, 41)⁴¹

The synthetic scheme for (41) is shown in Figure 2.25.

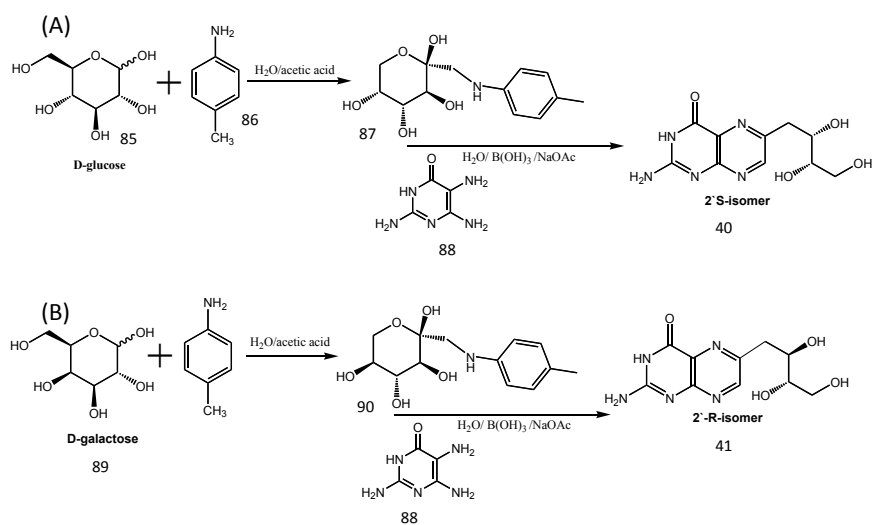


Figure 2.25: Synthetic scheme for 2-amino-6-((2S/2R,3S)-2,3,4-trihydroxybutyl)pteridin-4(3H)-one (40, 41).

2.5.51 Synthesis of (2R,3S,4R,5R)-2-((p-toluidino)methyl)-tetrahydro-2H-pyran-2,3,4,5-tetraol (**87**)

Glacial acetic acid (30 μ L) was added to a mixture of d-glucose (1.08 g, 6mmol), *p*-toluidine (772 mg, 7 mmol) in water (1 mL). The mixture was rotated on a rotary evaporator (sealed without vacuum) at 90°C for 2 h (during this time the product precipitated from the reaction mixture). After cooling to room temperature, ether-ethanol (3:1, 20 mL) was added. Upon stirring at room temperature for an additional 2 h, the mixture was filtered, washed with ether (10 mL), ether-ethanol (5:1, 20 ml mL), ether (10 mL), and dried under vacuum to give aminoalcohol **87** as a light brownish white solid (0.6 g, 41%). ¹H NMR (DMSO-*d*₆) ppm 6.88 (d, 2H), 6.55 (d, 2H), 5.44 (s, 1H), 4.85 (m, 1H), 4.36 (m, 3H), 3.85 (d, 1H), 3.66-3.55 (m, 3H), 3.48 (d, 1H), 3.27 (dd, 1H), 2.99 (dd, 1H), 2.14 (s, 3H)

2.5.52 Synthesis of 2-amino-6-((2S,3S)-2,3,4-trihydroxybutyl)pteridin-4(3H)-one (**40**)

A mixture of 2,5,6-triaminopyrimidin-4-ol (210 mg, 1.5 mmol), *p*-tolyl-D-isoglucosamine (198 mg, 0.73), sodium acetate (225 mg) and boric acid (60 mg) in water (5 ml) was heated in a stream of argon for 6 h on a water bath. A grayish brown solid separated out. The product was filtered and washed with acetone (20 mL) and ethanol till the filtrate was colorless. This was followed by an ether wash. The buff colored solid was dissolved in 1N HCl (30 ml). The solution was treated with charcoal and filtered. The resulting filtrate was neutralized with ammonia and the neutralized solution was left

in the cold room overnight. This resulted in a yellow precipitate, (0.11 g, 56%). ¹H NMR (DMSO-*d*₆) ppm 8.28 (s, 1H), 6.90 (bs, 2H), 4.66 (m, 2H), 4.38 (bs, 1H), 3.83, 3.76 (2bs, 1H), 3.45 (m, 1H), 3.39 (m, 2H), 3.12 (m, 1H), 2.81 (m, 1H).

2.5.53 Synthesis of (2R,3S,4R,5R)-2-((*p*-toluidino)methyl)-tetrahydro-2H-pyran-2,3,4,5-tetraol (90)

Glacial acetic acid (30 μL) was added to a mixture of d-glucose (1.08 g, 6 mmol), *p*-toluidine (772 mg, 7 mmol) in water (1 mL). The mixture was rotated on a rotary evaporator (sealed without vacuum) at 90 °C for 2 h (during this time the product precipitated from the reaction mixture). After cooling to room temperature, ether-ethanol (3:1, 20 mL) was added. Upon stirring at room temperature for an additional 2 h, the mixture was filtered, washed with ether (10 mL), ether-ethanol (5:1, 20 mL), ether (10 mL), and dried under vacuum to give aminoalcohol **90** as a light brownish-white solid (0.63 g, 43%). ¹H NMR (DMSO-*d*₆) ppm 6.88 (d, 2H), 6.55 (d, 2H), 5.44 (s, 1H), 4.85 (m, 1H), 4.36 (m, 3H), 3.85 (d, 1H), 3.66-3.55 (m, 3H), 3.48 (d, 1H), 3.27 (dd, 1H), 2.99 (dd, 1H), 2.14 (s, 3H).

2.5.54 Synthesis of 2-amino-6-((2R,3S)-2,3,4-trihydroxybutyl)pteridin-4(3H)-one (41)

A mixture of 2,5,6-triaminopyrimidin-4-ol (210 mg, 1.5 mmol), *p*-tolyl-D-isoglucosamine (198 mg, 0.73 mmol), sodium acetate (225 mg) and boric acid (60 mg) in water (5 mL) was heated in a stream of argon for 6 h on water bath. A grayish brown

solid separated out. The product was filtered and washed with acetone (20 mL) and ethanol till the filtrate was colorless. This was followed by ether wash. The buff colored solid was dissolved in 1N HCl (30 ml). The solution was treated with charcoal and filtered to remove the charcoal. The resulting filtrate was neutralized with ammonia and the neutralized solution was left in the cold room overnight. This resulted in yellow precipitate, (0.1 g, 51%). ^1H NMR ($\text{DMSO-}d_6$) ppm 8.54 (s, 0.5H), 8.28 (s, 0.5H), 6.90 (bs, 2H), 4.66 (m, 2H), 4.38 (bs, 1H), 3.83, 3.76 (2bs, 1H), 3.45 (m, 1H), 3.39 (m, 2H), 3.12 (m, 1H), 2.81 (m, 1H).

3. THIAMIN PYRIMIDINE SYNTHASE

3.1 Introduction to thiamin pyrimidine synthase - ThiC

Thiamin pyrophosphate is an essential cofactor in all forms of life.⁵⁰ It plays a key role in amino acid and carbohydrate metabolism. Thiamin pyrophosphate biosynthesis has been extensively studied.^{51,52} There are unique biosynthetic pathways in bacteria and eukaryotes.⁵³⁻⁵⁶ The bacterial thiamin pyrimidine synthase, ThiC, a radical AdoMet enzyme, catalyzes a remarkable rearrangement reaction where it converts aminoimidazole ribonucleotide (**AIR**, **1**) to the thiamin pyrimidine - 4-amino-5-hydroxymethyl-2-methylpyrimidine phosphate (**HMP-P**, **2**) and S-Adenosyl methionine (**AdoMet**, **3**) to 5'-Deoxyadenosine (**5'dA**, **5**) as shown in Figure 3.1.^{1,26-28}

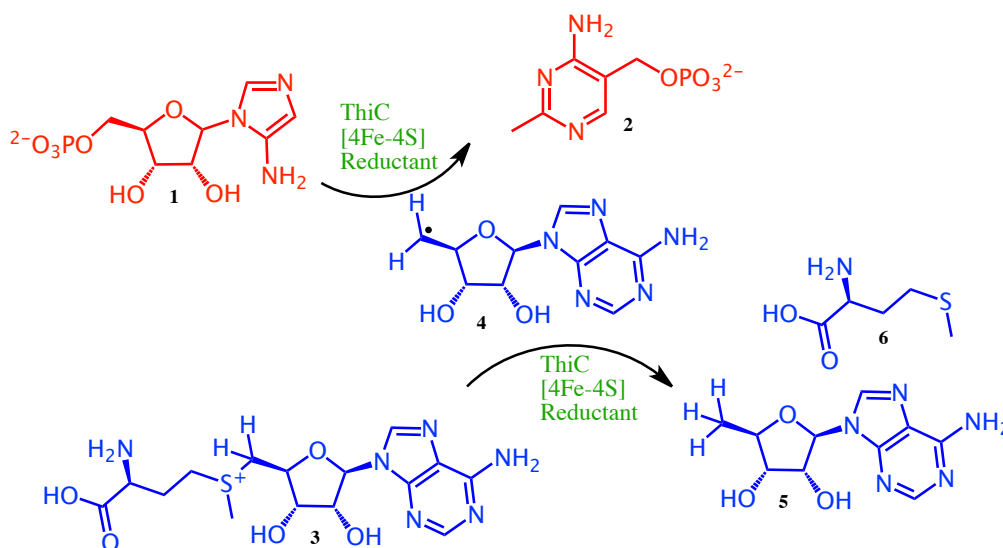
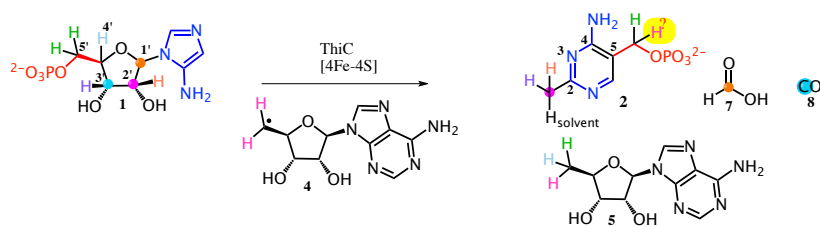


Figure 3.1: ThiC catalyzed conversion of AIR (**1**) to HMP-P (**2**) and AdoMet (**3**) to 5'dA (**5**) and methionine (**6**).

Previous studies have established the C, N and H labeling pattern on HMP and 5'dA. It has been shown that ThiC is a novel radical SAM enzyme where one molecule of 5'-deoxyadenosyl radical is involved in two hydrogen atom abstractions (Figure 3.2). Figure 3.2 illustrates the C, N and H labeling pattern on HMP-P and 5'dA.^{1,26,27,57-59}

(A)



(B)

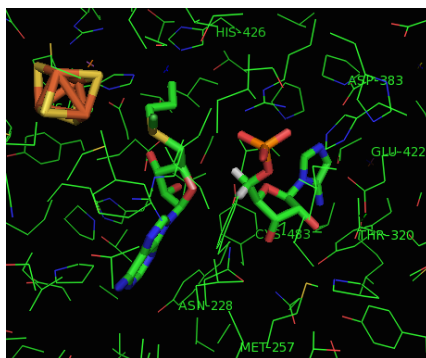


Figure 3.2: C, N and H labeling pattern on HMP-P and 5'dA in the ThiC-catalyzed reaction and active site of At.ThiC.

Previous studies with cell free extract demonstrated that ThiC converted 5'-²H₂-AIR to monodeuterio HMP-P (**22**) and the origin of the product C5' hydrogen remained unknown (Figure 3.2). We wanted to investigate the origin of this hydrogen atom.

Current mechanistic proposal for ThiC-catalyzed reaction is shown in Figure 3.3.

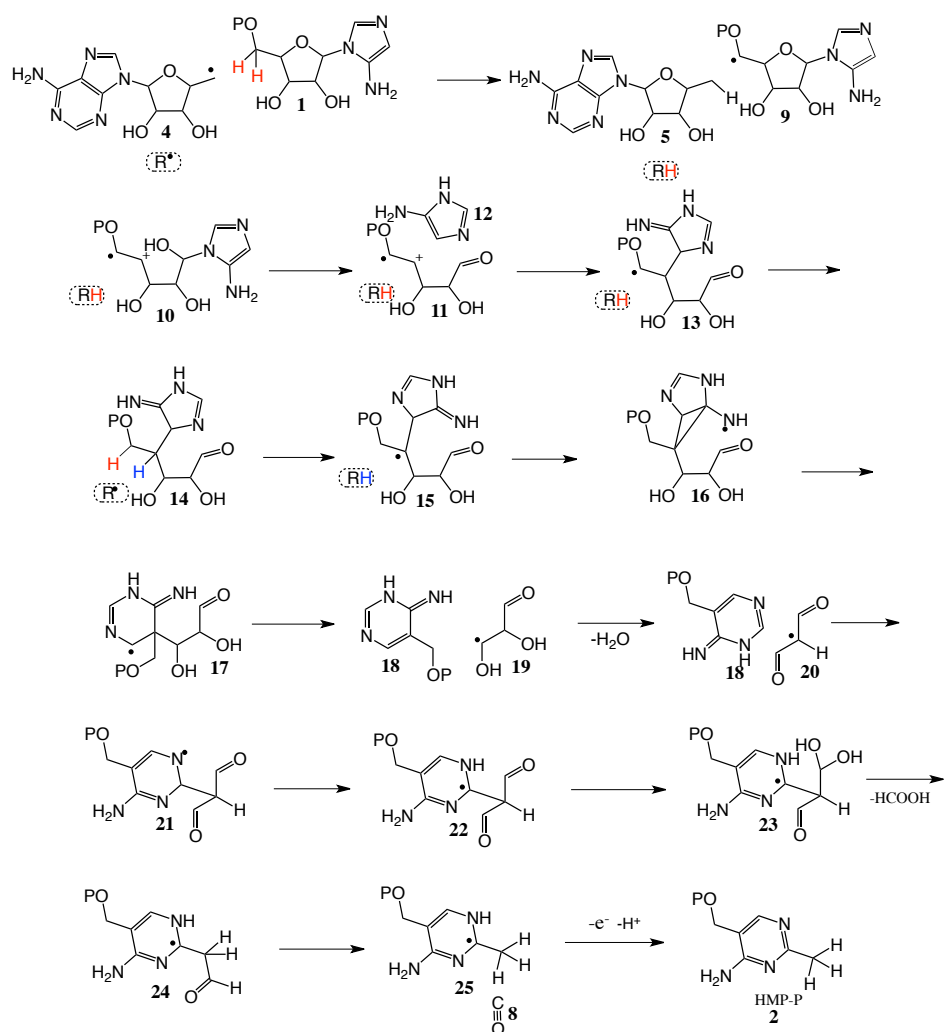


Figure 3.3: Mechanistic proposal for ThiC-catalyzed reaction.

It involves a radical rearrangement reaction wherein a 5'-deoxyadenosyl radical (4) is generated at the active site of ThiC. This in turn abstracts a hydrogen atom from C5' of AIR to generate a radical on AIR (9). This is followed by β bond scission to give radical cation (10) and C-N bond cleavage to give (11). Addition to the carbocation

gives **13**. Transfer of hydrogen atom from 5'dA regenerates 5'dA radical (**4**) and gives intermediate **14**. The regenerated 5'dA radical abstracts a hydrogen atom from the 4' position to give **15**. Radical addition to heterocycle gives (16), followed by β bond scission gives ring expanded compound **17**. β bond scission gives **18** and **19**. **19** undergoes dioldihydratase like reaction to generate **20** that undergoes radical addition to give **21**. Radical rearrangement give **22**. Addition of water and loss of formate gives 24. Loss of CO (**8**) followed by loss of electron gives final product HMP-P (**2**).²⁷

3.2 Results and discussion

3.2.1 Identification of the origin of the C5' hydrogen of HMP-P

Based on the mechanistic proposal there is a transfer of hydrogen atom from adenosyl radical onto intermediate **13** to give **14**. If the early steps of the mechanism are correct, this hydrogen atom transferred from adenosyl radical should end up at C5' of HMP-P (**2**).

To test this, the two reactions shown in Figure 3.4 were carried out and the resulting HMP-P was dephosphorylated and analyzed by ESI MS. The first reaction was performed using purified ThiC with 5'-²H₂-AIR and unlabeled AdoMet, the experiment previously carried out with cell free extract, and as expected gives monodeuterio-HMP (**27**) as indicated by the $m/z = 141.1$ Da peak in the mass spectrum (Figure 3.4). The second ThiC reaction, using AdoMet enzymatically synthesized from universally deuteriated ATP and 5'-²H₂-AIR, gave dideuterio-HMP (**29**) ($m/z = 142.1$ Da). This experiment confirms that one of the C5' hydrogens of HMP-P is derived from the

adenosyl radical and completes the identification of the origin of all of the atoms generated in the complex ThiC-catalyzed rearrangement reaction.

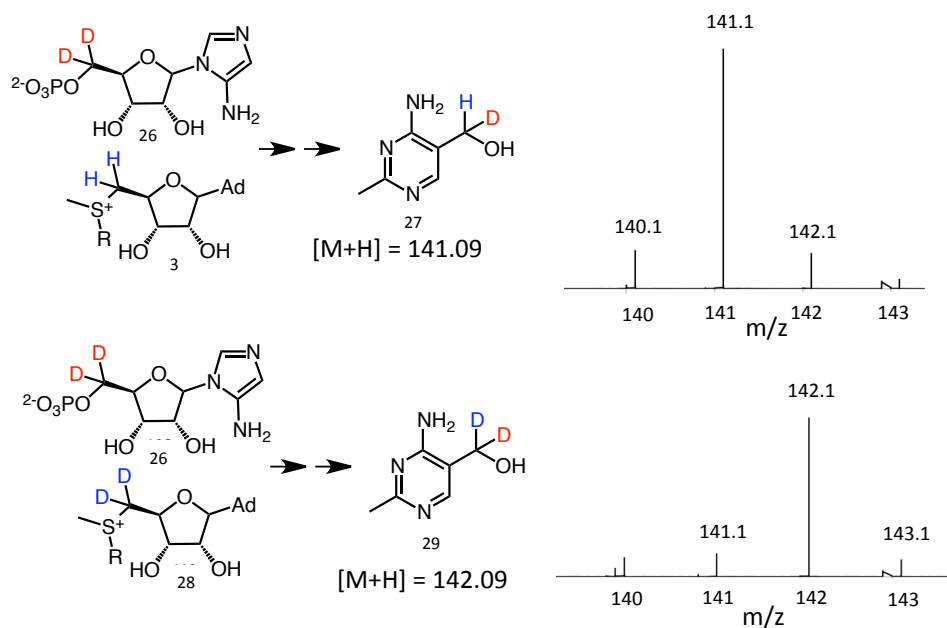


Figure 3.4: Incorporation of a deuterium atom from AdoMet. (A) $m/z = 141.1$ corresponds to monodeuterio HMP (B) $m/z = 142.1$ corresponds to the dideuterio HMP-P.

3.2.2 Stereochemistry of the transfer of hydrogen atom from 5'dA on to HMP-P

The ThiC catalyzed conversion of 5'-²H₂-AIR and unlabeled AdoMet to HMP-P results in the generation of a chiral center at C5' of HMP-P (Figure 3.4, compound **27**). Our next task was to determine the stereochemistry of this center in the enzymatic reaction product. For this, we synthesized the 1-(S)-camphanic esters of unlabeled HMP,

R -5'- ^2H -HMP and S -5'- ^2H -HMP^{60,61} and demonstrated that R - and S -monodeuterio HMP could be differentiated by NMR analysis of these esters (Figure 3.5).

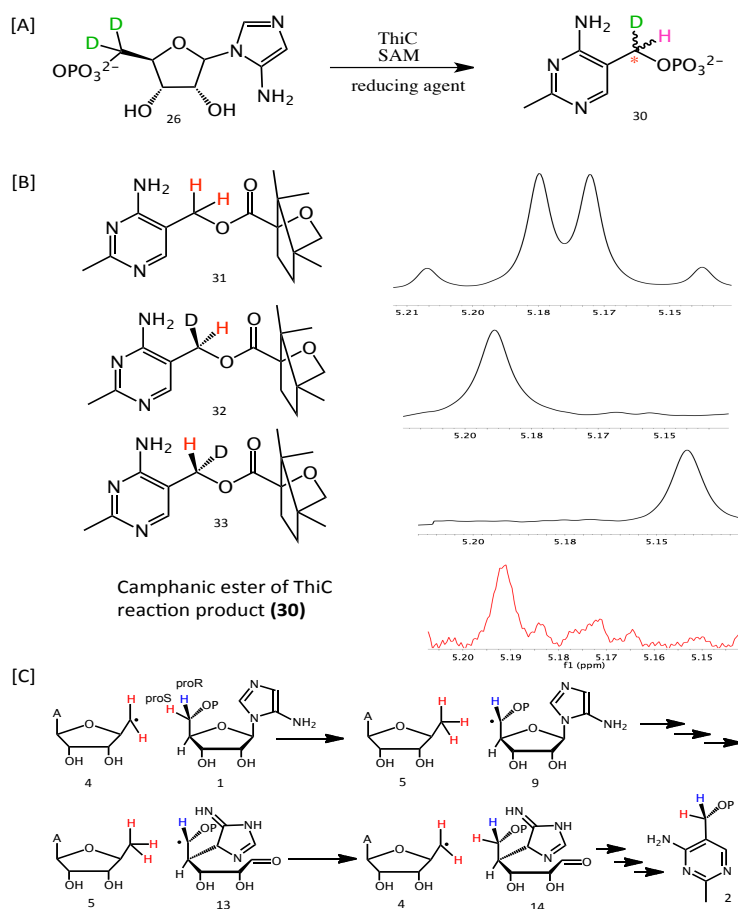


Figure 3.5: Stereochemical analysis of the deuterium atom incorporated from AdoMet. (A) ThiC reconstitution with 5'- $^2\text{H}_2$ -AIR and SAM generates chiral centre on mono deuterated HMP as indicated by *. (B) The top three NMR traces are the reactions of standards for HMP with 1-(S)-camphanic chloride. The bottom trace represents the reaction of HMP purified by ThiC reconstitution with 5'- $^2\text{H}_2$ -AIR and unlabeled AdoMet followed by phosphatase treatment. This shows that the hydrogen atom on mono deuterated HMP-OH from ThiC is on pro S face.

3.2.3 Summary of active-site mutant studies for ThiC

The ThiC catalyzed transformation is amazingly complex. To understand the mechanistic details of this reaction, it would be of significant value to trap AIR derived intermediates in the ThiC catalyzed reaction. With this view, several ThiC active site¹ mutants were tested. Table 3.1 summarizes the results of this study.

Table 3.1 ThiC - active site mutant studies.

Active site mutant	5'dA detection	AIR derived product detection
C.c. ThiC M248L	5'-deoxyAdenosine is formed in levels comparable to wt. C.c. ThiC. 5' hydrogen atom from AIR is abstracted. But 4' hydrogen atom from AIR is not abstracted.	No AIR derived product was detected by LCMS or ³² P assays. Analyzed the protein by trypsin digest to look for modification. But no modification detected
C.c. ThiC C474S	5' and 4' H atom abstracted from AIR.	NMR experiments indicate product is unstable or more than one product formed.

Table 3.1 Continued.

Active site mutant	5'dA detection	AIR derived product detection
C.c. ThiC H417A	5' and 4' H atom abstracted from AIR. 5'dA formed in low levels.	HMP-P formed in very low amounts. Detected by ³² P assays. Also, detected by LCMS
C.c. ThiC H481A	5'-deoxyadenosine formed in low levels	HMP-P formed in very low amounts
C.c. ThiC S333A	No 5'dA formation detected. Isolated protein did not bind [4Fe-4S] cluster.	NA
C.c. ThiC R377K	5'-deoxyAdenosine is formed in very low levels. However, no deuterium atom incorporation from AIR was found	No AIR derived product detected
C.c. ThiC Y277F	5' and 4' H atom abstracted from AIR	HMP-P not detected. Possibly trace levels of AIR derived product observed.

Table 3.1 Continued.

Active site mutant	5'dA detection	AIR derived product detection
C.c. ThiC Y440F	5'DeoxyAdenosine formed in very low levels. No other product detected	No AIR derived product detected
C.c. ThiC H417A- H481A	Very low levels of 5'-deoxyadenosine detected	Trace levels of HMP-P detected
A.t. ThiC N228S	5'dA formed	HMP-P formed. No intermediate detected
A.t. ThiC T320A	5'dA formed	HMP-P formed. No intermediate detected
A.t. ThiC D383N	5'dA formed	HMP-P formed. No intermediate detected
A.t. ThiC M257L	5'dA formed	Possible intermediates detected at trace levels.
A.t. ThiC C484S	5'dA formed	HMP-P formed. No intermediate detected.

Table 3.1 Continued.

Active site mutant	5'dA detection	AIR derived product detection
A.t. ThiC T320C	5'dA formed	HMP-P formed. No intermediate detected.
A.t. ThiC M257C- T320C- E422C	5'dA formed	HMP-P not formed. No AIR derived product detected.
A.t. ThiC M257C- T320C- E422C- L259C	5'dA formed	HMP-P not formed. No AIR derived product detected.

It can be seen from the Table 3.1 that in case of some of the mutants, AIR derived intermediates can be detected. However, trace levels of products were detected making it impossible for complete NMR characterization of the products.

3.3 Conclusion

We demonstrated that one of the C5' hydrogens of HMP-P was derived from the adenosyl radical. This completed the identification of the origin of all of the atoms

generated in the complex ThiC-catalyzed rearrangement reaction. We have previously demonstrated that adenosyl radical abstracts the proS hydrogen from the C5 position of AIR. At some point during the reaction, 5'dA transfers the hydrogen atom on to AIR derived intermediate, which eventually forms HMP-P (mechanistic proposal shown in Figure 3.3). The HMP-P stereochemistry demonstrates that this hydrogen atom abstraction occurs from the si face of the radical resulting in overall retention of stereochemistry for the C5' hydrogen atom replacement reaction.

We performed several active-site mutant studies with a view to trap and characterize intermediates in the ThiC catalyzed reaction. In case of some of the mutants, AIR derived intermediates can be detected. However, trace levels of products are formed thus making it impossible for complete NMR characterization of these products.

3.4 Experimental

3.4.1 Over-expression of C.c. ThiC

A full length clone of C.c. ThiC in pET28 vector was co-transformed with pDB1282, a plasmid encoding genes responsible for the Fe/S cluster biogenesis machinery, into *E. coli* B834(DE3). A 15 mL overnight culture of the resulting strain in LB was used to inoculate 1.8 L of sterilized M9 minimal medium, supplemented with 100 mg/L ampicillin and 40 mg/L kanamycin, and was allowed to grow at 37 °C till the OD600 reached 0.2 – 0.25. At this point, ferrous ammonium sulfate, L-cysteine and L-arabinose were added to final concentrations of 100 µM, 300 µM and 0.2% (w/v)

respectively and the growth was allowed to continue with slow shaking (100 rpm). Once the OD₆₀₀ reached 0.65 – 0.7, the cultures were cooled with ice-water and IPTG was added to a final concentration of 10 μM. The protein overexpression was continued at 15 °C at 50 rpm for 24 hours. The flasks were then incubated at 4 °C for 3 hours and the cells were then harvested and stored under liquid nitrogen till future use.

3.4.2 Over-expression of A.t. ThiC

Previous studies reported¹¹ that overexpression of full-length AtThiC containing 644 residues results in insoluble protein whereas overexpression of ΔN71-AtThiC with residues 1-71 removed results in soluble protein with high yield (1,2). In the present study, ΔN71-AtThiC was cloned into a modified pET-28 plasmid that encodes the following hexahistidine-tagged protein product:

NH₂- MGSDKIHSHHHSSGENLYFQGHMK₇₂...K₆₄₄-COOH”.

This plasmid was transformed into *E. coli* BL21(DE3) cells. Large-scale cultures were grown in baffled shake flasks containing 1.5 L of LB medium, 0.051 g chloramphenicol, and 0.06 g kanamycin. The flasks were shaken at 180 rpm and 37 °C until an optical density at 600 nm (OD₆₀₀) of 0.5-0.55 was reached and then moved to a 4 °C cold room. About 1.5 hours later, 200 mg ferrous ammonium sulfate, 200 mg L-cysteine, and 36 mg isopropyl β-D-1-thiogalactopyranoside (IPTG) were added per flask and the flasks were shaken at 90 rpm and 15 °C for about 20 hours. The flasks were then moved to the cold room for about 2 hours before being pelleted by centrifugation, flash frozen, and stored in liquid N₂.

3.4.3 Purification of A.t. ThiC and C.c. ThiC

For enzyme purification, the cell pellets were thawed at room temperature in an anaerobic chamber and suspended in lysis buffer (100 mM Tris-HCl, pH 7.5) in the presence of 2mM DTT, lysozyme (0.2 mg/ml) and benzonase (100 units). This mixture was then cooled in an ice-bath for 2 hrs. The suspension of cells was then sonicated and centrifuged to give the cell-free extract. The enzyme was then purified using standard Ni-NTA chromatography. The column was first incubated with the lysis buffer. The cell-free extract was then passed over the column, which was then washed with 5-6 column volumes of wash buffer (100 mM Tris-HCl, 300 mM NaCl, 20 mM imidazole, 2mM DTT, pH 7.5). The protein was then eluted using 100 mM Tris-HCl, 300 mM NaCl, 250 mM imidazole, 2 mM DTT, pH 7.5. The purified enzyme was buffer exchanged into 100 mM potassium phosphate, 30% glycerol, 2 mM DTT, pH 7.5 using a 10DG column and the purified enzyme was stored in liquid nitrogen.

3.4.4 Over-expression and purification of S-adenosylmethionine synthetase

SAM synthetase-GFP over-expression plasmid was a gift from Dr. David P. Barondeau's lab. This plasmid was transformed in *E. coli* BL21(DE3) cells. 5ml per litre of the starter culture was added to 6 liters of Luria Broth media. The cells were allowed to grow till OD₆₀₀ reached 0.6. Then the cells were cooled to 4⁰ C for one hour. Then 0.5mM of IPTG was added to the media. The culture was shaken at 15⁰ C for 12 hrs.

The cells were then harvested by centrifugation. The cells were suspended in lysis buffer (100mM potassium phosphate, 300mM NaCl, 10mM imidazole). They were

sonicated and centrifuged to remove the cell debris. The protein was purified by Ni-NTA column. After loading the protein on Ni-NTA column, the column was washed with wash buffer (100mM potassium phosphate buffer, 300mM NaCl, 50mM imidazole, pH 7.5, 5 column volumes). The protein was eluted off the column using 250mM imidazole. The protein was desalted in 100mM potassium phosphate buffer, 30% glycerol, pH 7.5, using 10DG desalting columns. The protein was stored in -80°C.

3.4.5 ThiC-SAM synthetase coupled assays

50 μ L of SAM synthetase (200 μ M) was incubated in an anaerobic chamber with 5mM of ATP and 5mM of methionine in a buffer containing 100mM Tris-HCl pH 8, 20mM MgCl₂, 200mM KCl. The assays were allowed to stand in the anaerobic chamber for 3 hrs. ThiC reconstitution assays were set up in an anaerobic chamber. 200 μ L of 280 μ M ThiC was incubated with excess of dithionite for 10 mins. Then 6.7 μ L of 30mM AIR was added to the ThiC reconstitution mixture. This was followed by addition of SAM from the SAM synthetase mixture.

3.4.6 ThiC assay conditions

ThiC reconstitution assays were set up in an anaerobic chamber. 200 μ L of 280 μ M ThiC was incubated with excess of dithionite for 10 mins. Then 6.7 μ L of 30mM AIR was added to the ThiC reconstitution mixture. This was followed by addition of 7 μ L of 50mM SAM.

3.4.7 Alkaline phosphate treatment of HMP-P purified after ThiC

reconstitution

Alkaline phosphatase $2\mu\text{L}$ (1000 units) was added per ml of HMPP purified after adjusting the pH of the solvent containing HMPP to 7.5. Then $5\mu\text{l}$ of MgCl_2 (1M) was added to this mixture. The mixture was incubated at 37°C for 6 hours.

3.4.8 Sample preparation for mass spectrometry experiments

The buffer exchanged HMP was concentrated using speed vacuum. When $500\mu\text{l}$ of solvent was remaining, 10 ml of water was added to it. Then this sample was again subjected to speed vacuum to concentrate it. This process was done at least three times to ensure maximum removal of ammonium formate. This resulted in optimum signal for mass spectrometry experiments.

3.4.9 Enzymatic sample - derivatization for stereochemistry experiment

Around 60 ml of HMP was buffer exchanged. The entire HMP buffer exchanged was concentrated to 5 ml using speed vacuum. It was diluted to 12ml using water. Again it was concentrated to $500\mu\text{l}$. Then 10ml of water was added to this mixture and it was again concentrated to $500\mu\text{l}$. This was done three times. The $500\mu\text{l}$ remaining was stripped to dryness using speed vacuum.

3.4.10 Reference standard sample – derivatization for stereochemistry

experiment

Dry HMP was dissolved in 200 μ l of dry dichloromethane. 4 μ L of dry pyridine was added to this mixture under argon. The mixture was allowed to stir for 10 min under argon. 1.5mg of 1-(S)-camphanic chloride was then added to this mixture and the reaction was allowed to stir overnight under argon. Then 3ml of ethyl ether and 200 μ l of water was added to this mixture. Separate the organic phase from the aqueous phase. Anhydrous sodium sulfate is then added to the organic phase. This is then passed through a cotton plug for filtration. The organic solvent was then removed in vacuo and the product was analyzed by NMR (CDCl₃). In all NMR experiments the chemical shifts were referenced to chloroform chemical shift.

3.4.11 HPLC purification of HMP-P from ThiC reconstitution mixture

The ThiC reconstitution assays were purified by reverse phase C18 column using HPLC. (Supelcosil, SPLC-18, 5 μ m, 25cmx10mm). Following conditions were used for HPLC purification. Solvent A: H₂O, solvent B: 100mM potassium phosphate pH 6.6, solvent C: methanol. 0min – 100%B, 7min – 10%A, 90%B, 12min – 25%A, 60%B, 15%C, 17min – 25%A, 10%B, 65%C, 19min – 100%B, 29min 100%B. For stereochemistry analysis several ThiC assays were purified to collect HMPP and for each mass spectrometry experiments three ThiC assays were purified.

3.4.12 HPLC buffer exchange of Alkaline phosphatase mixture

The alkaline phosphatase mixture was again purified by HPLC using C18 column (Supelcosil, LC-18DB, 5 μ m, 25cmx4.6mm) to collect HMP. The solvents that were used for HPLC were; Solvent A – H₂O, Solvent B – 5mM ammonium formate, Solvent C – methanol. Following was the gradient used: 0 min – 100%B, 1min- 100%B, 6 min – 20%A, 20%B, 60%C, 11 min – 100%B, 17 min – 100%B.

3.4.13 Synthetic scheme for camphanic esters of HMP (31, 32, 33)^{60,61}

The synthetic scheme for (31) and (33) is shown in Figure 3.6.

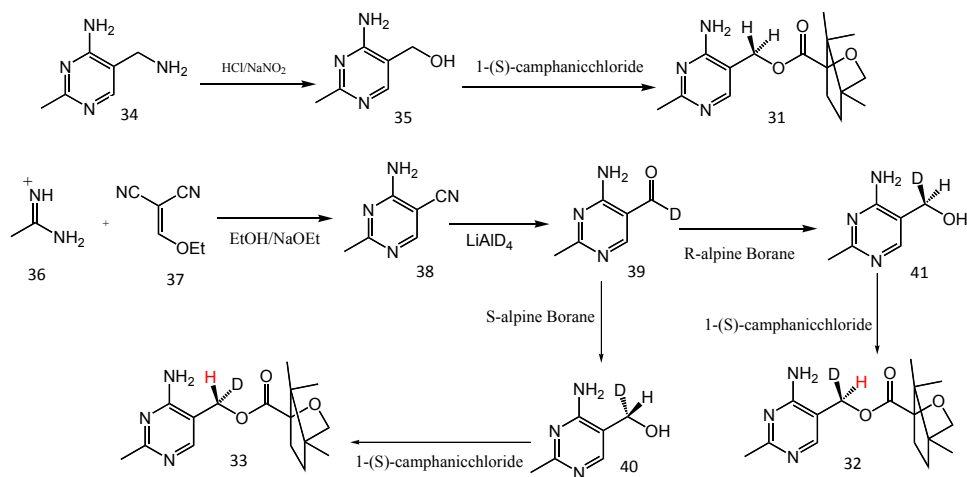


Figure 3.6: Synthetic scheme for camphanic esters of HMP (31, 32, 33).

3.4.14 Synthesis of 4-amino-5-(hydroxymethyl)-2-methylpyrimidine (HMP, 35)

10ml of 5% HCl was added to 136 mg of Grewe diamine at 0⁰ to 5⁰ C. The mixture was allowed to stir for 10 mins at this temperature. It was then heated to 90⁰ C. Then 10 ml of 10mM solution of NaNO₂ was then added drop wise at this temperature. After the completion of addition the reaction mixture was immediately cooled and then titrated to pH 8.5 using 40% NaOH solution.

3.4.15 Synthesis of 4-amino-5-cyano-2-methylpyrimidine (38)

0.95 g of acetimidine hydrochloride (36) was dissolved in 200ml of anhydrous ethanol. 0.3g of sodium was then dissolved in anhydrous ethanol and this solution was added to the acetimidine solution. The mixture was allowed to stirred till no further solid precipitation was observed. It was then filtered. 1.22g of ethoxymethylene malonontrile (37) was dissolved in 10ml of anhydrous ethanol and was added to the above filtrate. The mixture was allowed to stir for 3.5hrs. The product of this reaction is then filtered and analyzed by NMR. The yield of this reaction is about 64%.

3.4.16 Synthesis of 4-amino-5-carbaldehyde-2-methylpyrimidine (39)

100mg of 4-amino-5-cyano-2-methylpyrimidine were added to 10ml of dry THF. This mixture was cooled down to -10⁰ C. This mixture was allowed to stir at -10⁰ C for 30 mins. Then 29 mg of lithium aluminum deuteride was added in parts such that the temperature does not increase beyond -5⁰ C. The reaction mixture was allowed to stir for

2 hrs. Then 5ml of methanol was added to this mixture. Flash column was used to purify the product. 5% methanol and ethyl acetate were used for silica gel flash chromatography. The solvent was evaporated in vacuo and a pure white solid was obtained.

3.4.17 Synthesis of 4-amino-5-R-D-(hydroxymethyl)-2-methylpyrimidine (41)

150 mg of aldehyde was mixed with 12ml of dry THF. 4.2 ml of S-alpine borane was added to this mixture under argon. The reaction mixture was allowed to stir for 3 hrs. After 3 hours, 4 ml of methanol and 4ml of water was added to this mixture. The R isomer was purified using silica gel flash column. 35% methanol in ethyl acetate was used for silica gel chromatography.

3.4.18 Synthesis of 4-amino-5-S-D-(hydroxymethyl)-2-methylpyrimidine (40)

Exactly same procedure was followed as above. Except in this case, R-alpine borane was used instead of S-alpine borane for the reduction of (39) to (40) as shown in the Figure 3.6.

3.4.19 Preparation of camphanic ester of HMP (31, 32, 33)

10mg of dry HMP was dissolved in 1ml of dry dichloromethane. 16 μ L of dry pyridine was added to this mixture under argon. The mixture was allowed to stir for 10 min under argon. 15mg of 1-(S)-camphanic chloride was then added to this mixture and the reaction was allowed to stir for 2hrs. Then 3ml of ethyl ether and 1ml of water was

added to this mixture. Separate the organic phase from the aqueous phase. Anhydrous sodium sulfate is then added to the organic phase. This is then passed through a cotton plug for filtration. The organic solvent was then removed in vacuo and the product was analyzed by NMR (CDCl_3). The two diastereomeric hydrogen atoms (Figure 3.5B) were confirmed by dqf COSY and HSQC experiments. The overlapping doublet of doublet in Figure 3.5B for compound **31** couples to each other (geminal A-B system). HSQC demonstrates that these two hydrogen atoms are on the same carbon atom.

4. ANAEROBIC VITAMIN B₁₂ BIOSYNTHESIS – HYDROXYBENZIMIDAZOLE SYNTHASE

4.1 Background and introduction

ThiC, thiamin pyrimidine synthase catalyzes a remarkable reaction, where aminoimidazole ribotide (**AIR, 1**) is converted to 4-amino-2-methyl-5-hydroxymethyl pyrimidine (**HMP-P, 3**), carbon monoxide (**CO, 6**), and formate (**5**) (Figure 4.1).^{1,27} Several studies labeling and mechanistic studies have been performed on the thiamin pyrimidine synthase, ThiC.^{1,26,27,58} It has been shown that ThiC belongs to the radical SAM family of enzymes and generates 5'-deoxyadenosyl radical (**5'-dA radical, 2**), which sequentially abstracts hydrogen atom from 5' and 4' position of AIR.²⁷

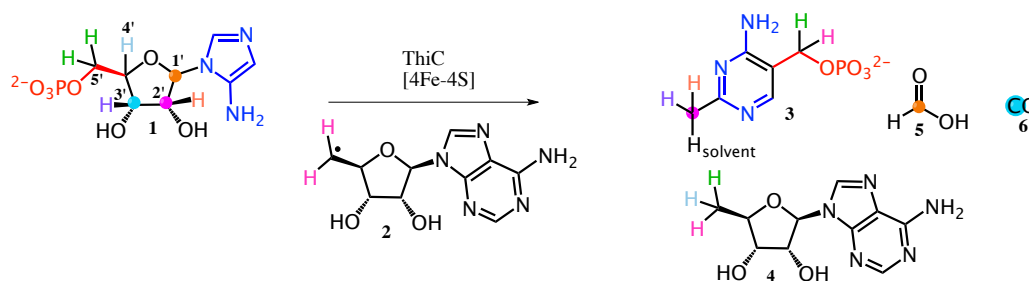


Figure 4.1: ThiC-catalyzed reaction - C, N and H labeling pattern on HMP-P and 5'dA.

We extensively tried to investigate the mechanistic details of ThiC catalyzed reaction. We also observe possible AIR derived intermediates in this complex reaction. However, these are generated only at trace levels. Also, ThiC, like several other radical

AdoMet enzymes, does a fraction of a turn-over making it very challenging to trap trace level products.

We decided to look for ThiC paralogs from different organisms that work better or catalyze different, more tractable chemistry. Bioinformatics search for thiamin biosynthetic genes (in particular ThiC) in the SEED database (<http://theseed.uchicago.edu/FIG/index.cgi>) revealed that there are several microorganisms that have more than one copies of ThiC. From the set of organisms that have multiple copies of ThiC, we observed that there is a subset of organisms where one of these copies of ThiC (which we named as ThiC-1) was clustered with vitamin B₁₂ biosynthetic genes. Also, many of these organisms are listed as anaerobic microorganisms. Anaerobic biosynthesis of vitamin B₁₂ has been extensively studied⁶²⁻⁷². However, the gene product(s) responsible for the biosynthesis of the “lower ligand” of vitamin B₁₂ – dimethylbenzimidazole is (are) unknown. In the aerobic pathway, BluB – the flavin destructase catalyzes the oxidative conversion of flavin mononucleotide (FMN, **7**) to dimethylbenzimidazole (DMB, **8**) as shown in the Figure 4.2.^{73,74}

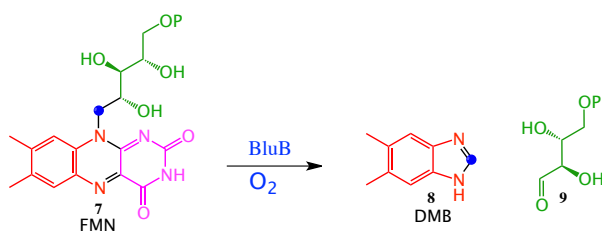


Figure 4.2: BluB catalyzed DMB biosynthesis.

Based on these observations, we decided to test the in vitro enzymatic activity of ThiC-1.

4.2 Results and discussion

4.2.1 Reconstitution of ThiC-1 as hydroxybenzimidazole synthase (HBI synthase)

We decided to synthesize and clone the nucleotide sequence of *Desulfuromonas acetoxidans* ThiC paralog (ThiC-1) clustered with vitamin B₁₂ biosynthetic genes. We heterologously co-overexpressed in *E. coli* with plasmid containing genes from *suf* operon for [4Fe-4S] cluster biosynthesis. ThiC-1 as isolated binds to a [4Fe-4S] cluster as shown in Figure 4.3A. The enzymatic assays with HBI synthase in presence of AIR, SAM and dithionite results in the formation of 5'-dA (**4**) as shown by the signal at 31min in the HPLC chromatogram (Figure 4.3B). This was confirmed by LCMS. Also, a unique signal was observed at 22.7 min only in the full reaction where all the components were present and not observed in any of the controls where either of ThiC-1, AIR, SAM or dithionite was absent (Figure 4.3B). This signal had an [M+H]⁺ of 135.05 Da (Figure 4.3D) which is identical to that of 5-HB.

To confirm the formation of 5-hydroxybenzimidazole (5-HB) we co-injected a reference standard for 5-HB with the ThiC-1 full reaction. The enzymatic product and the reference standard co-elute as shown in (Figure 4.3).

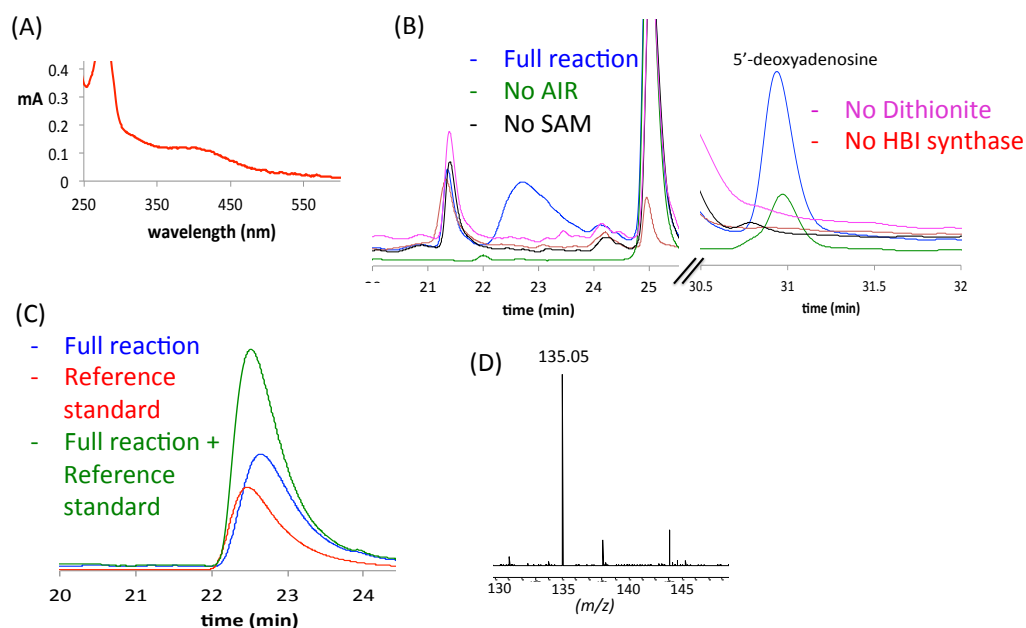


Figure 4.3: Reconstitution of ThiC-1 as HBI synthase. (A) UV-Vis spectrum of HBI synthase as isolated. (B) HPLC (254nm) chromatograms for HBI synthase reactions with controls. A unique signal observed in the full reaction at 22.7min retention time. (C) Red chromatogram – reference standard for 5-HB. Blue chromatogram - enzymatic reaction containing all the components - HBI synthase, AIR, SAM and dithionite (full reaction). Green Co-injection of the reference standard corresponding to 5-HB and the full reaction. This indicates that the reference standard and the enzymatic product co-elute. (D) MS indicates an $[M+H]^+ = 135.05$ Da for the enzymatic product. This is consistent with the $[M+H]^+$ for 5-HB.

Similar to ThiC, ThiC-1 uses AIR (**1**) and AdoMet as a substrate. SAM is converted to 5'-deoxyadenosine (**5'-dA**, **6**). However, unlike the ThiC reaction, ThiC* catalyzed reaction converts AIR to 5-hydroxybenimidazole (**5-HB**, **10**). 5-HB (**10**) has been previously proposed to be an intermediate in the anaerobic dimethylbenzimidazole /vitamin B₁₂ biosynthesis.⁶⁹ Our study identifies the gene product responsible for the formation of this key ligand of vitamin B₁₂. We renamed ThiC-1 as hydroxybenzimidazole synthase (**HBI synthase**).

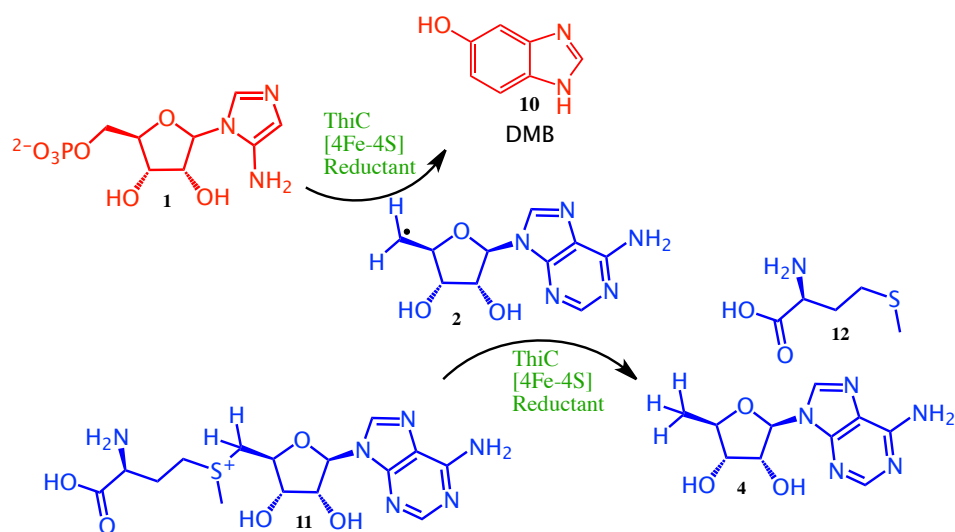
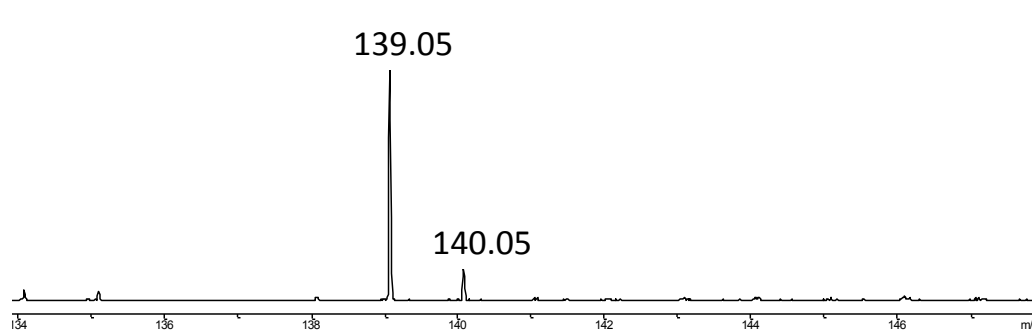


Figure 4.4: Reconstitution of ThiC-1 as a radical SAM enzyme as hydroxybenzimidazole synthase (HBI synthase).

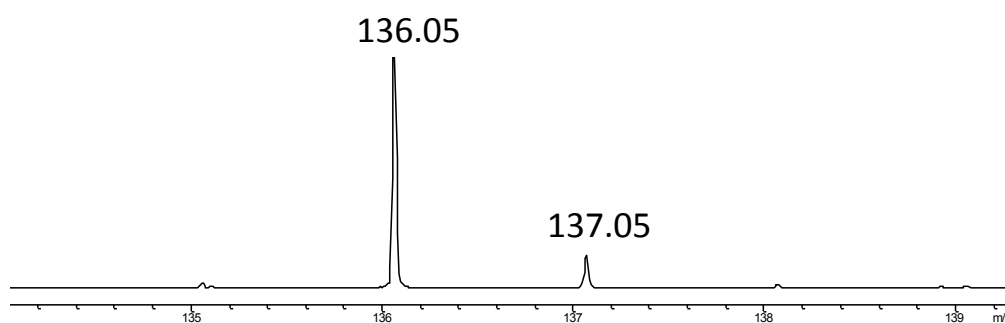
4.2.2 HBI synthase reactions with ^{13}C -labeled AIR isotopomers

HBI synthase reactions with ^{13}C -labeled AIR were analyzed by LCMS. Figure 4.5 and Table 4.1 summarizes these results. The reactions with $1',2',3',4',5'-^{13}\text{C}_5\text{-AIR}$ resulted in the $[\text{M}+\text{H}]^+ = 139.06$ Da for 5-HB indicating that only 4 of the 5 ^{13}C labeled carbons were incorporated in 5-HB. The reactions with $3'-^{13}\text{C-AIR}$ and $2'-^{13}\text{C-AIR}$ showed an $[\text{M}+\text{H}]^+ = 136.05$ Da thereby indicating a single ^{13}C incorporation in 5-HB formed in both these reactions. The reaction with $1'-^{13}\text{C-AIR}$ resulted in an $[\text{M}+\text{H}]^+ = 135.05$ Da indicating that $1'-\text{C}$ of AIR is not incorporated in 5-HB. The mass spectrum of each of these results is shown in Figure 4.5.

(A)



(B)



(C)

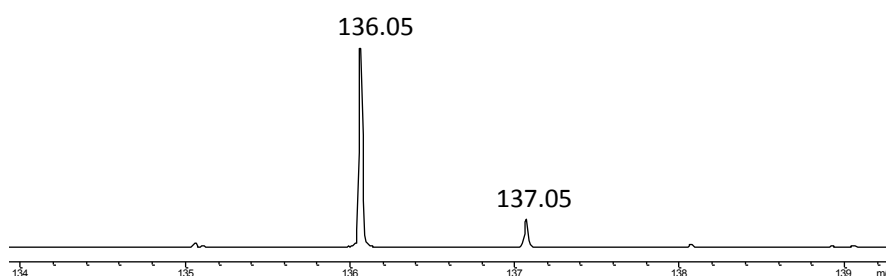


Figure 4.5: HBI synthase reactions with ^{13}C -AIR. (A) MS for 5-HB - HBI synthase reaction with $1',2',3',4',5'$ - $^{13}\text{C}_5$ -AIR. (B) MS for 5-HB - HBI synthase reaction with $3'$ - ^{13}C -AIR. (C) MS for 5-HB - HBI synthase reaction with $2'$ - ^{13}C -AIR (D) MS for 5-HB - HBI synthase reaction with $1'$ - ^{13}C -AIR

(D)

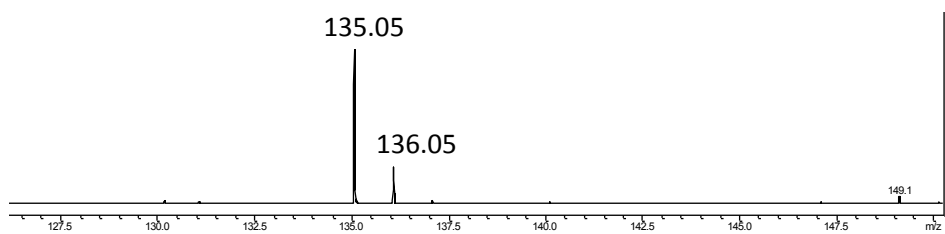


Figure 4.5 Continued.

Table 4.1 summarizes the LCMS results.

Table 4.1: Summary of HBI synthase reactions with ^{13}C -AIR.

Substrate	5-HB [M+H]⁺ Da
1',2',3',4',5'- $^{13}\text{C}_5$ -AIR	139.0
3'- ^{13}C -AIR	136.0
2'- ^{13}C -AIR	136.0
1'- ^{13}C -AIR	135.0
^{15}N -AIR	135.0/136.0

4.2.3 HBI synthase – fate of 1'-C of AIR

Having figured out that 1'-C of AIR is not incorporated into 5-HB, we wanted to determine the fate of 1'-C of AIR. HBI synthase reactions were performed with 1',2',3',4',5'-¹³C₅-AIR. NMR analysis of the small molecule pool of these HBI synthase reactions showed a unique signal that was observed in ¹³C-NMR (Figure 4.6) and DEPT 90 NMR (Figure 4.6D - 4.6F). The ppm shift and the observation of the DEPT 90 signal suggested the possible product could be formate (**5**). In order to confirm this, we spiked in a reference standard of formate (**5**) (final concentration 50mM) in the full reaction. This matched with the signal at 172 ppm in ¹³C-NMR (Figure 4.6D) and DEPT 90 NMR (Figure 4.6A). This suggests that the 1'-C of AIR is lost as formate (**5**).

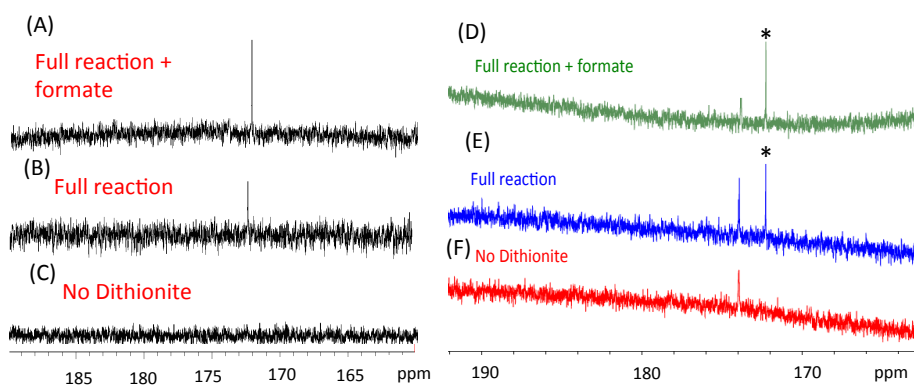
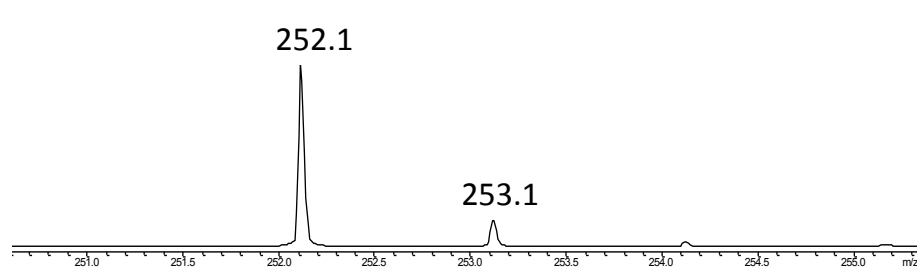


Figure 4.6: HBI synthase – fate of 1'-C of AIR (A-C) DEPT 90 NMR of small molecule pool of HBI synthase reactions with 1',2',3',4',5'-¹³C₅-AIR. (A) HBI synthase reaction with 1',2',3',4',5'-¹³C₅-AIR in presence of SAM, reductant. The reactions were spiked in with formate (10mM) after 2hrs. (B) HBI synthase reaction with 1',2',3',4',5'-¹³C₅-AIR in presence of SAM, reductant (C) No Dithionite – control. HBI synthase reaction with 1',2',3',4',5'-¹³C₅-AIR in presence of SAM and absence of dithionite. (D-F) ¹³C NMR of small molecule pool of HBI synthase reactions with 1',2',3',4',5'-¹³C₅-AIR. (D) Green – Full reaction + 50mM formate. (E) Blue – Full reaction. (F) Red – No Dithionite control.

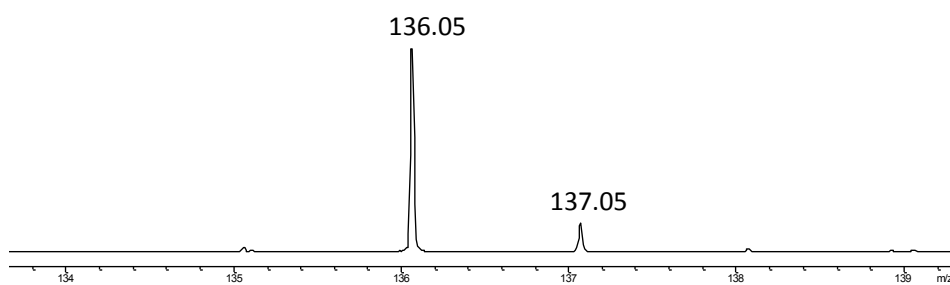
4.2.4 HBI synthase reactions with ^2H -labeled AIR isotopomers

HBI synthase reactions with ^{13}C -labeled AIR were analyzed by LCMS. Figure 4.7 - Table 4.2 summarizes the results. The reactions of HBI synthase with $5',5'\text{-}^2\text{H}_2\text{-AIR}$, followed by LCMS analysis suggested that the one of the deuterium atoms from $5',5'\text{-}^2\text{H}_2\text{-AIR}$ gets incorporated in to $5'$ -deoxyadenosine ($[\text{M}+\text{H}]^+=253.1$ Da) where as the other deuterium atom gets incorporated in 5-HB ($[\text{M}+\text{H}]^+=136.05$ Da). We then wanted to identify the preference of $5'$ -deoxyadenosyl radical to abstract pro R or pro S hydrogen atom from AIR. HBI synthase reactions with $5'\text{-R-}^2\text{H-AIR}$ revealed an $[\text{M}+\text{H}]^+=252.1$ Da for $5'$ -dA and $[\text{M}+\text{H}]^+=136.05$ Da for 5-HB indicating that the deuterium atom from $5'\text{-R-}^2\text{H-AIR}$ is not abstracted by $5'$ -deoxyadenosyl radical and is incorporated on the final product 5-HB. HBI synthase reactions with $5'\text{-S-}^2\text{H-AIR}$ revealed an $[\text{M}+\text{H}]^+=252.1/253.1$ Da for $5'$ -dA and $[\text{M}+\text{H}]^+=135.05$ Da/ 136.05 Da for 5-HB indicating that there is a preference for deuterium atom abstraction by $5'$ -dA radical from $5'$ pro S of AIR. Reactions with $4\text{-}^2\text{H-AIR}$ revealed that the deuterium atom from AIR is retained on the final product 5-HB and is not abstracted by $5'$ -dexoxyadenosyl radical. The mass spectrum of each of these results is shown in Figure 4.7.

(A) MS for 5'-dA



(B) MS for 5-HB



MS for 5'-dA

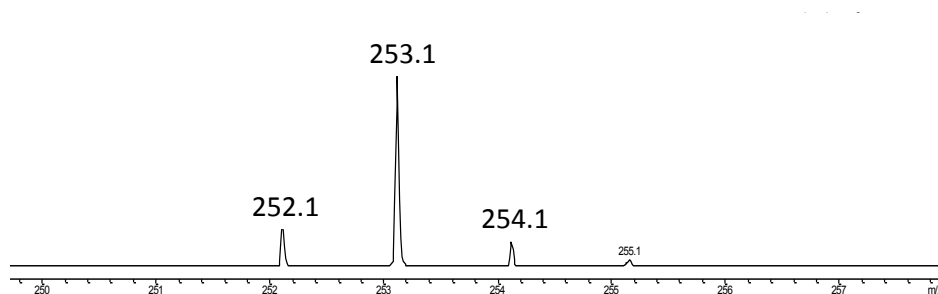
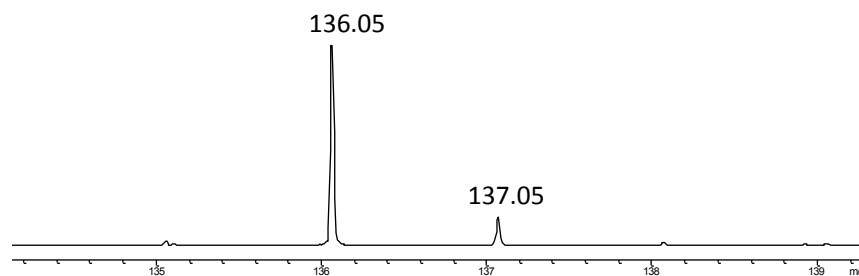
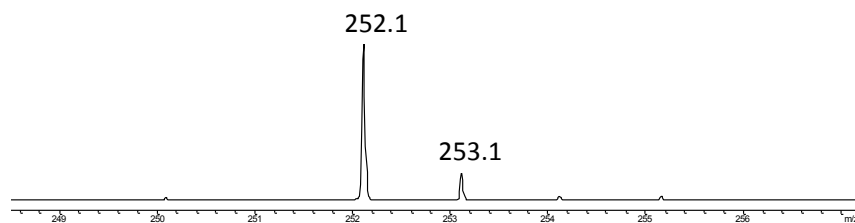


Figure 4.7: HBI Synthase reactions with ^2H -AIR. (A) HBI synthase reaction with AIR - MS for 5'-dA. (B) HBI synthase reaction with $5',5'\text{-}^2\text{H}_2$ -AIR - LCMS data for 5-HB and 5'-dA. (C) HBI synthase reaction with $5'\text{-R-}^2\text{H}$ -AIR - LCMS data for 5-HB and 5'-dA. (D) HBI synthase reaction with $5'\text{-S-}^2\text{H}$ -AIR - LCMS data for 5-HB and 5'-dA. (E) HBI synthase reaction with $4\text{-}^2\text{H}$ -AIR - LCMS data for 5-HB and 5'-dA.

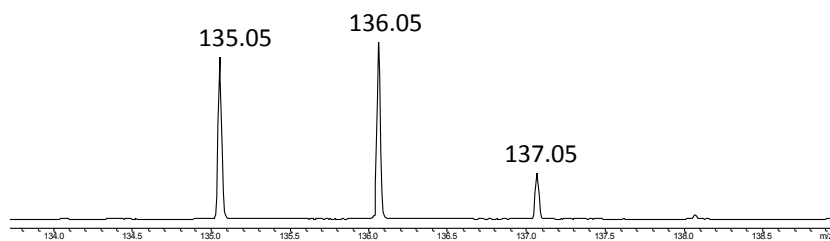
(C) MS for 5-HB



MS for 5'-dA



(D) MS for 5-HB



MS for 5'-dA

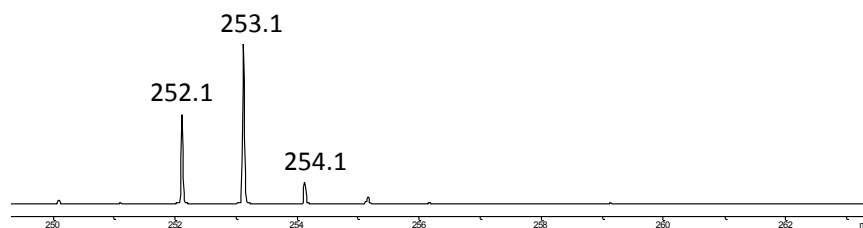
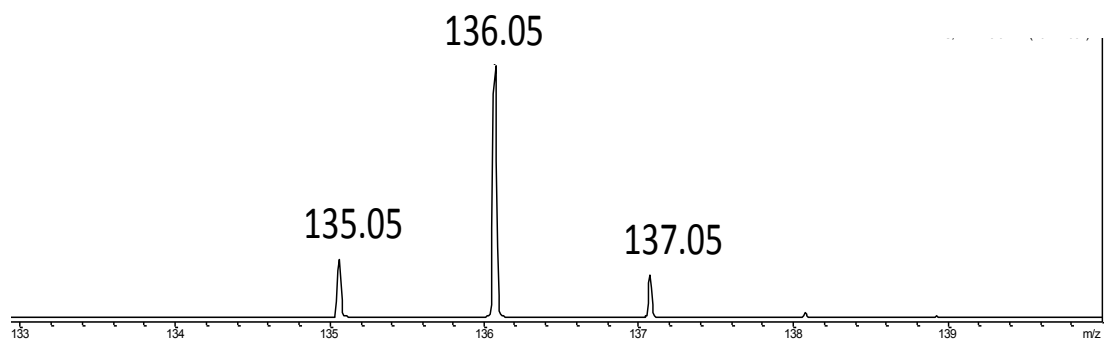


Figure 4.7 Continued.

(E)

MS for 5-HB



MS for 5'-dA

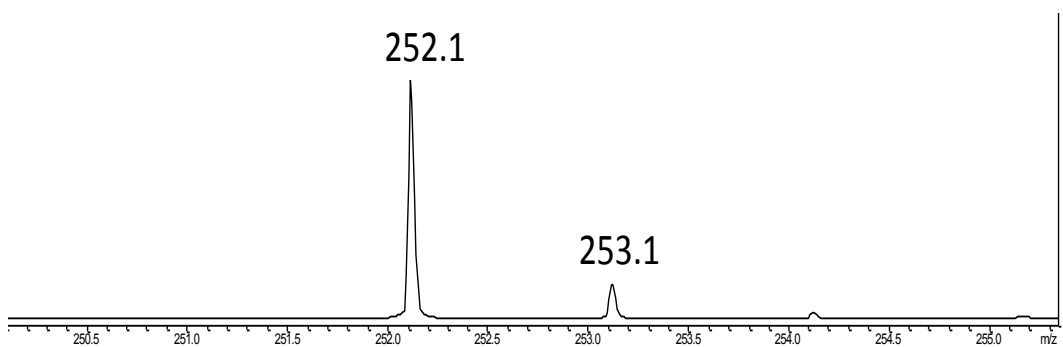


Figure 4.7 Continued.

Table 4.2 summarizes the LCMS studies of HBI synthase reaction with ^2H -AIR isotopomers. This table compiles and highlights the deuterium-labeling pattern on 5-HB and 5'-dA.

Table 4.2: HBI synthase reaction with ^2H -AIR isotopomers.

Substrate	5-HB $[\text{M}+\text{H}]^+ \text{ Da}$	5'dA $[\text{M}+\text{H}]^+ \text{ Da}$
Unlabeled AIR	135.0	252.0
5',5'- $^2\text{H}_2$ -AIR	136.0	253.0
5'-R- ^2H -AIR	136.0	252.0
5'-S- ^2H -AIR	135.0/136.0	252.0/253.0
4'- ^2H -AIR	135.0	252.0

This study shows that unlike ThiC where a single 5'dA radical sequentially abstracts 4' and 5' hydrogen atoms from AIR, in case of HBI synthase the 5'dA radical abstracts only the C5' hydrogen. There is a preference for the abstraction of pro S C5' hydrogen as compared to pro R C5'.

4.2.5 HBI synthase reactions with ^{15}N -AIR

AIR where the amino group was ^{15}N labeled was synthesized (^{15}N -AIR). HBI synthase reactions with ^{15}N -AIR followed by LCMS analysis revealed a mixture of 135.05 Da and 136.05 Da signals for 5-HB, there by indicating a mixture of ^{14}N and ^{15}N incorporated product in the final 5-HB (Figure 4.8).

MS for 5-HB

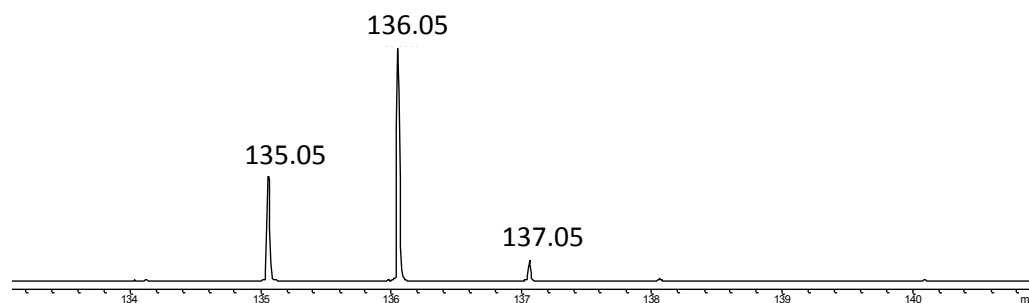


Figure 4.8: HBI synthase reaction with ^{15}N -AIR - LCMS data for 5-HB.

4.2.6 Characterization of labeling pattern on 5-HB

5-HB from HBI synthase reactions with AIR, 5',5'- $^2\text{H}_2$ -AIR, 4- $^2\text{H}_2$ -AIR and 2'- ^{13}C -AIR was isolated. ^1H -NMR was used to identify the location of label incorporation in 5-HB (Figure 4.9B-4.9F).

It can be seen that the ^1H NMR for the 5-HB isolated from the HBI synthase assays with unlabeled AIR (Figure 4.9C) matches with the standard 5-HB (Figure 4.9B). For the 5-HB isolated from the HBI synthase assays with 2'- ^{13}C -AIR, the doublet at 7.12 ppm splits into two doublets due to ^{13}C coupling to ^1H . This indicates that the carbon at 4 position of 5-HB generated has ^{13}C label. For the 5-HB isolated from the HBI synthase assays with 4'- ^2H -AIR, the doublet of doublet at 6.9 ppm almost vanishes, indicating ^2H incorporation at position 6 of the 5-HB isolated. For the 5-HB isolated from the HBI synthase assays with 5',5'- $^2\text{H}_2$ -AIR, the doublet 7.6 ppm vanishes, indicating ^2H incorporation at position 7 of the 5-HB isolated. The summary of the labeling pattern from these studies is demonstrated in Figure 4.9.

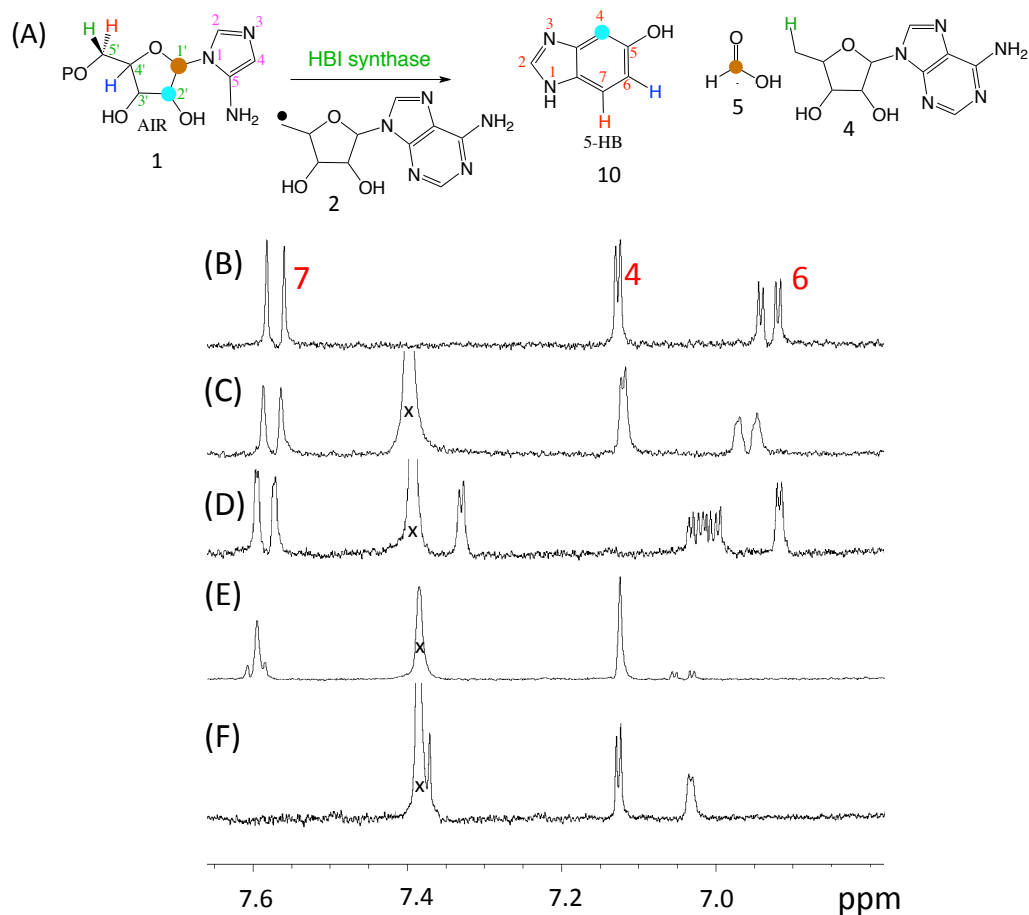


Figure 4.9: Characterization of the labeling pattern on 5-HB. (A) Summary of labeling pattern on 5-HB (B) ^1H NMR for 5-HB reference standard. (C)-(F): ^1H NMR of 5-HB purified from enzymatic reactions. Following were the substrates for each of these cases. (C) unlabeled AIR (D) $2'$ - ^{13}C -AIR (E) $4'$ - ^2H -AIR (F) $5',5'$ - $^2\text{H}_2$ -AIR.

4.2.7 Discussion

The aerobic and the anaerobic biosynthetic pathways for the corrinoid core in vitamin B₁₂ are extensively studied.⁶² The lower ligand of vitamin B₁₂ 5,6-dimethylbenzimidazole (**DMB, 8**) in the aerobic pathway involves a fascinating reaction catalyzed by BluB where FMN is converted to DMB in presence of oxygen (Figure 4.2). It was suggested that the aerobic and the anaerobic pathways are different for the DMB

biosynthesis.^{63,64} In case of the anaerobic pathway, previous feeding studies indicated that 5-HB and 5-hydroxy-6-methylbenzimidazole are the precursors to anaerobic DMB biosynthesis⁶⁹. Precursors to these benzimidazoles were identified as glycine and D-erythrose.^{63,65-67} Also, the gene(s) responsible for the biosynthesis of these precursors were unknown prior to our study.

We reconstituted HBI synthase as a radical SAM enzyme that catalyzes the conversion of AIR (**1**) to 5-HB (**10**). Our studies suggested that AIR was a direct precursor to 5-HB. This is consistent with the previous studies as D-erythrose is the precursor to ribose-5-phosphate. Also, glycine is a substrate of the phosphoribosylamine-glycine ligase, an enzyme on the AIR biosynthetic pathway (purine metabolism).

Several site-specifically isotopically labeled AIR were used to study the labeling pattern on 5-HB and 5'-dA. Table 4.1, Table 4.2 and Figure 4.9A summarize the labeling data for 5-HB (**10**). 1'-C of AIR does not get incorporated in 5-HB (**10**). It is converted to formate (**5**).

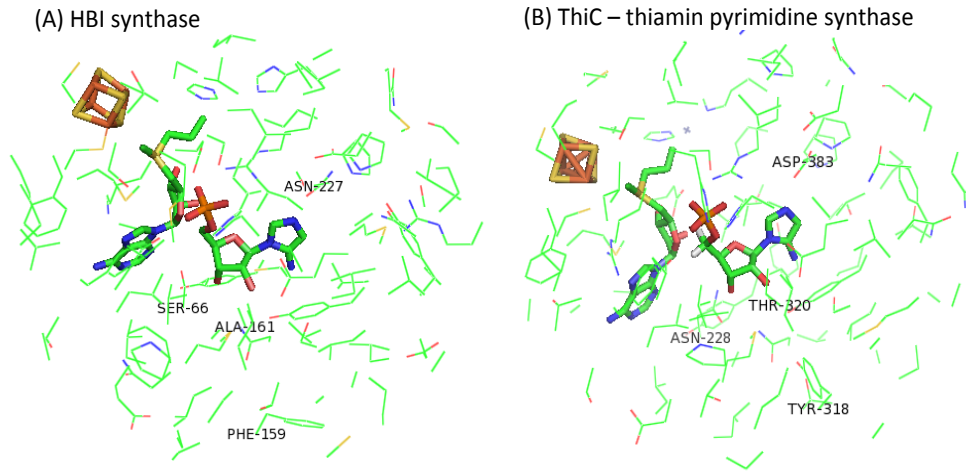
4.2.8 ThiC-HBI synthase homology model (Steve Ealick Lab, Cornell University)

We wanted to understand the structural details of HBI synthase. HBI synthase is homologous to thiamine pyrimidine synthase, ThiC. HBI synthase chemistry is similar to ThiC chemistry in terms of the generation of 5'-dA radical and abstraction of the pro S hydrogen atom by 5'-dA radical from C5' of AIR. However, two significantly different

molecules, 5-HB (**10**) and thiamin pyrimidine (**3**) are formed as final products in the HBI synthase and ThiC respectively.

We wanted to compare the active site of ThiC with HBI synthase to understand the differences in the reactivity. We have a high-resolution crystal structure of ThiC. A sequence alignment (Figure 4.10) and comparison of HBI synthase to ThiC demonstrates that most of the active site residues are conserved in HBI synthase. We made a homology model of HBI synthase based on ThiC structure (Figure 4.10A). Interestingly, the active site architecture remains very similar to ThiC. Key features that are different in HBI synthase are – serine in HBI synthase for an asparagine in ThiC between the AIR and SAM binding sites; alanine (HBI synthase) for threonine (ThiC) in the AIR ribose binding site, and a asparagine (HBI synthase) for aspartate (ThiC) in the imidazole binding site. This is an intriguing observation. We plan to study the mutant of HBI synthase with an intention to trap out reaction intermediates. We also plan to pursue structural studies on HBI synthase bound to 5-HB.

It is quite remarkable that based on the homology model (Figure 4.10), the active site architecture of HBI synthase remains very similar to ThiC considering that two significantly different molecules, 5-HB (**10**) and thiamin pyrimidine (**3**) are formed as final products in the HBI synthase and ThiC respectively.



(C)

	1	10	20	30	40	50	60	70	80	90	100	110	120	130
ThiC-1	----- ----- ----- ----- ----- ----- ----- ----- ----- ----- ----- ----- ----- ----- -----													
ThiC	----- ----- ----- ----- ----- ----- ----- ----- ----- ----- ----- ----- ----- ----- -----													
A.t. ThiC	NRASVHCTLHSLVYVCNKHNSGARKPLMSSLLPGFDVYVQAAATRFKKEITTTTRATLTFDPPPTTNSERAKQRKHTIDPSSPDFQIPSPFEECFPKSTKEHKVYVHEESGHVLYKPPFRVHLSGGEPAFDNY													
Consensus													
	131	140	150	160	170	180	190	200	210	220	230	240	250	260
ThiC-1	----- ----- ----- ----- ----- ----- ----- ----- ----- ----- ----- ----- ----- ----- -----													
ThiC	----- ----- ----- ----- ----- ----- ----- ----- ----- ----- ----- ----- ----- ----- -----													
A.t. ThiC	MKTQVEHVDGIIIEQHATVVAHDELSPEYIRTVHAEKIVIPNN-SNSTPKPVGIGKGLRTKVNASIGTSSDVTNYQAEVYRKATAEQAGADTLNELS ATLNEHAROGIITOTLRQAAIEGVDAEHLRARVAGTACIHNKVRKNGKPLAVGKGNSTKVNANIGTSKDOTSDNEHEKRVAVRAGAAHLDLS													
Consensus													
	261	270	280	290	300	310	320	330	340	350	360	370	380	390
ThiC-1	----- ----- ----- ----- ----- ----- ----- ----- ----- ----- ----- ----- ----- ----- -----													
ThiC	----- ----- ----- ----- ----- ----- ----- ----- ----- ----- ----- ----- ----- ----- -----													
A.t. ThiC	VGNLDRVREYLAAYNLVYGVPLVQAFCDATKRYGSAD-KLQPEELFOLTEQACEDGLAFMAIHGINRYITELRKHRYVGLVSKGGTSMSVSHNEHNRENPLVEQFDVRYVAILKKYDVCISLGN TGGPIDEIARRIETDQACIGSVPLVQARVDTIRAKKKRHYQHTYDETFDGIKKHLDGVDFTVHCGVTQITLDRMDREG-RHMDVSRGGSFTRAKHAFNKRENPLVEHFDLLELYRVDVLSLGN													
Consensus													
	391	400	410	420	430	440	450	460	470	480	490	500	510	520
ThiC-1	----- ----- ----- ----- ----- ----- ----- ----- ----- ----- ----- ----- ----- ----- -----													
ThiC	----- ----- ----- ----- ----- ----- ----- ----- ----- ----- ----- ----- ----- ----- -----													
A.t. ThiC	GLRGRADHSDHRAHQELTWCLEAQLGREGGCMVEGPGAMPDIEVFNILIAKRNHAPYMLGPISIDVVPQGDHSSRATGAAHQARYGADLCIYTPAEHLALPNEDDVRSQVREARYATYTG GFRPGLHARARQIQELLLGELTNRADHREIQPIEGPAPVDAQKKNIELQKPYEAGAPPYMLGPLYOLARVYHITLCAIGLARRSSGADPLCYVTPSEHLCLPNQDVAHEGVIASRATARRA GLRPSIYDANDTQAFELLTQELTIRARMEKQVQVNEGPGAPPHKIPENHOKLEMCNEAPEYTLGLTDTAPGYDHTSATGAAHTGALGLCYITPKHCLPNQDVAHEGVIASRATARRA GIKpG_ihDa_DrAQ_qELLi_gELt_raw#_#_Qv#_EGPGHvPd_!_aM!_!_Ok_!_cneAPXY_LGPI_TD_apGzDHTsATIGa_a_a_GadLICyITP_EHL_LPN_#Dv_GVIA_r1Asha													
Consensus													
	521	530	540	550	560	570	580	590	600	610	620	630	640	650
ThiC-1	----- ----- ----- ----- ----- ----- ----- ----- ----- ----- ----- ----- ----- ----- -----													
ThiC	----- ----- ----- ----- ----- ----- ----- ----- ----- ----- ----- ----- ----- ----- -----													
A.t. ThiC	DANKYDKGROROKRASKARQLQDKQFELALNPEQARQVRSRLPEEHS---CTHCG-NFCARNG-SKTLFDGDLQGDKC DVIKQVPGATEKHARAKKDLNEQFELSDLPYKARERRESKRADEHGA---CTHCG-DLCRVKYNDEEREELQKAS													
Consensus													

Figure 4.10: HBI synthase homology model based on ThiC structure. (A) Proposed active site of HBI synthase (ThiC-1 - *Desulfuromonas acetoxidans*) homology model to thiamine pyrimidine synthase (B) *Arabidopsis thaliana* ThiC - Thiamine pyrimidine synthase active site. The active site residues that differ in HBI synthase as compared to ThiC are labeled in this figure. (C) Sequence alignment of A.t. ThiC, D.a. ThiC and D.a. ThiC-1

4.2.9 Mechanistic proposal for HBI synthase catalyzed reaction

A mechanistic proposal consistent with our studies is shown in Figure 4.11.

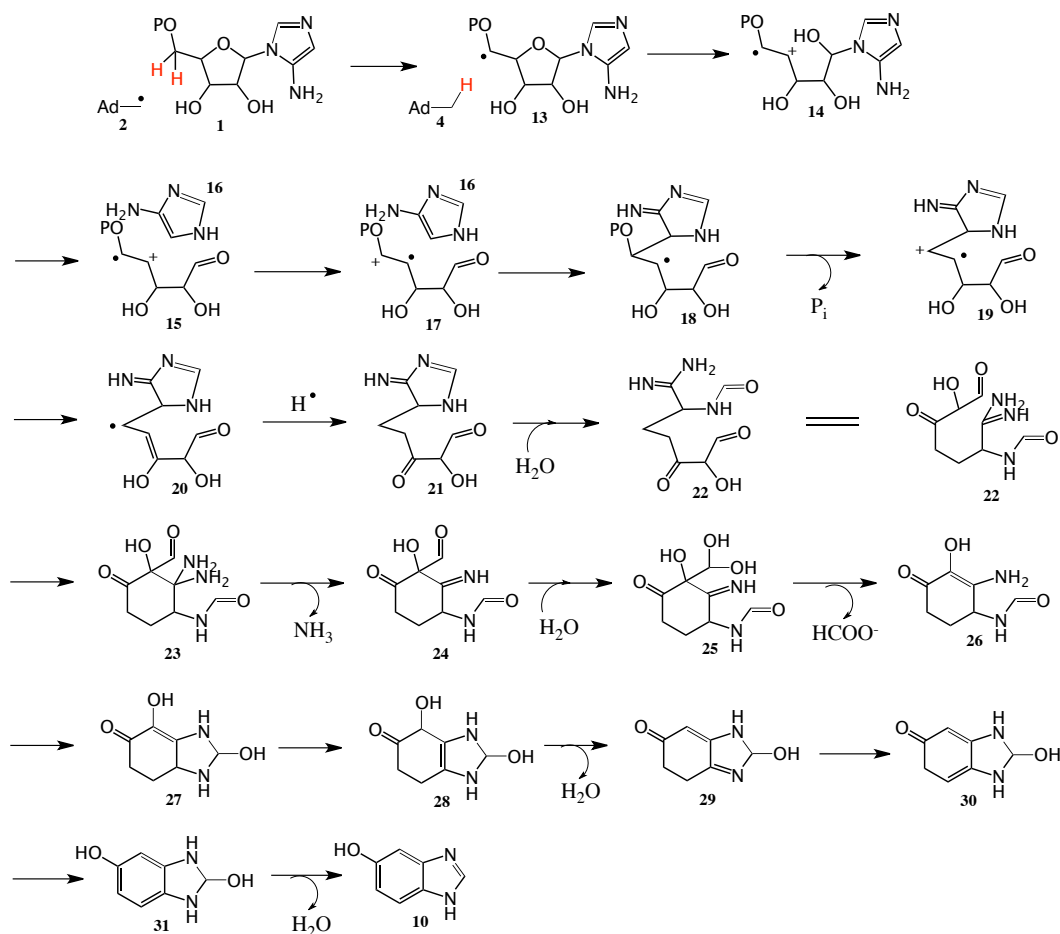


Figure 4.11: Mechanistic proposal for the HBI synthase catalyzed reaction.

In the first step, water attacks the C2 of AIR and opens up the heterocycle. A 5'-deoxyadenosyl radical (**2**) abstracts a pro S hydrogen atom AIR to generate a radical intermediate (**13**). β bond cleavage results in the formation of radical cation (**14**). The

cleavage of the C-N bond, followed by the C-C bond formation to connect the ribosyl part to the imidazole, gives intermediate **(15, resonance form 17)**. Nucleophilic attack at C5' connects **(16)** and **(17)** by a C-C bond to give **(18)**. Loss of phosphate gives **(19)**. Deprotonation, transfer of electron back to the [Fe-4S] cluster, tautomerization and addition of water gives **(22)**. Ring closure and loss of formate gives **(26)**. Ring closure followed by tautomerization and loss of water gives **(29)**. Tautomerization and loss of water gives the final compound **(5-HB, 10)**. The hypothetical intermediate **(23)** can be used to understand the scrambling of ^{15}N in 5-HB in the HBI synthase reactions with ^{15}N -AIR.

4.3 Conclusion

We identified and reconstituted hydroxybenzimidazole synthase involved in vitamin B₁₂ biosynthesis has solved an old and important puzzle in the anaerobic vitamin B₁₂ biosynthesis. Our studies suggested that AIR was a direct precursor to 5-HB. This is consistent with the previous studies as D-erythrose is the precursor to ribose-5-phosphate. Also, glycine is a substrate of the phosphoribosylamine-glycine ligase, an enzyme on the AIR biosynthetic pathway (purine metabolism).

Several site-specifically isotopically labeled AIR were used to study the labeling pattern on 5-HB and 5'-dA. Table 4.1, Table 4.2 and Figure 4.9A summarize the labeling data for 5-HB **(10)**. 1'-C of AIR does not get incorporated in 5-HB **(10)**. It is converted to formate **(5)**. We advance a mechanistic proposal consistent with our studies.

We are currently investigating the mechanistic details of this reaction using mechanistic probe molecules and X-ray crystallography

4.4 Experimental

4.4.1 Over-expression and purification of HBI synthase

The nucleotide sequence of *Desulformonas acetoxins* ThiC homolog (HBI synthase) clustered with vitamin B₁₂ biosynthetic genes was synthesized and cloned in THT vector (pET 28 vector that has a TEV protease cleavage site for removing the Histag). HBI synthase was co-expressed in the presence of a plasmid encoding the *suf* operon for in vivo [4Fe-4S] reconstitution in *E. coli* BL21 (DE3). An overnight 15 ml culture was grown in LB media in the presence of kanamycin (40mg/L) and chloramphenicol (25mg/L). This was then added to a minimal media (containing M9 minimal salts 1X, 27ml of 50% glucose, 7ml of 1M MgSO₄, 200µl of 1M CaCl₂, 40mg/L kanamycin and 25mg/L chloramphenicol. The cultures were incubated at 37⁰C with shaking (180 rpm) until the OD₆₀₀ reached 0.6 to 0.65. The cultures were then incubated at 4⁰C without shaking for 3 hrs. Then 50 mg of ferrous ammonium sulfate and 50 mg of cysteine were added. This was followed by induction of the culture with 70 µM IPTG. The culture was then incubated at 15⁰C with shaking (50 rpm) for 18 - 20hrs. The cultures were then incubated at 4⁰C for 3 hrs without shaking. The cells were then harvested and stored in liquid nitrogen overnight before enzyme purification. For enzyme purification, the cell pellets were thawed at room temperature in an anaerobic chamber and suspended in lysis buffer (100 mM Tris-HCl, pH 7.5) in the presence of

2mM DTT, lysozyme (0.2 mg/ml) and benzonase (100 units). This mixture was then cooled in an ice-bath for 2 hrs. The suspension of cells was then sonicated and centrifuged to give the cell-free extract. The enzyme was then purified using standard Ni-NTA chromatography. The column was first incubated with the lysis buffer. The cell-free extract was then passed over the column, which was then washed with 8-9 column volumes of wash buffer (100 mM Tris-HCl, 300 mM NaCl, 20 mM imidazole, 2mM DTT, pH 7.5). The enzyme was then eluted using 100 mM Tris-HCl, 300 mM NaCl, 250 mM imidazole, 2 mM DTT, pH 7.5. The purified enzyme was buffer exchanged into 100 mM potassium phosphate, 30% glycerol, 2 mM DTT, pH 7.5 using an Econo-Pac 10DG desalting columns (commercially available from *Bio-RAD*) and the purified enzyme was stored in liquid nitrogen. The protein as isolated binds to a [4Fe-4S] cluster as indicated by the UV-Vis spectrum shown in Figure 4.3A.

4.4.2 HBI synthase assays for LCMS and HPLC purification of 5-HB

HBI synthase (120 μ M) was incubated with dithionite (10mM), AIR (5mM), SAM (7mM) at room temperature for 60min. Controls were set up where either of AIR, SAM, dithionite or HBI synthase is absent. The protein was filtered out using 10kDa cut off filters and the small molecule pool was analyzed by HPLC and LCMS. These assays were done with unlabeled AIR, 5',5'-²H₂-AIR, 4-²H₂-AIR, 1',2',3',4',5'-¹³C₅-AIR, 5'-R-²H-AIR, 5'-S-²H-AIR, 1'-¹³C-AIR, 2'-¹³C-AIR, 3'-¹³C-AIR.

Same assay conditions were used for the purification of 5-HB for NMR characterization. These assays were done with unlabeled AIR, 5',5'-²H₂-AIR, 4-²H₂-AIR, 2'-¹³C-AIR.

4.4.3 Enzymatic assays for NMR analysis to determine the fate of 1'-C of AIR

HBI synthase (800μM) was incubated with dithionite (50mM), 1',2',3',4',5'-¹³C₅-AIR (20mM), SAM (30mM) at room temperature for 60min. Controls were set up where either of AIR, SAM, dithionite or HBI synthase are absent. The protein was filtered out using 10kDa cut off filters. The small molecule pool was analyzed by ¹³C and DEPT 90 NMR experiments.

4.4.4 HPLC conditions for co-elution experiment and purification of 5-HB

HPLC -1260 series Agilent. LC-18 column - ((Supelcosil LC-18-T column (15cm x 3mm, 3μm)). Following gradient was used: A: water, B: 5mM ammonium formate, C: methanol. Following gradient was used - 0 min: 100%B; 7 min: 100%B; 25 min: 7%A, 70%B, 23%C; 27 min: 25%A, 75%C; 29 min - 25%A, 75%C; 30 min: 100%B; 45 min – 100%B).

4.4.5 LCMS conditions for HBI synthase assays

HPLC conditions - HPLC - 1260 series Agilent. LC-18 column - ((Supelcosil LC-18-T column (15cm x 3mm, 3μm)). Following gradient was used - A: 5mM ammonium

formate, B: 75% methanol and 25% water. Following gradient was used - 0 min: 100% A; 7 min: 100% A; 25 min: 70% A, 30% B; 26 min: 100% B; 28 min – 100% B; 29 min: 100% A; 40 min – 100%A). MS conditions for LCMS experiments - Capillary, -4500 V; Capillary offset, -500 V; Nebulizer gas, 3.0 bar; Dry gas, 10.0 L/min; Dry gas temperature, 200°C; Funnel 1 RF, 200.0 Vpp; Funnel 2 RF, 250.0 Vpp; ISCID, 0.0 eV; Hexapole RF, 200 Vpp; Quadrupole, Ion energy, 5.0 eV; Low mass, 100 *m/z*; Collision cell, collision energy, 10.0 eV; Collision RF, 150.0 Vpp, Transfer time, 100.0 μ s; Prepulse storage, 5.0 μ s. Data was processed with DataAnalysis ver. 4.0 SP4

4.4.6 Synthetic scheme for AIRs (36)²⁷

The synthetic scheme for AIRs (36) is shown in Figure 4.12. Dr. Sameh H.

Abdelwahed synthesized all the labeled AIRs isotopomers.

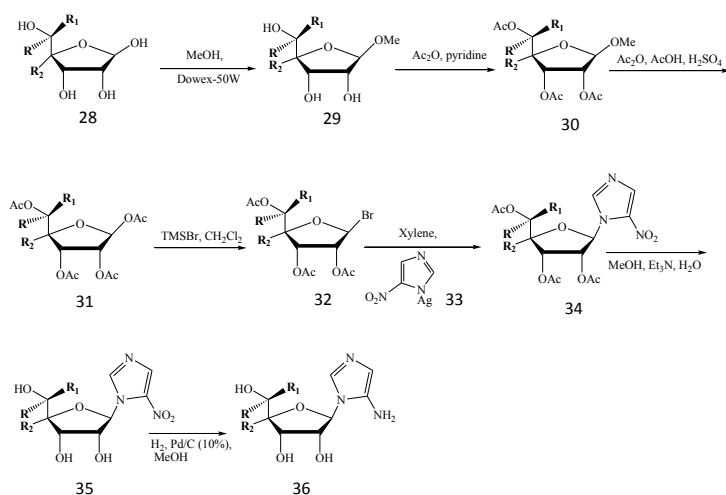


Figure 4.12: Synthetic scheme for AIRs (36).

4.4.7 Synthesis of methyl a/b-D-ribofuranoside (29)

Methyl a/b-D-ribofuranoside (1.4 g, 8.5 mmol) was coevaporated twice with deuterium oxide (99.8 % atom D, 5.00 ml each) and dissolved in the same solvent (28 ml), deuterated Raney-Ni (settled volume: 15 ml) was added with bubbling Argon through the mixture for 10 min. The reaction mixture was refluxed with stirring at 110°C in an oil bath for 7 days in an atmosphere of Argon. The mixture was filtered through celite, washed with water, and the combined aqueous phases were evaporated to give an oily product (0.52, 51%). ¹H NMR (acetone-d₆ + D₂O, 300 MHz) δ 4.71(s, 1H), 3.55 (s, 0.5H), 3.27 (s, 3H); ¹³C NMR (acetone-d₆, 75 MHz) δ 108.8, 103.4 (C1), 84.1 (C4), 74.9 (t, J = 23.1), 71.4 (t, J = 22.2 Hz), 62.5 (quintet, J = 20.4 Hz), 54.7.

¹H-NMR (D₂O) (a): 4.92 (s, 1H) H-1; 4.02 (s, 0.3H) H-4; 3.37 (s, 3H) OCH₃; (b) 4.83 (s, 1H) H-1; 3.93 (s, 0.7H) H-4; 3.33 (s, 3H) OCH₃. ¹³C-NMR (D₂O) (a): 103.5 C1; 84.9 C4; 55.8 OCH₃; (b): 108.3 C1; 83.1 C4; 55.52 OCH₃.

4.4.8 Synthesis of 1-O-Methyl-2,3,5-tri-O-acetyl-a/b-D-ribofuranoside (30)

To a cooled (ice-bath) solution of **29** (0.3 g, 1.75 mmol) in anhydrous pyridine (5 ml) acetic anhydride (0.5 ml, 564 mg, 5.48 mmol) was added with stirring. The stirring was continued for 4 hr. at room temperature. Usual work-up and drying gave a thick oil (0.4 g, 80%). (b): 4.87 (s, 1H) H-1; 4.09 (d) H-4; 3.40 (s, 3H) OCH₃; (a) 5.10 (s, 1H) H-1; 4.29 (d) H-4; 3.37 (s, 3H) OCH₃; 2.11 - 2.06 (3xs, 9H) 3xOAc (a+b)

4.4.9 Synthesis of 1,2,3,5-tetra-O-acetyl- α/β -D-ribofuranoside (**31**)

(0.4 g, 1.39mmol) of **30** was dissolved in glacial acetic acid (10ml) and acetic anhydride (1.4 ml, 1.56mmol) and treated with sulfuric acid (0.2 ml) with ice-cooling. After 3 h at room temperature, the solution was stirred with ice-water, extracted with chloroform, washed with water, then aqueous sodium hydrogen carbonate, dried over MgSO₄ and evaporated to give compound **31** as pale yellow syrup (0.4 g, 92 %). ¹H-NMR of main components (CDCl₃): (b): 6.16 (s, 1H) H-1; 4.36 (s) H-4# (a): 6.42 (s, 1H) H-1; 4.44 (s) H-4#; 2.2 -2.1 (4xs, 12H) 4xOAc (a+p). For mix of anomers : ¹H NMR (CDCl₃, 300 MHz) d 6.32, 6.06 (s, 1H), 4.34, 4.27 (s, 0.5 H), 2.07 (s, 3H), 2.01 (s, 3H), 1.96 (s, 3H)

4.4.10 Synthesis of 5-nitro-1-(2,3,5-tri-O-acetyl- β -D-ribofuranoside (**34**)

To a solution of **31** (0.4 g, 1.26 mmol) in dichloromethane (5 mL) at -76°C, bromotrimethylsilane (1.5 mL, 10.9 mmol) was added dropwise and the temperature was allowed to rise to room temperature overnight. Bromo trimethylsilane and trimethylsilyl acetate were removed in vacuo at 20°C. The crude product was dissolved in 5 mL of dry xylene. This solution was then added dropwise to a mixture of the silver salt of 4-nitroimidazole (0.5 g, 2.2 mmol) in xylene (12 mL) at reflux. The reaction mixture was refluxed for 1 h, cooled, and filtered. The solvent was evaporated in vacuo (45 °C bath) and the residue dissolved in 10 mL CHCl₃. The solution was washed (NaHCO₃, H₂O), dried (MgSO₄), and concentrated. The product was purified by flash column chromatography (1 : 1 ethyl acetate : hexanes) to give 120 mg of a colorless oil

(26%). ¹H NMR (CDCl₃, 300 MHz) δ 8.11 (s, 1H), 8.04 (s, 1H), 6.45 (s, 1H), 4.48 (s, 0.5H), 2.17 (s, 3H), 2.16 (s, 3H), 2.06 (s, 3H).

4.4.11 Synthesis of 5-nitro-1-(β -D-ribofuranoside)imidazole (35)

34 (120 mg, 0.32 mmol) was dissolved in methanol (2 mL), and water (0.8 mL) and triethylamine (0.8 mL) were added. The mixture was stirred for 12 h at room temperature and the solvent was removed in vacuo. The residue was dissolved in 2 mL of water and lyophilized to provide 80 mg (99%) of a pale yellow oil. ¹H NMR (MeOD, 300 MHz) δ 8.54 (s, 1H), 7.91 (s, 1H), 6.20 (s, 1H), 3.98 (s, 0.5H).

4.4.12 Synthesis of 5-amino-1-(β -D-ribofuranoside)imidazole (36)

35 (80 mg, 0.33 mmol) was dissolved in anhydrous methanol (30 mL). 30 mg of 10% Pd/C was added and the mixture was hydrogenated at atmospheric pressure and room temperature for 3 h. The catalyst was removed by filtration and solvent removed in vacuo to give a colorless oil (100%). ¹H NMR (D₂O, 300 MHz) δ 7.60 (s, 1H), 6.43 (s, 1H), 5.66 (s, 1H), 4.12 (s, 0.5H)

C-labeled AIR analogs: [1'-¹³C]AIRs and [3'-¹³C]AIRs were made from [1-¹³C]ribose and [3-¹³C]ribose respectively by the same procedure described above and then enzymatic phosphorylated.

5. SUMMARY AND OUTLOOK

5.1 Summary

The studies presented in this dissertation provide insightful details in the early steps of molybdopterin biosynthetic pathway. Mechanistic details of the complex radical rearrangement reaction catalyzed by MoaA were elucidated.^{38,41,45} Studies on thiamin pyrimidine synthase, ThiC resulted in the completion of product labeling studies. Bioinformatics investigations on ThiC resulted in the identification and first report of the in vitro reconstitution of the elusive benzimidazole biosynthesis in the anaerobic vitamin B₁₂ biosynthetic pathway.

5.1.1 Molybdopterin biosynthesis

The genes responsible for molybdopterin biosynthesis have been known since 1980s. However, the chemical details of the early steps of this biosynthetic pathway were yet to be elucidated.³² The biosynthesis of molybdopterin is similar in plants, animals and microorganisms. The first steps in the molybdopterin biosynthesis are catalyzed by MoaA and MoaC use guanosine-5'-triphosphate (**1**; GTP) as the precursor to synthesize cyclicpyranopterininmonophosphate (cPMP). Previous labeling studies had established that in the conversion of GTP to cPMP by MoaA-MoaC, the C8 of GTP is inserted between the C2' and C3' carbons. This is an unprecedented reaction catalyzed in ribose chemistry. Also, it was shown that MoaA is a member of the radical-SAM superfamily of proteins and harbors two [4Fe-4S]^{2+,1+} clusters. The N-terminal [4Fe-4S]

cluster is likely to be responsible for the reductive cleavage of SAM to the 5'-deoxyadenosyl (5'-dA) radical and L-methionine and the second cluster binds to N1 of GTP. A 2.35 Å crystal structure of MoaA shows the two clusters at the active site as well as the orientation of 5'-deoxyadenosine (5'dA) as compared to GTP.²⁹⁻³¹

We demonstrated that MoaA catalyzes the first step in molybdopterin biosynthesis where guanosine-5'-triphosphate (GTP, **1**) is converted to pterin (**15**, Figure 5.1).⁴¹ Meanwhile, a study from Kenichi Yokoyama's lab suggested that (**4**) was the product of MoaA.⁴⁴ We expressed MoaA in *E. coli* (MoaC⁻) and showed that we formed pterin as the product of MoaA. This provided the first conclusive evidence that pterin (**15**) was the product of MoaA. Thus, we demonstrated that MoaA catalysis involves a remarkable rearrangement reaction where the C8 of GTP is inserted between the C2' and C3' carbon atoms of GTP to give the final pterin (**15**).⁴¹

To get mechanistic insights in to the MoaA-catalyzed chemistry, we identified the position of hydrogen atom abstraction by 5'-deoxyadenosyl radical. We used 2',3'-dideoxyGTP as a substrate analog and trapped a novel intermediate (**27**). We further trapped the radical (**2**) by using 2'-chloroGTP. We characterized the products of MoaA reaction with 2'-chloroGTP.⁴¹

We decided to explore the use of 2'-deoxyGTP to probe the later steps of the reaction. MoaA reaction with 2'-deoxyGTP resulted in the formation of a stereo-specific product pterin. This suggested that the formation of this pterin was primarily or exclusively occurring at the MoaA active site because non-enzymatic chemistry would

result in the scrambling of stereochemistry at C3 of the pterin substituent. This study clarified the later step of MoaA-catalyzed transformation.

Based on all these studies we revised our mechanistic proposal for the MoaA-catalyzed reaction (as outlined in Figure 5.1)⁴¹

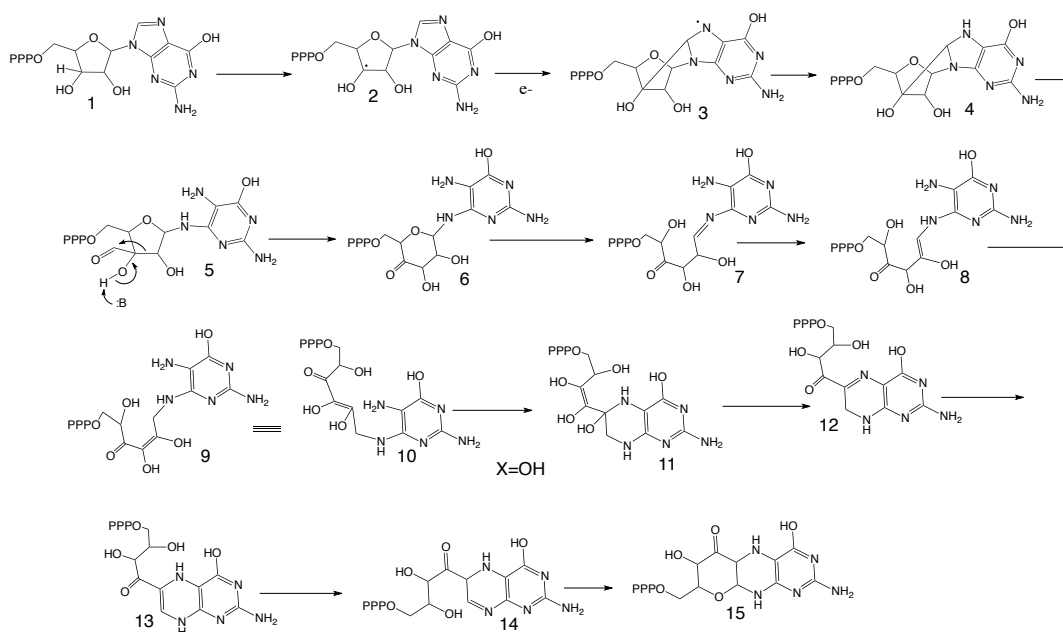


Figure 5.1: Mechanistic proposal for MoaA-catalyzed transformation

5.1.2 Thiamin pyrimidine synthase – ThiC

We demonstrated that one of the C5' hydrogens of HMP-P was derived from the adenosyl radical. This completed the identification of the origin of all of the atoms generated in the complex ThiC-catalyzed rearrangement reaction. We have previously demonstrated that adenosyl radical abstracts the proS hydrogen from the C5 position of

AIR (unpublished). At some point during the reaction, 5'dA transfers the hydrogen atom on to AIR derived intermediate, which eventually forms HMP-P. The HMP-P stereochemistry demonstrates that this hydrogen atom abstraction occurs from the si face of the radical resulting in overall retention of stereochemistry for the C5' hydrogen atom replacement reaction.

We performed several active-site mutant studies with a view to trap and characterize intermediates in the ThiC catalyzed reaction. In case of some of the mutants, AIR derived intermediates can be detected. However, trace levels of products are formed thus making it impossible for complete NMR characterization of these products.

5.1.3 Anaerobic vitamin B₁₂ biosynthesis – hydroxybenzimidazole biosynthesis

In our pursuit to study the mechanistic details of the ThiC catalyzed transformation, we decided to investigate ThiC homologs from different organisms that work better or catalyze different, more tractable chemistry. Bioinformatics search for thiamin biosynthetic genes (in particular ThiC) in the SEED database (<http://theseed.uchicago.edu/FIG/index.cgi>) revealed that there are several microorganisms that have more than one copies of ThiC. From the set of organisms that have multiple copies of ThiC, we observed that there is a subset of organisms where one of these copies of ThiC (which we named as ThiC*) was clustered with vitamin B₁₂ biosynthetic genes. Also, many of these organisms are listed as anaerobic

microorganisms. Anaerobic biosynthesis of vitamin B₁₂ has been extensively studied.^{62-69,71,72} However, the gene product(s) responsible for the biosynthesis of the “lower ligand” of vitamin B₁₂ – dimethylbenzimidazole was (were) unknown.

We identified and reconstituted hydroxybenzimidazole synthase (HBI synthase) involved in vitamin B₁₂ biosynthesis has solved an old and important puzzle in the anaerobic vitamin B₁₂ biosynthesis. Our studies suggested that AIR was a direct precursor to 5-HB. This was consistent with the previous studies as D-erythrose is the precursor to ribose-5-phosphate. Also, glycine is a substrate of the phosphoribosylamine-glycine ligase, an enzyme on the AIR biosynthetic pathway (purine metabolism).

Several site-specifically isotopically labeled AIR were used to study the labeling pattern on 5-HB and 5'-dA. Based on these studies, we advanced a mechanistic proposal consistent with our studies so far.

The mechanistic proposal for HBI synthase-catalyzed transformation is shown in Figure 5.2

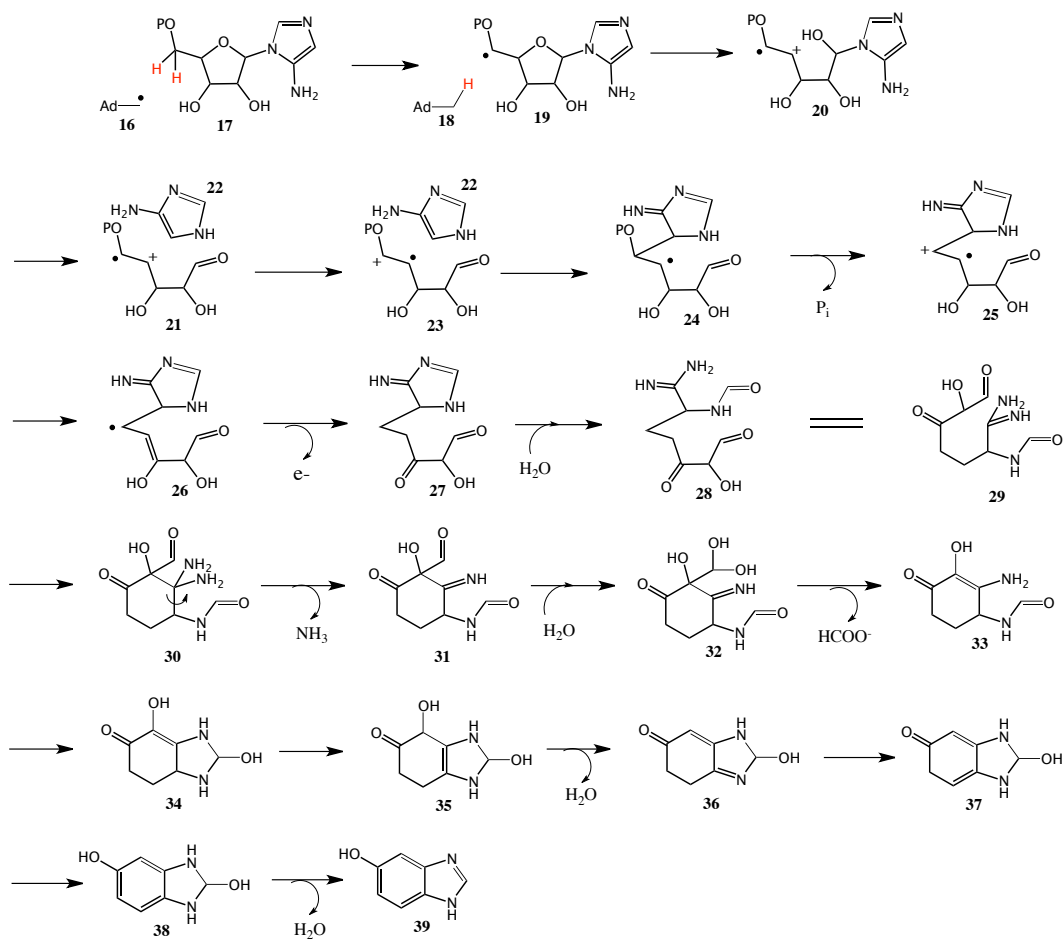


Figure 5.2: Mechanistic proposal for HBI synthase-catalyzed transformation

5.2 Outlook

Based on all our studies, my general opinion is that the critical step to study radical AdoMet enzymes is the robust reconstitution of [4Fe-4S] cluster and protein activity. This, to me, is the “corner stone” to proceed for performing mechanistic and structural studies on these enzymes.

5.2.1 Molybdopterin biosynthesis - crystallography

The crystal structure (2FB3) is not a particularly high-resolution structure (2.35Å). For example, the binding of the purine to the second iron sulfur cluster has been shown by Hoffman group using ENDOR spectroscopy to be incorrect. In addition, the binding site for the deoxyadenosine makes no sense in the context of a deoxyadenosyl radical abstracting a hydrogen atom from C3' of GTP. Therefore, it seems that the MoaA structure is not yet at the level where we can reliably predict residues involved in catalysis. High-resolution structure with GTP and SAM/SAH bound will be highly informative.

5.2.2 Thiamin pyrimidine synthase – ThiC – trapping of organic radicals

Rapid freeze quench followed by high-field EPR studies have been recently used by the Britt Lab to study organic radicals generated in the radical AdoMet enzymes.^{23,75} In our lab, we also have the synthetic expertise to make site-specifically labeled AIR isotopomers and make highly quality ThiC. With all these technical expertise, rapid freeze quench followed by high-field EPR studies seems to be a promising tool to study ThiC catalyzed chemistry.

5.2.3 Testing HBI synthase homologs– anaerobic vitamin B₁₂ biosynthesis

With a view to find a more robust HBI synthase homolog for crystallographic studies, it may be of value to screen HBI synthase homologs from different organisms.

5.2.4 HBI synthase – EPR studies

Rapid freeze quench followed by high-field EPR studies seems to be a promising tool to study HBI synthase catalyzed chemistry. Kinetic studies on HBI synthase are recommended before performing the EPR studies.

5.2.5 AIR analogs to study HBI synthase and ThiC reactions

Using substrate analogs has been significantly useful to elucidate the mechanistic details of MoaA catalyzed transformation.^{38,41,45} Testing AIR analogs with a view to trap out intermediates in the ThiC and HBI synthase reactions may be highly informative.

REFERENCES

- (1) Chatterjee, A.; Li, Y.; Zhang, Y.; Grove, T. L.; Lee, M.; Krebs, C.; Booker, S. J.; Begley, T. P.; Ealick, S. E. *Nat. Chem. Biol.* **2008**, *4*, 758.
- (2) Wuebbens, M. M.; Rajagopalan, K. V. *J. Biol. Chem.* **1995**, *270*, 1082.
- (3) Mahanta, N.; Fedoseyenko, D.; Dairi, T.; Begley, T. P. *J. Am. Chem. Soc.* **2013**, *135*, 15318.
- (4) Szu, P.-H.; Ruzsyczky, M. W.; Choi, S.-h.; Yan, F.; Liu, H.-w. *J. Am. Chem. Soc.* **2009**, *131*, 14030.
- (5) Kamat, S. S.; Williams, H. J.; Raushel, F. M. *Nature* **2011**, *480*, 570.
- (6) Kamat, S. S.; Williams, H. J.; Dangott, L. J.; Chakrabarti, M.; Raushel, F. M. *Nature* **2013**, *497*, 132.
- (7) Kudo, F.; Hoshi, S.; Kawashima, T.; Kamachi, T.; Eguchi, T. *J. Am. Chem. Soc.* **2014**, *136*, 13909.
- (8) Meunier, B.; de Visser, S. P.; Shaik, S. *Chem. Rev.* **2004**, *104*, 3947.
- (9) Nam, W. *Acc. Chem. Res.* **2007**, *40*, 522.
- (10) Banerjee, R.; Ragsdale, S. W. *Annu. Rev. Biochem.* **2003**, *72*, 209.
- (11) Frey, P. A.; Hegeman, A. D.; Ruzicka, F. J. *Crit. Rev. Biochem. Mol. Biol.* **2008**, *43*, 63.
- (12) Moss, M.; Frey, P. A. *J. Biol. Chem.* **1987**, *262*, 14859.
- (13) Lieder, K. W.; Booker, S.; Ruzicka, F. J.; Beinert, H.; Reed, G. H.; Frey, P. A. *Biochemistry* **1998**, *37*, 2578.

- (14) Cospser, N. J.; Booker, S. J.; Ruzicka, F.; Frey, P. A.; Scott, R. A.
Biochemistry **2000**, *39*, 15668.
- (15) Lepore, B. W.; Ruzicka, F. J.; Frey, P. A.; Ringe, D. *Proc. Natl. Acad. Sci. U. S. A.* **2005**, *102*, 13819.
- (16) McCarty, R. M.; Somogyi, A.; Lin, G.; Jacobsen, N. E.; Bandarian, V.
Biochemistry **2009**, *48*, 3847.
- (17) McCarty, R. M.; Bandarian, V. *Chem. Biol.* **2008**, *15*, 790–798.
- (18) McCarty, R. M.; Krebs, C.; Bandarian, V. *Biochemistry* **2013**, *52*, 188.
- (19) Dowling, D. P.; Bruender, N. A.; Young, A. P.; McCarty, R. M.;
Bandarian, V.; Drennan, C. L. *Nat. Chem. Biol.* **2014**, *10*, 106.
- (20) Shepard, E. M.; Duffus, B. R.; George, S. J.; McGlynn, S. E.; Challand,
M. R.; Swanson, K. D.; Roach, P. L.; Cramer, S. P.; Peters, J. W.; Broderick, J. B. *J. Am. Chem. Soc.* **2010**, *132*, 9247.
- (21) Tron, C.; Cherrier, M. V.; Amara, P.; Martin, L.; Fauth, F.; Fraga, E.;
Correard, M.; Fontecave, M.; Nicolet, Y.; Fontecilla-Camps, J. C. *Eur. J. Inorg. Chem.*
2011, 1121.
- (22) Kuchenreuther, J. M.; Myers, W. K.; Stich, T. A.; George, S. J.;
Nejatyjahromy, Y.; Swartz, J. R.; Britt, R. D. *Science* **2013**, *342*, 472.
- (23) Kuchenreuther, J. M.; Myers, W. K.; Suess, D. L. M.; Stich, T. A.;
Pelmenschikov, V.; Shiigi, S. A.; Cramer, S. P.; Swartz, J. R.; Britt, R. D.; George, S. J.
Science **2014**, *343*, 424.

- (24) Duffus, B. R.; Ghose, S.; Peters, J. W.; Broderick, J. B. *J. Am. Chem. Soc.* **2014**, *136*, 13086.
- (25) Decamps, L.; Philmus, B.; Benjdia, A.; White, R.; Begley, T. P.; Berteau, O. *J. Am. Chem. Soc.* **2012**, *134*, 18173.
- (26) Lawhorn, B. G.; Mehl, R. A.; Begley, T. P. *Org. Biomol. Chem.* **2004**, *2*, 2538.
- (27) Chatterjee, A.; Hazra, A. B.; Abdelwahed, S.; Hilmey, D. G.; Begley, T. *P. Angew. Chem., Int. Ed.* **2010**, *49*, 8653.
- (28) Coquille, S.; Roux, C.; Mehta, A.; Begley, T. P.; Fitzpatrick, T. B.; Thore, S. *J. Struct. Biol.* **2013**, *184*, 438.
- (29) Haenzelmann, P.; Schindelin, H. *Proc. Natl. Acad. Sci. U. S. A.* **2004**, *101*, 12870.
- (30) Hanzelmann, P.; Schindelin, H. *Proc. Natl. Acad. Sci. U. S. A.* **2006**, *103*, 6829.
- (31) Lees, N. S.; Hanzelmann, P.; Hernandez, H. L.; Subramanian, S.; Schindelin, H.; Johnson, M. K.; Hoffman, B. M. *J. Am. Chem. Soc.* **2009**, *131*, 9184.
- (32) Leimkuehler, S.; Wuebbens, M. M.; Rajagopalan, K. V. *Coord. Chem. Rev.* **2011**, *255*, 1129.
- (33) Hille, R. *Trends Biochem. Sci.* **2002**, *27*, 360.
- (34) Schwarz, G.; Mendel, R. R. *Annu. Rev. Plant Biol.* **2006**, *57*, 623.
- (35) Reiss, J.; Bonin, M.; Schwegler, H.; Sass, J. O.; Garattini, E.; Wagner, S.; Lee, H.-J.; Engel, W.; Riess, O.; Schwarz, G. *Mol. Genet. Metab.* **2005**, *85*, 12.

- (36) Schwarz, G.; Santamaria-Araujo, J.; Wolf, S.; Lee, H.J.; Adham I.M.; Grone H.; Schwegler, H.; Sass, J.O.; Otte, T.; Hanzelmann, P.; Mendel R.R.; Engel, W.; Reiss, J. *Hum. Mol. Genet.* **2004**, *13*, 1249-55.
- (37) Wuebbens, M. M.; Rajagopalan, K. V. *J Biol Chem* **1995**, *270*, 1082.
- (38) Mehta, A. P.; Hanes, J. W.; Abdelwahed, S. H.; Hilmey, D. G.; Hanzelmann, P.; Begley, T. P. *Biochemistry* **2013**, *52*, 1134.
- (39) Johnson, J. L.; Hainline, B. E.; Rajagopalan, K. V. *J Biol Chem* **1980**, *255*, 1783.
- (40) Santamaria-Araujo, J. A.; Fischer, B.; Otte, T.; Nimtz, M.; Mendel, R. R.; Wray, V.; Schwarz, G. *J. Biol. Chem.* **2004**, *279*, 15994.
- (41) Mehta, A. P.; Abdelwahed, S. H.; Xu, H.; Begley, T. P. *J. Am. Chem. Soc.* **2014**, *136*, 10609.
- (42) Johnson, J. L.; Wuebbens, M. M.; Rajagopalan, K. V. *J Biol Chem* **1989**, *264*, 13440.
- (43) Viscontini, M. *Methods Enzymol.* **1971**, *18*, 678.
- (44) Hover, B. M.; Lokszejn, A.; Ribeiro, A. A.; Yokoyama, K. *J. Am. Chem. Soc.* **2013**, *135*, 7019.
- (45) Mehta, A. P.; Abdelwahed, S. H.; Begley, T. P. *J Am Chem Soc* **2013**, *135*, 10883.
- (46) Stubbe, J.; Nocera, D. G.; Yee, C. S.; Chang, M. C. Y. *Chem Rev* **2003**, *103*, 2167.

- (47) Chatgililoglu, C.; Ferreri, C.; Terzidis, M. A. *Chem. Soc. Rev.* **2011**, *40*, 1368.
- (48) Greenberg M., D. E. *Radical and Radical Ion Reactivity in Nucleic Acid Chemistry. Wiley Series of Reactive intermediates in Chemistry and Biology.*, John Wiley & Sons, Inc., Hoboken, New Jersey.
- (49) Berger, A.; Schiltz, E.; Schulz, G. E. *Eur. J. Biochem.* **1989**, *184*, 433.
- (50) Eijkman, C. *Ned Tijdschr Geneeskde* **1990**, *134*, 1654.
- (51) Kluger, R. *Chem. Rev.* **1987**, *87*, 863.
- (52) Agyei-Owusu, K.; Leeper, F. J. *FEBS J.* **2009**, *276*, 2905.
- (53) Jurgenson, C. T.; Begley, T. P.; Ealick, S. E. *Annu. Rev. Biochem.* **2009**, *78*, 569.
- (54) Park, J.-H.; Dorrestein, P. C.; Zhai, H.; Kinsland, C.; McLafferty, F. W.; Begley, T. P. *Biochemistry* **2003**, *42*, 12430.
- (55) Chatterjee, A.; Schroeder, F. C.; Jurgenson, C. T.; Ealick, S. E.; Begley, T. P. *J. Am. Chem. Soc.* **2008**, *130*, 11394.
- (56) Hazra, A.; Chatterjee, A.; Begley, T. P. *J. Am. Chem. Soc.* **2009**, *131*, 3225.
- (57) Yamada, K.; Kumaoka, H. *Biochem. Int.* **1982**, *5*, 771.
- (58) Yamada, K.; Kumaoka, H. *J Nutr Sci Vitaminol (Tokyo)* **1983**, *29*, 389.
- (59) Tazuya, K.; Morisaki, M.; Yamada, K.; Katagi, T.; Kumaoka, H. *Bitamin* **1985**, *59*, 621.

- (60) Nicewonger, R.; Costello, C. A.; Begley, T. P. *J. Org. Chem.* **1996**, *61*, 4172.
- (61) Reddick, J. J.; Nicewonger, R.; Begley, T. P. *Biochemistry* **2001**, *40*, 10095.
- (62) Scott, A. I. *J. Org. Chem.* **2003**, *68*, 2529.
- (63) Lamm, L.; Hoerig, J. A.; Renz, P.; Heckmann, G. *Eur. J. Biochem.* **1980**, *109*, 115.
- (64) Hoellriegl, V.; Lamm, L.; Rowold, J.; Hoerig, J.; Renz, P. *Arch. Microbiol.* **1982**, *132*, 155.
- (65) Lamm, L.; Heckmann, G.; Renz, P. *Eur. J. Biochem.* **1982**, *122*, 569.
- (66) Vogt, J. R. A.; Lamm-Kolonko, L.; Renz, P. *Eur. J. Biochem.* **1988**, *174*, 637.
- (67) Vogt, J. R. A.; Renz, P. *Eur. J. Biochem.* **1988**, *171*, 655.
- (68) Munder, M.; Vogt, J. R. A.; Vogler, B.; Renz, P. *Eur. J. Biochem.* **1992**, *204*, 679.
- (69) Renz, P.; Endres, B.; Kurz, B.; Marquardt, J. *Eur. J. Biochem.* **1993**, *217*, 1117.
- (70) Endres, B.; Weurfel, A.; Volgler, B.; Renz, P. *Biol. Chem. Hoppe-Seyler* **1995**, *376*, 595.
- (71) Schulze, B.; Vogler, B.; Renz, P. *Eur. J. Biochem.* **1998**, *254*, 620.
- (72) Keck, B.; Munder, M.; Renz, P. *Archives of Microbiology* **1998**, *171*, 66-68.

(73) Taga, M. E.; Larsen, N. A.; Howard-Jones, A. R.; Walsh, C. T.; Walker, G. C. *Nature* **2007**, *446*, 449.

(74) Cooper, A. J. L.; Pinto, J. T. *Chemtracts* **2006**, *19*, 474.

(75) Kuchenreuther, J. M.; Myers, W. K.; Stich, T. A.; George, S. J.; NejatyJahromy, Y.; Swartz, J. R.; Britt, R. D. *Science* **2013**, *342*, 472.

APPENDIX

The appendix describes a summary of ThiC activity studies with substrate analogs. We tested several ThiC substrate analogs with a view to trap ThiC-reaction intermediates. Figure A1 demonstrates the substrate analogs that were tested. However, no/trace levels of products were detected in these reactions making it impossible for complete NMR characterization of the products formed.

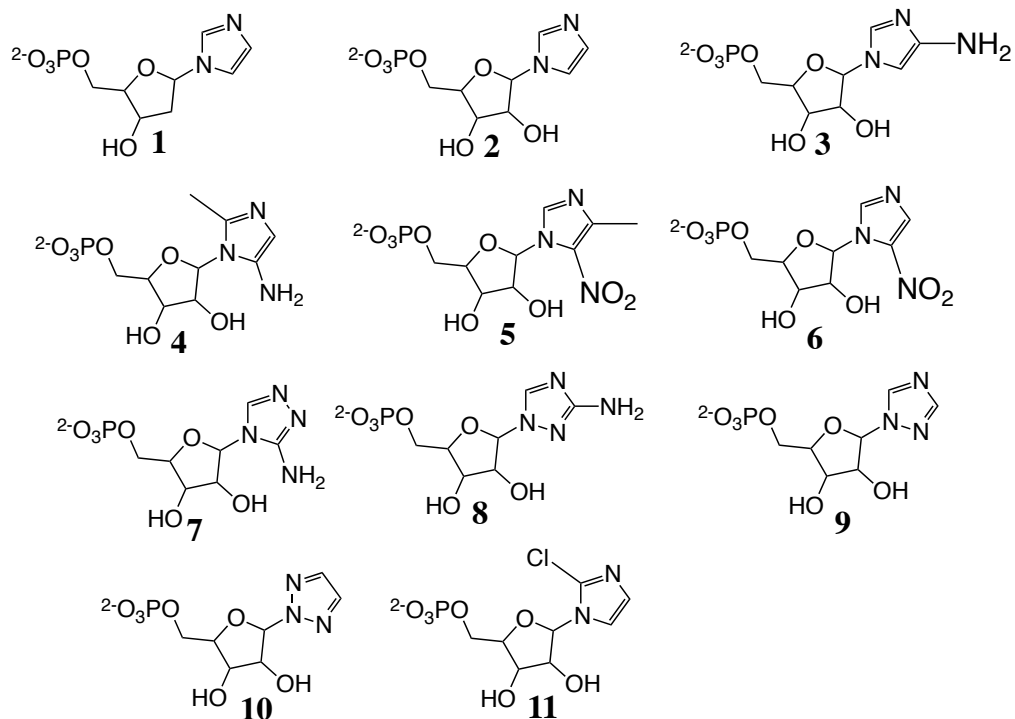


Figure A1: Substrate analogs that were tested for ThiC-catalyzed reactions.